Universiteit Utrecht

Multicomponent Transport of Contaminants Released into the Environment following the Application of Phosphogypsum

Benjamin Ebbers, 3018423

Master Thesis
August, 2011

Advisors:

Prof. M. Th. van Genuchten

Dr. D. Jacques

Prof. S.M. Hassanizadeh

Prof. M. Th. van Genuchten

       Department of Mechanical Engineering, COPPE/LTTC
       Federal University of Rio de Janeiro, UFRJ
       Rio de Janeiro, Brazil
       Tel. +55-21-32-64-70-25

Dr. D. Jacques

       Unit: Performance Assessments
       SCK•CEN
       Mol, Belgium
       Tel. +32 14 33 21 11

Prof. S. M. Hassanizadeh

       Department of Earth Sciences
       Faculty of Geosciences
       Utrecht University
       Utrecht, the Netherlands
       Phone: +31 (0)302537464

Abstract

In this study, the subsurface fate and transport of radioactive contaminants released from phosphogypsum, a by-product of the phosphate fertilizer industry was studied, using the HP-1 multicomponent transport modeling program. HP-1 combines Hydrus 1D, a model simulating one-dimensional variably saturated water flow and multicomponent transport in soil systems and sediments, with PHREEQC, which can be used to a broad range of low-temperature biogeochemical reactions in water, soils and sediments. A literature search was conducted to identify the most important parameters that influence the mobility of radium released from the phosphogypsum. Two PHREEQC approaches, the "EC-model" and the "K_d-model", were developed using data obtained from the literature to account for the dynamic behavior of radium in the vadose zone. Results of these approaches were used in PHREEQC batch experiments and compared with literature data. The EC-model, which uses ionic exchange constants from literature, is dynamic and well suited for spatially and temporally variable geochemical conditions. The K_d-model, which relates the radium distribution coefficient, K_d, to various soil parameters, is a linear approach and highly empirical, thus accounting to a lesser extent for transient geochemical conditions then the EC-model. HP-1 was used to model the long-term fate and transport of phosphogypsum applied to a typical Dutch agricultural soil profile, the Fimic Anthrosol. A 20-year simulation with the EC model showed relatively fast migration of radium, caused by high concentrations of Ca^{2+}, H^+ and SO_4^{2-}. Only an estimated 20% of the initial radium remained in the column. By comparison, the K_d model predicted relatively strong bonding of radium in the top 10 cm of the soil, but also steady leaching of radium from the column. Adding terms to account for transient changes in the calcium concentration and pH caused relatively small variations in the concentration with pH having the largest impact on radium migration in long-term simulations.

Table of Contents

CHAPTER 1 - Introduction

1.1 - Motivation

Agricultural operations typically try to enhance crop growth by optimizing soil conditions and nutrient availability with the help of fertilizers. With the rise of the chemical industry, artificial fertilizer production was optimized to satisfy specific requirements and make fertilizers more applicable to a variety of soil conditions. Inorganic phosphate fertilizers are among a long list of inorganic fertilizers used to provide plants of phosphate. Although fertilizers as such are beneficial, the production of inorganic phosphate fertilizers is not without consequences and byproducts. For example, phosphogypsum (PG) created during fertilizer production causes environmental concerns.

Phosphate fertilizer is chemically produced in several steps. The first step is the treatment of sedimentary or igneous phosphate ores, composed mainly of apatite, with concentrated sulfuric acid, resulting in the production of phosphoric acid, hydrated calcium sulphate (phosphogypsum) and hydrogen fluoride [Rutherford et al. 1994]:

$$Ca_{10}(PO_4)_6F_2 + 10\,H_2SO_4 + 20\,H_2O \rightarrow 10\,CaSO_4 \cdot 2\,H_2O + 2\,HF \tag{1.1}$$
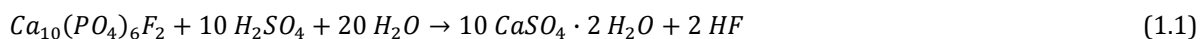
Phosphoric acid, depending on the experimental conditions and stochiometry of the reaction, is further processed to different types of phosphate fertilizers, being single superphosphate (SSP), monocalcium phosphate, triple superphosphate (TSP) or variations with ammonium resulting in monoammonium phosphate (MAP) and diammonium phosphate (DAP) [Saueia & Mazilli, 2006].

Phosphogypsum, when crystallized, is separated from the liquid phase by filtration, mixed with water and sluiced to a disposal or holding area. The amount of phosphogypsum being produced is significant. For each ton of phosphoric acid, approximately 5 ton of phosphogypsum is produced [Rutherford et al. 1994]. Worldwide production of phosphogypsum has been estimated to be about 100 to 280 megaton per year [Yang et al. 2009].

Phosphate ores are often enriched with radioactive elements, originating from the natural presence of [238]U and [232]Th [Tayibi et al. 2009]. During the wet phosphate production reaction, these naturally occurring impurities, besides radionuclides also heavy metals, are released and redistributed between the end-products. In addition to these impurities, the end- products also contain the remains of reactants and by-products, thus making phosphogypsum a potentially toxic waste product.

To a large extent, the type of fertilizer being processed dictates the selective separation of naturally occurring radium, uranium and thorium concentrations. During wet phase phosphate fertilizer production, it is thermodynamically favorable for [238]U to become incorporated into the fertilizer (at that stage phosphoric acid) while the daughter product of [238]U, [226]Ra, incorporates into phosphogypsum. About 80% of [226]Ra is concentrated in PG while around 86% of [238]U and 70% of [232]Th end up in the phosphoric acid [Haridasan et al., 2009, Rutherford et al. 1996].

Mainly due to the elevated levels of ^{226}Ra, but also because of other impurities, wet phosphogypsum is generally considered to be an undesired by-product, or even a (radioactive) waste product, with its usage greatly restricted by government regulations. For example, its general usage was in 1989 officially banned by the U.S. Environmental Protection Agency (EPA), while in 1992 the same restrictions were enforced by the European Union [Tayibi et al. 2009]. From that time on there were only three permitted options for managing phosphogypsum waste; (1) stacking (figure 1.1), (2) disposal or dumping in waterways (figure 1.2), seas or oceans, or (3) usage in research [EPA, 2004].

Figure 1.1. Phosphogypsum stacks near a phosphate fertilizer industrial plant in Polk County, Florida [DEP].

Stacking of phosphogypsum can lead to several risks for environmental and human health in surrounding areas. The risks may involve: (1) atmospheric contamination with fluoride or other toxic elements; (2) groundwater pollution with mobile anions, acidity, trace elements or radionuclides; (3) radon gas; (4) inhalation of radioactive dust; and (5) direct exposure to gamma radiation [Rigi et al. 2005, Rutherford et al. 1994].

One way of discarding the massive amount of phosphogypsum being produced is disposal or dumping in seas and oceans. A study conducted by a committee of the Health Council of the Netherlands investigated the impact of phosphogypsum discharge on the marine environment of the Nieuwe Waterweg near the North Sea coast. Increased concentrations of ^{226}Ra in the seawater and ^{231}Pa, ^{210}Po and ^{210}Pb in the sea bottom were found downstream of the discharge area, leading to increased concentrations of radionuclides in marine organisms and ultimately exposure of radionuclides to humans when eating fishery products from the North Sea [van der Heijde et al. 1988]. Several studies did lead to a change in waste policy and stricter regulations enforced by the EU regarding the disposal of phosphogypsum in maritime environments [OSPAR Commission, 2002]. In 1998 these regulations resulted in a complete ban on the release of phosphogypsum in rivers in Spain, as well as stricter regulation in the Netherlands [Villa et al. 2009].

Figure 1.2. Drainpipe for wastewater and
phosphogypsum in White Springs, Florida [DEP].

Notwithstanding the ban on the use of phosphogypsum for many applications and direct usage, research indicates there are several potential environmentally safe and economically feasible applications. For example, usage as a road base, an agricultural soil amendment, landfill cover and as material to make ceramic roofing tiles [Florida Industrial and Phosphate Research Institute].

PG's most feasible and extensively reported application is in agriculture as a soil amendment. For this reason its application is studied in this thesis. Phosphogypsum is beneficial for (1) highly weathered soil, with low exchange capacities and/or low levels of extractable nutrients; (2) soils with high sodicity resulting in dense subsoil horizons, and those with variable sodicity at the surface which are prone to dispersion and crusting; (3) acid soils with high levels of Al; (4) calcareous soils [Rutherford et al. 1994].

1.2 - Agricultural Soils in the Netherlands

Agriculture is and has been for many centuries an important factor in the Dutch economy. As land availability is low compared to most other countries, an efficient use and maintenance of agricultural soils is required. Many parts of the Netherlands that were originally not useable for agriculture purposes have therefore been prepared and reclaimed. An example is the 'Enkeerdgrond' or 'Loopodzolgrond' [De Bakker and Schelling, 1989]. This soil, also catalogued as a Plaggept by USDA (1975) and a Fimic Anthrosol by FAO (1988), is an agricultural soil typically located on higher, sandy grounds in the middle, eastern and northern regions of the Netherlands (figure 1.3). The soil is formed under anthropogenic influence mainly by the agricultural practice of applying manure and peat on sandy soils for hundreds of years. This resulted in the formation of thick A-horizons, in many cases thicker than 50 cm and relative rich in organic matter (2.5-8%). B- and C-horizons are typically found about 50 to 100 cm below the surface. The C-horizon, the base soil, is primarily made of fine drift sand (figure 1.4) [de Vries and Leeters, 2001, Jongmans and Peek].
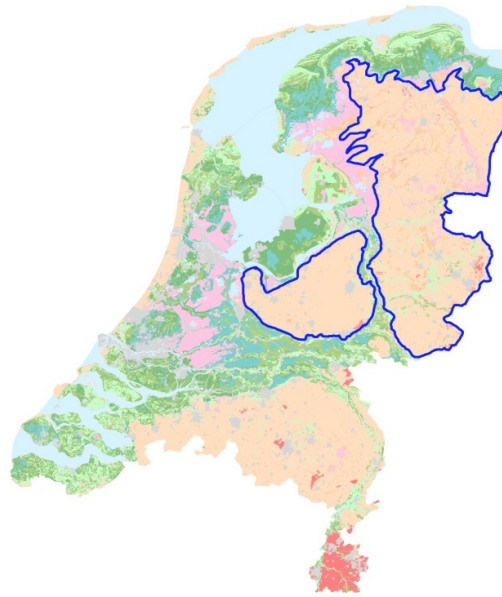
Figure 1.3. Soilmap of the Netherlands, [Alterra, Wageningen 2006]. Highlighted, inside of the blue lines, are sandy areas of the middle, eastern and northern part of the Netherlands were Fimic Anthrosols are typically found.

Intensive usage of the Enkeerdgrond over recent decennia has depleted most of the soils as well as compacted the top layers. Because of this and due to soil acidity, the base soil is non-calcareous, with the soil pH often ranging between about 3.7 and 4.3. This suggests that a soil conditioner such as PG could be used to increase production of these soils. For this reason the Enkeerdgrond, will be used as the experimental medium for our research under Dutch climate conditions.

Figure 1.4. (left) Vertical soil profile of a typical Enkeerdgrond [Niewsarchief Bibliotheek Wageningen UR, 2010]. The thick dark top layer (the A-horizon) is either dark brown or black coloured and rich of organic matter. Below this is a small transition layer, whose light grey color indicates that some leaching took place, a possible remnant of an earlier Podzol. This layer transgresses into the red-brown B-horizon where leachates have precipitated in the base soil. The yellow sand below this layer is part of the base soil or C-horizon; (right) Elevation of the soil surface level due to anthropogenic application of manure and peat over hundreds of years, thus creating a typical Enkeerdgrond [NBV, 2011].

1.3 - Research Objectives

It is important to understand and predict the long-term fate of impurities released from PG when used as a soil conditioner in agricultural settings, data not yet available from field studies. Knowledge of the evolution, interaction and migration of the pollutants through the soil is important and can be obtained through a combination of literature, theoretical and experimental research.

The main focus of this study is on the migration of phosphogypsum (PG) and the incorporated radionuclide, ^{226}Ra, since PG is considered a potential contaminant because of its relative high levels of radium. Assuming its regular use as a condition in agricultural operations, its fate and transport in the soil will be studied with HP-1 as a modeling tool.

A literature study will be carried first to categorize and summarize empirical data from earlier studies on the geochemistry of radium and to establish a database with important parameters affecting radium geochemistry and mobility.

PHREEQC models will be developed next to simulate the interaction of radium with the soil using the parameters found in the literature.

Implementation of the PHREEQC code into HP-1 code [Jacques et al., 2006] and its subsequent incorporation as a geochemical module within HYDRUS-1D [Šimůnek et al., 2009] results in generic models which can be used for situations where phosphogypsum is used as a soil conditioner in agricultural soils.

Long term simulations will be carried out, preferably over a time period of 100 to 200 years, to obtain data which are not available yet from field studies about the migration of radium in the soil.

Results from the models can eventually be applied to large-scale field situations to make long-term predictions of multi-component transport and radium migration when PG is applied as a soil amendment.

CHAPTER 2 - Literature on the Geochemistry of PG and Radium.

A small introduction on phosphogypsum, the production process and its structure has already been given in the section 1, this chapter will further elaborate on some characteristics of phosphogypsum. Since phosphogypsum is considered toxic mainly due to the relative high amount of incorporated radium [Tayibi et al. 2009], most of the literature research will be about this radionuclide and its release from the PG as well as its interaction with the soil and important soil parameters that influence this interaction.

2.1 - Phosphogypsum

PG is a chemical compound that mainly consists of mixture of calcium sulphate dihydrate ($CaSO_4.2H_2O$), also known as gypsum, and bassanite ($CaSO_4.0.5H_2O$). Included in this mixture are some impurities, such as radionuclides, trace elements and products of the phosphate fertilizer production process, such as phosphate [Rutherford et al. 1994].

Although phosphate fertilizer production processes and phosphate rock used in the process differs per factory or country and results in phosphogypsum having different characteristics, some characteristics are generally the same. [Canut et al. 2008], using phosphogypsum produced in Brazil, to determine some of these characteristics. The phosphogypsum particles are covered by micropores (<500 Å), have a specific surface area of 17.5 $m^2.g^{-1}$, a total pore volume of 0.05 $cc.g^{-1}$ and an average pore diameter of 107 Å. The grainsize of the phosphogypsum can be categorized as fine (<100mm). Impurity concentrations depend mainly on the origin of the phosphate rock used in the production process.

Physico-chemical conditions existing in and leaching of PG are of major importance to determine solubility and redox stability of phosphogypsum, as well as radionuclide release from stacks to terrestrial environments. Solubility of PG is determined by many parameters and is a complex system, yet the influence of some of the general parameters is clear. Salinity, the ionic strength, of the percolating water has a small but significant impact on PG solubility. [Papanicolaou et al. 2009] showed, by measurement of SO_4^{2-} concentrations in PG stack solutions. Consequently the increased solubility of phosphogypsum in saline stack fluids results in increased uranium levels in the solutions. The pH has an insignificant effect at the solubility of phosphogypsum in the range between 4 and 8.

Particle size of the phosphogypsum granules has a dominant influence on the dissolution rate. For example solutions with 1.0-mm phosphogypsum granules reach Ca saturation of 90%, whereas solutions with 5.0-6.0 mm granules reach only 35% saturation after 24 hours. Scanning of the particles exposed to relative long term dissolution showed formation of as Al-phosphate precipitate which coated the granules and might have inhibited further dissolution [Frenkel et al. 1989]. Reported solubility product constant of $CaSO_4$, K_s, equals $2.5x10^{-5}$.

Knowledge of PG dissolution could be important because it is responsible for increased concentration of Ca^{2+} and SO_4^{2-} in the soil, which in turn can influence mobility of radium. Extra information about the parameters influencing PG dissolution is available in the literature; however the focus of this study lies not on the dissolution of PG but on the release of radium from the PG.

2.2 - Radium in Phosphogypsum

Radium, a radioactive chemical element discovered in 1898, has four isotopes, ^{223}Ra, ^{224}Ra, ^{226}Ra and ^{228}Ra. Throughout this report the terms ^{226}Ra, Ra-226, Ra and radium will be used indiscriminately and will refer all to the Radium-226 isotope. Other isotopes of radium are not considered in this study.

^{226}Ra is the most abundant of the radium isotopes and is formed by alpha decay of ^{230}Th within the ^{238}Ur decay series. It is an earth alkali metal, which means that it is divalent and has similar properties as Mg, Ca, Sr and Ba. ^{226}Ra is of environmental concern because it follows similar biological pathways as Ca, resulting in possible accumulation in bone tissue of organisms. Having a half-life of 1620 year, ^{226}Ra is also considered hazardous because it decays into ^{222}Rn gas by alpha decay. This element, also an alpha particle emitter, is a concern due to its relative short half-life, 3.8 days, and its high mobility [Rutherford et al. 1994]. Its short half-life is of concern because relative much energy is released in a short time span, increasing the damage it can inflict on organic tissue.

For the pH conditions of most natural waters, and in general over a wide range of pH values (pH 3-10), dissolved radium will be present primarily as the uncomplexed Ra^{2+} cation [EPA, 2004]. In environments with high sulphate concentrations however, typical of PG stacks and possibly in situations where soil is mixed with PG, it is common that the mobility of ^{226}Ra is controlled by the precipitation and dissolution of calcium (Ca), strontium (Sr) and barium (Ba) sulphates. The solubility product constants (25^oC) for radium sulphate and barium sulphate are $10^{-10.4}$ and 10^{-10}, respectively [Rutherford et al. 1994].

Precipitation of radium is only possible when the solid-solution solids (Ba, Sr, Ra) SO_4 and (metal, Ra) CO_3, and the levels of sulphate and carbonate are relatively high. In other words, only when the soil solution reaches equilibrium with these solids, they will precipitate until then either Ra^{+2} or $RaSO_4$ (aq) will control the speciation of radium [Langmuir and Riese, 1985, Rutherford et al. 1994].

Although radium sulphate is thought to be the main speciation of radium in PG, in some experiments other forms of solid radium have been observed. For example, radium is known to incorporate in $CaAl_3(PO_4)_2(OH)_5*H_20$ [Cañete et al. 2007] and is also present the iron-oxide fraction [Santos et al. 2006]. No thermodynamic properties are known about these precipitates; therefore they will not be included in our models.

2.3 - Radium Leaching from Phosphogypsum

Data from leaching experiments are important to estimate the leaching rate of radium from the PG when applied in agricultur. To better understand the processes of ^{226}Ra leaching, several studies have been used.

In continuous leaching experiments of ^{226}Ra from a fertilizer process sludge, consisting of $CaCO_3$ and $CaSO_4$ at a ratio of 85:15, three states of radium could be identified (figure 2.1); a loosely bound fraction which desorbs initially (batch numbers 5 to 11); a fraction of the loosely bound radium moving down the column in a desorption-sorption cycle (batch numbers 11 through 19); and a chemically exchanged fraction which steadily leaches out (batch numbers 20 and higher) [Paul et al. 1984].

The first two factions are essentially one entity, thus bringing the total number of states down to two, one loosely bound state which accounted in the study of Paul et al. (1984) for 40% of the total activity, and the chemically exchanged fraction. Both fractions however are not a fixed amount and the size is dependent on the condition of leaching (e.g. the pH and ionic strength of the percolating water).
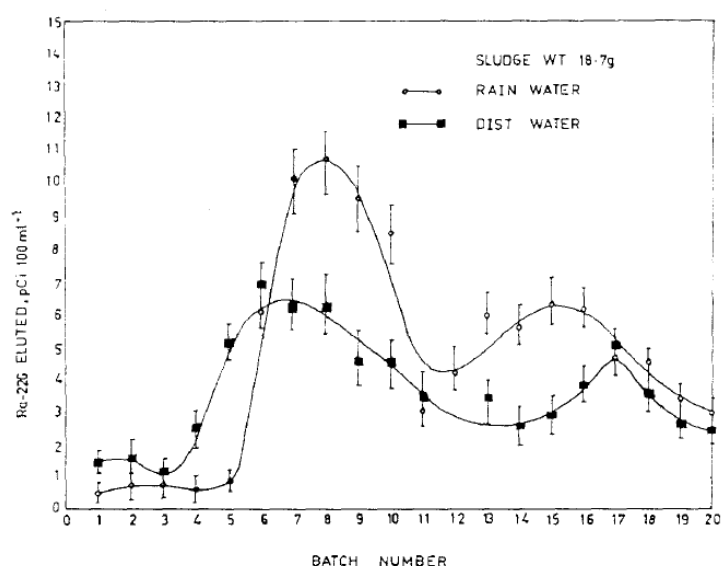

Figure 2.1. From Paul et al., (1984). The leaching of ^{226}Ra from $CaCO_3$:$CaSO_4$ (85:15) sludge by column elution and the usage of two types of eluants: rain- and distilled water. The first peak is designated to be the loosely bound fraction (1), the second peak could be the loosely bound radium that moves down the column in a desorption-sorption cycle (2). The long tailing is attributed to the chemically exchanged fraction which steadily leaches out.

Since radium, to a lesser extent, is also present in the form of $RaSO_4$ (aq) [Rutherford et al 1994], a form relatively inert to electrostatic interactions, the first peak may not necessarily consist of only Ra^{2+}, such suggested by Paul et al. (1984). The retardation of Ra^{2+} due to electrostatic interactions may then explain the second peak, which logically would consist of mostly Ra^{2+}. The electrostatic interactions would then effectively separate $RaSO_4$ and Ra^{2+}. The long tailing could result from slow dissolution of PG particles and thus cause the slow release of $RaSO_4$ incorporated therein.

The same leaching trend, consisting of a quick-desorption stage, a stage with desorption-sorption cycles and a steady-state leaching stage, was also observed by [Cañete et al. 2007] who studied the leachability of Philippine phosphogypsum (figure 2.2) in a column experiment, leached with de-ionized water. The total leached activity was only around 5% of the initial Ra present, which suggests that Philippine PG strongly binds the radionuclide to its matrix. Except for the first few leachates which were acidic, the pH of the later leachates, leveled off at around 5.6.
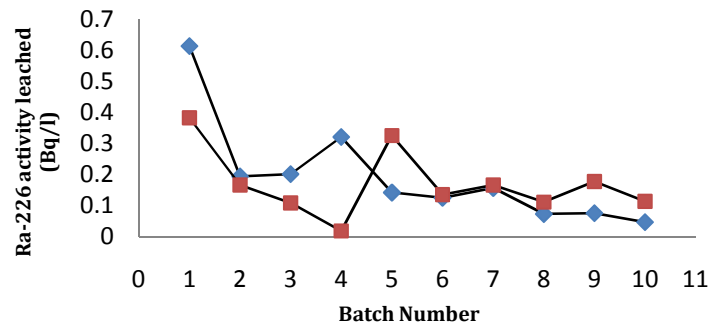

Figure 2.2. ^{226}Ra activity concentrations (Bq.l^{-1}) after leaching (blue) or washing (red) [Cañete et al. 2007]

The effect of using different leachants as described by [Paul et al. 1984] can also be seen in a study performed by Haridasan et al. (2002), who examined the dissolution characteristics of ^{226}Ra from PG with distilled water and rainwater (figure 2.3).
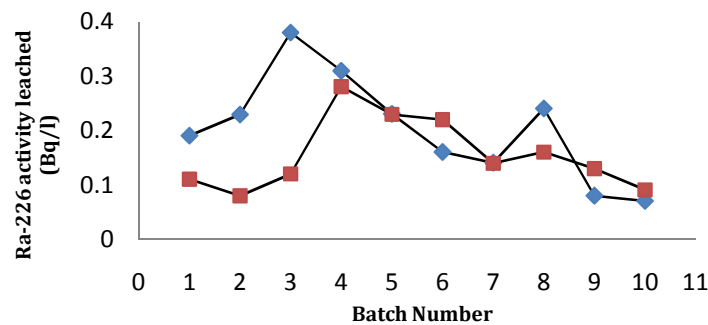
Figure 2.3. from Haridasan et al. (2002). Leaching of ^{226}Ra from phosphogypsum with distilled water (blue) or rain water (red).

Next to studying the effect of using different leachates, Haridasan et al. (2002) also simulated leaching under natural leaching conditions. One kilogram of PG was uniformly spread in a rectangular PVC tray of 0.25 square meters and was exposed to a total of 762 mm rainwater, with a pH varying from 4 to 6.1, for one month. The pH of the leachates varied from 2.8 to 5.5. The maximum and minimum ^{226}Ra activities in the leachates were 0.53 and 0.07 Bq.l^{-1}. From the initial ^{226}Ra activity (850 Bq), only 0.9% or 7.38 Bq was leached out in a month. Even though this quantity is low, a trend similar to the other leaching studies could be observed (figure 2.4).

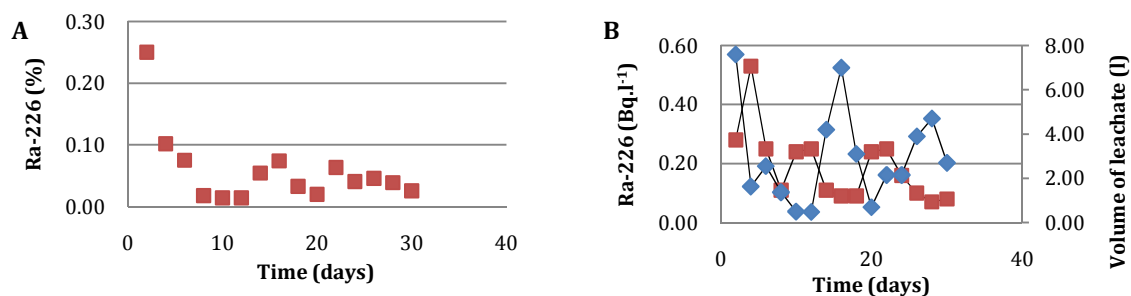*Figure 2.4. ^{226}Ra release from PG over a month period using 762 mm of rainwater as (A) a percentage of the initial ^{226}Ra activity, and (B) the concentration in the leachate (Bq.l^{-1}) (red), and volume of leachate (blue).*

Paul et al. (1984) concluded that several parameters such as pH and ionic strength of the leachate, dictate the leaching of the loosely bound fraction of ^{226}Ra from a PG stack. This conclusion was supported by two other studies [Cañete et al. 2007, Haridasan et al. 2002]. However, these studies contradicted each other about which of the leachants released and caused radium to migrate more. Paul et al. (1984) observed more leaching when using rainwater, while Haridasan et al. (2002) observed more leaching when using distilled water. Paul et al. (1984) stated that rainwater has a lower pH and higher ionic strength then distilled water. The lower pH results in a higher dissolution rate of the phosphogypsum, hence a quicker release of radium from the stack. The higher ionic strength results in a higher mobility of Ra due to competition with ions from rainwater on the ion exchange sites. Haridasan et al. (2002) stated that usage of rainwater results in less radium leaching compared to using distilled water. The main reason is that the rainwater contains dissolved ions, especially sulphate, from the atmosphere, which makes $CaSO_4$ less likely to dissolve, and Ra^{+2} to release slower. The effect of higher ionic strength on the mobility of Radium was not addressed.

Although the total amount of ^{226}Ra leached was different for each study, all three studies showed similar trends regarding the release over time of ^{226}Ra from PG as described in great detail by Paul et al. (1984). Also, most studies indicate that only a small amount of ^{226}Ra is released (0.9%) after one year as reported by Haridasan et al. (2002). This can be used as a guideline for the amount of ^{226}Ra released, or total PG dissolution, in our models.

Over short time periods, leaching of ^{226}Ra from soils with water brought to pH 5.5 by CO_2, can reasonably be approximated by Fick's law of diffusion. Diffusion coefficients for radium range from 5 x 10^{-11} to 10^{-13} cm^2 day^{-1}. These coefficients can also provide another basis for estimating the fraction that would be leached over long periods [Nathwani and Phillips, 1978].

2.4 - Radium Mobility in (top)soils

2.4.1 - Radium Speciation and Adsorption Mechanisms

As stated before, for the pH conditions found in most natural waters and in general over a wide range of pH values (pH 3-10), dissolved radium will be present primarily as the uncomplexed Ra^{2+} cation [EPA, 2004].

Other aqueous complexes that have been identified in experimental settings, and could influence radium mobility in some environments, are $RaOH^+$, $RaCl^+$, $RaCO_3$ (aq) and $RaSO_4$ (aq). Some of their thermodynamic properties have been identified by Langmuir and Riese (1985) (table 2.1). The formation constants and solubility products for the species $RaOH^+$, $RaCl^+$, $RaCO_3$ (aq), $RaCO_3$ (s), $RaSO_4$ (aq) and $RaSO_4$ (s) were added to the PHREEQC database, which was renamed phreeqcUB.dat (attachment A).

Table 2.1 Formation constants (log K_{as}) of radium complexes or solubility products (log K_{sp}) of radium solids [Langmuir and Riese, 1985]

Formation Reactions	log K_{as} or log K_{sp}
1) $Ra^{2+} + OH^- = RaOH^+$	0.50
2) $Ra^{2+} + Cl^- = RaCl^+$	-0.10
3) $Ra^{2+} + CO_3^{2-} = RaCO_3$ (aq)	2.50
4) $RaCO_3$ (s) $= Ra^{2+} + CO_3^{2-}$	-8.30
5) $Ra^{2+} + SO_4^{2-} = RaSO_4$ (aq)	2.75
6) $RaSO_4$ (s) $= Ra^{2+} + SO_4^{2-}$	-10.26

Note: Not all values listed in the table are measured values; some are obtained by plotting K values of similar complexes, formed with related alkali earth elements like Ca, Sr and Ba, against the effective cation radii in their appropriate coordination.

Concentrations of radium in natural waters, and even in waters associated with uranium mining and nuclear waste disposal sites, are rarely high enough to reach saturation with pure radium solid. Aqueous radium concentrations are therefore limited instead by adsorption or solid solution formation. For a Ra solid solution to play an important role, the host mineral must be close to saturation [Langmuir and Riese, 1985]. High sulphate concentrations in the soil solution are thought to induce radium precipitation [Vandenhove and van Hees (2007)] as noted earlier. However, the question remains whether or not sulphate concentrations found in soils will be high enough to do so.

The process dominating the migration of radium through a soil depends on the speciation of radium under given circumstances. As radium dissolves to Ra^{+2}, it mainly adsorbs to soil and organic matter through ion exchange [EPA, 2004]. Laili et al (2010) observed that the adsorption of radium ions increased with increasing pH, which is another indication that radium ions mainly adsorb onto coir pith surfaces (a substitute for organic matter) in this case, through an ion-exchange mechanism.

Two types of adsorption of radium ions from the solution exist: (A) Rapid physical adsorption by weak van der Waals forces, basically caused by electrostatic charges such as the adsorption of cations which can be easily replaced by ions that possess special adsorptivity, ion-exchange; and (B) specific chemical

adsorption through the formation of strong chemical bonds with the top layer of a soil. This latter form is most commonly found in barium bearing minerals, such as barite and barium salts where radium from the aqueous solution and barium ions from the mineral surface, due to their similarity, are relative easily exchanged [Wang et al, 1993]. None of these minerals are found extensively in our PG stack or soil. The first form of adsorption (ion exchange) will therefore be the main form of adsorption and immobilization of radium in our models.

2.4.2 - Important Soil Parameters Influencing Radium Mobility

Since radium mobility is mainly dominated by adsorption through ion exchange, the cation exchange capacity (CEC) is an important parameter of the soil. The value of the CEC of a soil is mostly determined by two factors, the amount of organic matter and soil texture, including mineralogical composition. There are several parameters of the soil (solution) which influence the amount of exchange sites available for radium (e.g. pH, ionic strength, and concentrations of bivalent cations). This section will elaborate on the influence of these parameters on the radium distribution coefficient (K_d). The data of both K_d and the soil parameters will be transformed to logarithmic values and linearly correlated through a trendline. The slope of this trendline will give an estimate of the change in the radium distribution coefficient through changing soil conditions, and thus can be used as a way to influence of soil parameters on the migration of radium.

Radium Concentration

Radium isotope concentrations are usually given in picocuries (1 pCi = 10^{-12} Ci), decays per second (1 pCi = 0.037 dps) or Becquerel (Bq). One gram of ^{226}Ra is equal to 1 Ci. Given the conversion factor of 1 Ci = 3.7×10^{10} Bq, one gram of ^{226}Ra is also equal to 3.7×10^{10} Bq.

The influence of the radium concentration on the amount adsorbed on a soil is often expressed using either a Freundlich or Langmuir isotherm when relationships are not linear. When for example it is limited by adsorption on a heterogeneous medium, the Freundlich isotherm can be used, which is described as:

$$S_e = K_f \times C_e^{1/n} \tag{2.1}$$

where C_e is the equilibrium concentration (Bq.ml^{-1}), S_e is the amount of radium adsorbed (Bq.g^{-1}) and K_f and $1/n$ are constants indicative of adsorption capacity and intensity, respectively. This equation can be linearized in a logarithmic form as follows

$$log\, S_e = log\, K_f \times {^1/_n}\, C_n \tag{2.2}$$

From the slopes and intercepts of the straight lines the parameters $1/n$ and K_f can be calculated. For a linear relationship between the concentration adsorbed on the soil and in the solution, the $1/n$ parameter has to be or close to 1.

The Langmuir Isotherm equation, usually used for a solid-liquid system, can be described as

$$q_e = \frac{K_1 K_2 C}{1 + K_2 C} \qquad (2.3)$$

where K_1 is the adsorption maximum (pCi.g^{-1}) and K_2 is a constant related to the bonding energy of the soil with radium (l.pCi^{-1}). This equation, upon rearrangement can also be written as

$$\frac{C}{q_e} = \frac{1}{K_1 K_2} \frac{C}{K_1} \qquad (2.4)$$

Freundlich parameters found by Laili et al. (2010) for the absorption of radium on coir pith in the presence of humic acids were 1.061 and 3586 (Bq.g^{-1}) for $1/n$ and K_f, respectively, for a pH of 9 and radium concentrations ranging from 0.2 to 1.0 Bq.ml^{-1}. Since $1/n$ approached one, the adsorption onto organic matter as a function of the amount of radium in the solution was close to linear.

The Freundlich isotherm has also been used to describe radium adsorption on Maifanshih rock at pH 7.6, 30 °C and between radium concentration ranges from 0.074 Bq.ml^{-1} to 1.85 Bq.ml^{-1} [Wang et al. 1993]. Under those experimental conditions $1/n$ and K_f were 1.66 and 0.458 Bq.g^{-1} respectively.

Nashwani and Phillips (1979a) described the adsorption of radium for a wide variety of soils, over a radium equilibrium concentration range from 3.70*10^{-5} to 3.70 Bq.ml^{-1}. They noted that sorption was in accordance with the Freundlich and the Langmuir isotherm equation. Values for the Freundlich isotherm constants $1/n$ and K_f, ranged from 2.09 to 17.86 and 0.43 to 231.09 Bq.g^{-1}, respectively. However, under the influence of Ca^{+2} concentrations ranging from 0.005 to 0.0005 M in the solution, values of $1/n$ and K_f changed slightly; they were generally lower, ranging from 4.69 to 14.08 and 0.37 to 65.91 Bq.g^{-1}, respectively.

Organic Matter

Vandenhove and van Hees (2007) determined the radium distribution coefficient, K_d, for nine soil types with distinct characteristics, and established relationships with several of the soil properties.

K_d was found to be clearly linearly related to the organic matter (OM) content (figure 2.5) as well as with the cation exchange capacity (CEC):

$$K_d = 0.71 \times CEC - 0.64 \qquad (2.5)$$
$$K_d = 27 \times OM - 27 \qquad (2.6)$$

or

$$\log K_d = 0.9305 \times \log CEC - 0.0047 \qquad (2.7)$$
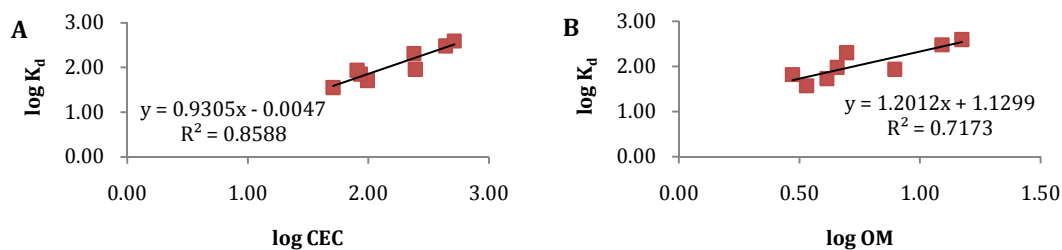$$\log K_d = 1.2012 \times \log OM - 1.1299 \qquad (2.8)$$

Figure 2.5. The relation between the log of the radium distribution coefficient, K_d, and (A) cation exchange capacity (CEC); (B) organic matter content (OM) [Vandenhove and van Hees, 2007].

The variation in the CEC of the soils could be explained by the OM fraction (R^2 = 0.91) and to a lesser extent by clay content (R^2 = 0.35) [Vandenhove and van Hees, 2007]. The correlations found by Vandenhove and van Hees (2007) however, were not consistent with K_d values found in a data compilation study a few years later [Vandenhove et al. 2009].

Natural organic materials can be divided into humic acids (HA), fulvic acids (Fa) and humin. Generally, humic acids are complex natural organic soil compounds which result from decomposition of organic matter and are responsible for much of its metal ion absorbing capability. [Laili et al. 2010] investigated the influence of humic acids and pH on the adsorption of radium using coir pith (CP) to eliminate factors such as mineralogical composition of the medium, which, as shown later, can affect the radium distribution coefficient as well. Results of this study are described in the subchapter "pH" since it involves mainly the influence of pH on the changing adsorption capacity of organic matter. The increased adsorption effect of humic acids on ^{226}Ra in the study of Laili et al. (2010) was mainly observed at neutral and alkaline pH values. This was explained by non-polar carboxylic groups that dissociate into ΞHA-COO$^-$ at pH values between of 4 and 6, thus providing additional radium adsorption surfaces.

Soil Textural Fractions

Besides organic matter, radium is known to adsorb to both clays and mineral oxides present in soils, especially near neutral and alkaline conditions [EPA, 2004]. To define a soil textural class, generally three textural fractions are defined: clay, silt and sand. These three fractions reflect particle size differences and usually also different mineralogical compositions. Variations in these fractions will thus influence the adsorption capacity of the soil differently.

Nathwani and Phillips (1978) found that the total amounts leached from a soil and the maximum concentrations reached in the leachate were much greater for coarse (e.g. sands) and medium-textured soils than for fine-textured soils (e.g. clays). Fine-textured soils therefore provide a higher sorption capacity and a low leaching rate.

Fine-textured soils generally have a higher CEC than medium- or coarse-textured soils, resulting in a higher sorption capacity of radium. The higher CEC is established by the naturally negative charge of clay mineral surfaces, leading to increased adsorption of (especially bivalent) cations. Another reason is that fine-textured soils consist of relatively small particles compared to medium- and coarse-textured soils which results in a much higher reactive surface area. However, even though together with organic matter, clay minerals are the dominant constituents contributing to the sorption of radium onto soil, organic matter is said to adsorb about ten times as much radium as clay [Simon and Ibrahim, 1990].

Cañete et al. (2008) studied radium migration through four different soils (two loamy, one clayey loam and one sandy loam soil) exposed to a phosphogypsum extract having a pH of about 3.72 (table 2.2).

Table 2.2. Activity reduction of radium after passing through 4 types of soil.

Soil Type	Initial Activity Extract (mBq.l[-1])	Activity after passing through soil (mBq.l[-1])	Activity Reduction (%)
Loam Soil 1	1,491 +/- 30.6	28.5 +/- 4.13	98.09
Loam Soil 2	1,491 +/- 30.6	N.D.	>98.99
Clay Loam	1,491 +/- 30.6	N.D.	>98.99
Sandy Loam	1,491 +/- 30.6	14.5 +/- 6.74	90.27

These results indicate that there are some differences in adsorption of radium depending on the soil texture, even at a low pH (3.72). Sandy loam had the smallest ^{226}Ra retardation; both the loam soil and clay loam soil did show more radium retardation.

Serne (1974) measured K_d values for radium on four sandy, arid soil samples using simulated river water solutions. The pH values of the soil/river water suspensions ranged from 7.6 to 8.0. The soil consisted primarily of quartz and feldspar, with 2-5 percent calcite and minor amounts of muscovite and smectite. The K_d values, which ranged from 214 to 467 ml.g^{-1}, could be related to the cation exchange capacity (CEC) values of these soils. Because our study deals with a sandy soil, albeit with varying organic matter content, similar K_d values should be expected. However, since the pH of the soils in the modeling experiments are expected to be significant lower, the K_d value should be lower as well. The effect of pH is discussed more thoroughly in a later section.

Even though the effects of clay minerals may not be significant at the pH levels found in arid soils, clay minerals still have an effect on the mobility or radium as it migrates through a soil. This will especially be the case in situations where the pH of the soil and adjacent groundwater increase, for example in deeper layers of the soil. To show the difference between different soil types, Thibault et al. (1990) reported K_d values for several types of soil (table 2.3). The wide range of the results is noteworthy given the relatively limited number of observations.

Table 2.3. Distribution coefficients of radium for various soil types. [Thibault et al. 1990].

Soil Type	K_d Values (ml.g^{-1}) Geometric Mean (2004)	Number of Observations	Range
Sand	500	3	57 - 21,000
Silt/Loam	36,000	3	1,262 – 530,000
Clay	9,100	8	696 – 56,000
Organic	2,400	1	N.A.

The K_d values of Thibault et al. (1990) were later revised downward by Sheppard et al (2006) as more experimental data became available. They were lowered to 53, 46, 34 and 200 ml.g^{-1} for sand, silt, clay and organic soils, respectively. Sheppard et al (2006) further recommended using an average K_d value of 47 ml.g^{-1} irrespective of soil type.

A subsequent compilation by Sheppard et al. (2009), using a total of 67 data from several studies [Sheppard et al. 2006; Thibault et al. 1990; and Vandenhove and Van Hees 2007] resulted in an equation (using only 30 points, R^2=0.13) that linked radium K_d with the clay fraction of a soil as follows:

$$logK_d = 0.0599 \times log(clay\ fraction) + 1.56 \tag{2.9}$$

The fact that pH is not introduced into this equation may have been due to the fact that clay minerals, even if present in small amounts, always adsorb some radium due to their natural negative surface, and that aqueous speciation of radium is insensitive to pH.

Nathwani and Phillips (1979a) derived useful coefficients relating soil properties to the Freundlich and Langmuir equation parameters, values are given in table 2.4.

Table 2.4. Correlation coefficients relating soil properties to Freundlich and Langmuir equation parameters [Nathwani and Phillips (1979a)].

	Freundlich		Langmuir	
	K_f (pCi.g^{-1})	n	K_1 (pCi.g^{-1})	K_2 (l.pCi^{-1})
Clay %	0.581	0.14	0.690	0.522
OM %	0.902	0.05	0.910	0.881
CEC	0.810	0.03	0.810	0.812
Sand %	0.521	0.002	0.648	0.648

Relationships between log K_d and the size of the clay or sand fractions were also evident in the study by Nathwani and Philips (1979) who measured the log K_d for varying Ca^{2+} concentrations (figure 2.6). Although the values of log K_d changed due to changing calcium concentrations, the slopes of the regression lines did not differ significantly and thus are considered insensitive to calcium concentration at these levels.
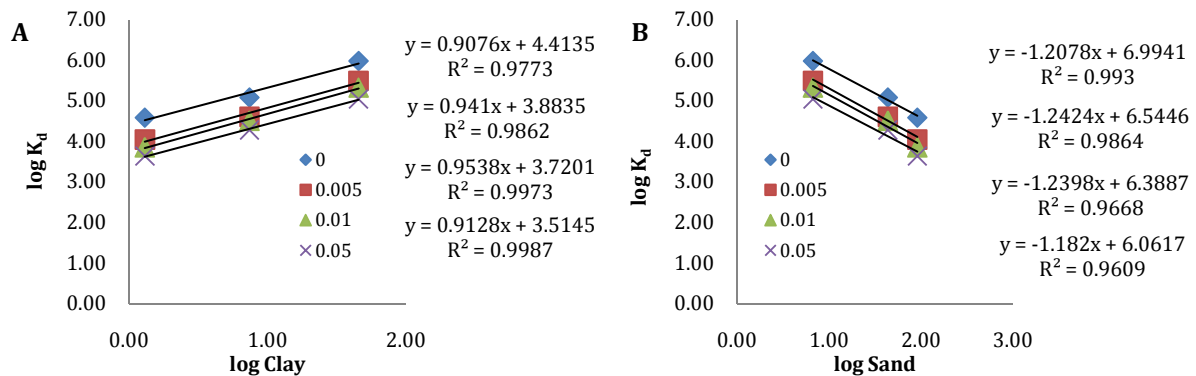

Figure 2.6. Data from Nathwani and Phillips (1979) giving a direct relationship between the log of the radium liquid solid partition constant (K_d, originally in ml.g^{-1}) and the log of the (A) clay and (B) sand fractions of the soil for four different concentrations of calcium.

Ionic Strength

Concentrations of cations in the soil solution, usually affected strongly by the ionic strength of a solution, can influence adsorption behavior of radium in a soil due to competition on the exchange sites of the soil.

Powell et al. (2010) analyzed two different soil types, a fine- and coarse-textured soil for pH 5.5, with ionic strength values (also given as NaCl concentrations) of 0.1 and 0.02 mol.l^{-1} [NaCl], with and without addition of strontium [table 2.5]. The mass of strontium added was 6 to 7 order of magnitude greater than the mass of radium.

Plotting log of the distribution coefficient for radium versus the log of the NaCl concentrations gives a relationship between the distribution coefficient for radium and the ionic strength for both the clay soil (figure 2.7a) and the sandy soil (figure 2.7b).

Table 2.5. K_d [ml.g^{-1}] values and standard deviation by Powell et al. (2010) for adsorption of radium on clay and sandy soils under varying ionic strengths and the addition of Sr.

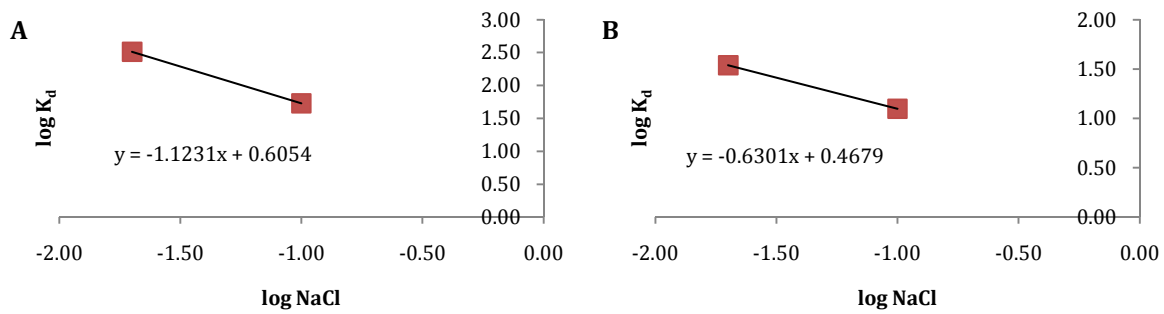|	[NaCl] = 0.1 M	[NaCl] = 0.02 M, Sr present.	[NaCl] = 0.02 M, no Sr present.
Clayey sediment	30.35 +/- 0.66	185.1 +/- 25.63	326.2 +/- 33.64
Sandy sediment	9.05 +/- 0.36	24.95 +/- 2.97	34.55 +/- 4.13

Figure 2.7. Log K_d plotted against the log of the ionic strength (NaCl) [M] for (A) fine-textured and (B) coarse-textured soils [Powell et al. 2010].

Linear interpolation between the results (figure 2.7) resulted in the following relationship between K_d and NaCl concentration for fine-textured soils

$$logK_d = -1.1231 \, log \, [NaCl] + 0.6054 \tag{2.10}$$

and coarse-textured soils

$$logK_d = -0.6301 \, log[NaCl] + 0.4679 \tag{2.11}$$

pH

The pH is known to play an important role in the adsorption of divalent ions onto the absorbent, thus influencing the cation exchange capacity of a soil and potentially facilitating the leaching of soil bound cations including ^{226}Ra. The pH range at which adsorption of cations begins to increase on mineral surfaces depends on the values of the point of zero charge (PZC) for each type of mineral or soil mixture as a whole, including its organic matter. In general, at pH values less than PZC, the mineral surface serves as a strong adsorbent for anions. At pH values greater than the PZC, the surface strongly adsorbs dissolved cationic constituents [EPA, 2004].

Nathwani and Phillips (1978) concluded that the leachate acidity significantly increases leaching rates, and therefore results in enhanced mobility in soils. A study of Cañete et al. (2008) reported high levels of ^{226}Ra activity in one of their wells, presumably caused by the intrusion of spilled H_2SO_4 from a plant in the vicinity of the monitoring well.

Because adsorption of cations is coupled with a release of H^+ ions, cation adsorption onto the soil is greatest at high pH values [EPA, 2004]. Because of the low pH of soil solutions generally found in most sandy soils, clay minerals may not have much influence on the migration of radium through such soils [Vandenhove and van Hees (2007)]. As concluded in the earlier section on soil texture, the effect of clay minerals on radium adsorption in our situation, a coarse-textured soil with pH ranging generally from 4 to 6, may therefore not be significant.

Meier et al. (1994) measured the adsorption of radium using site-specific waters and crushed sedimentary rocks from the Gorleben salt dome in Germany. In the pH range from approximately 4 to 9, the adsorption and desorption of radium increased with increasing pH. Values of K_d measured for the adsorption of radium on a sandy sediment in groundwater were 6.7, 12.6, 26.3 and 26.3 ml.g^{-1} at pH values of 6, 7, 8, and 9, respectively (figure 2.8). For the same system, the desorption K_d values were 10.9, 31, 38, and 29 ml.g^{-1} at pH values of 6, 7, 8, and 9. Linear interpolation between the log of the adsorptive K_d and pH gives an indication of radium adsorption on sandy sediments and its pH dependency and resulted in the following relationship
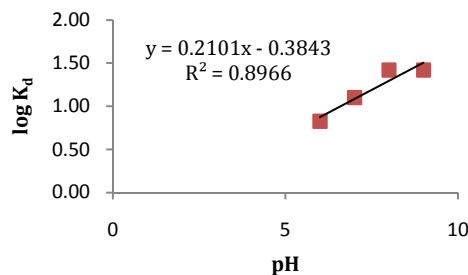
$$logK_d = 0.2101 \times pH - 0.3843 \tag{2.12}$$

Figure 2.8. Radium distribution coefficient for adsorption (ads K_d) and desorption (des K_d) plotted against pH. Linear interpolation was used for the adsorption K_d [Meier et al. 1994]

Laili et al. (2010) studied the adsorption of radium on coir pith (CP, an organic matter substitute) under influence of humic acids. Similar to soil minerals, the amount of adsorption sites available on organic matter surfaces for radium is lower at low pH values due to protonation of adsorption sites. This also results in electrostatic repulsion between radium ions and the positively charged CP surface, leading to less radium adsorption (figure 2.9)
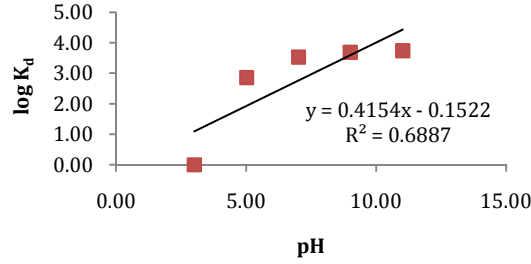
Figure 2.9. Effect of pH on the distribution coefficient (K_d) on the adsorption of radium ions onto CP under the presence of HA's, (50 ml and 0.2 g CP) [Laili et al. 2010].

Linear interpolation between the results (figure 2.9), resulted in the following relationship between log K_d and pH

$$logK_d = 0.4145 \times pH - 0.1522 \tag{2.13}$$

The PZC of coir pith was measured to be at pH 6.3, while a significant increase in adsorption was observed at pH values higher than 6.3 (figure 2.9). This can be explained by electrostatic attraction between the negatively charged CP surface and Ra ions. pH thus influences the radium adsorption onto CP surfaces significantly when humic acids are present. Hence determination of the PZC of a soil is important in the modeling studies.

Competitive Bivalent Cations

Most cations present in the soil solution are known to compete with radium for adsorption sites on soil particle surfaces. Due to their similarity to radium, changing concentrations of especially bivalent alkaline earth elements such as Mg, Ca, Sr and Ba can strongly influence adsorption behavior of radium [Vandenhove and van Hees, 2007; Nathwani and Phillips, 1979b].

Nathwani and Phillips (1979b) observed a decrease in adsorption of radium with increasing Ca^{2+} concentrations over a range of 0.005 to 0.05 mol.l^{-1} in the soil solution. Relationships between K_d and the concentration of calcium ($[Ca^{2+}]$) were established (figure 2.10) for three different soils: Wendover, a silty clay, Grimsby, a silty loam and St. Thomas, a sandy soil. Nathwani and Phillips (1979b) concluded that when radium is adsorbed in the presence of a large amount of Ca^{2+} ions covering many adsorption sites, the slope of the isotherm will be influenced more by the maximum adsorption capacity (CEC) of the soil than its affinity for radium. Values for 1/n (Freundlich parameter) under varying Ca^{2+} concentrations ranged from 4.69 to 14.08 while K_f values ranged from 10.1 to 1779.1, depending mostly on soil type and organic matter present.
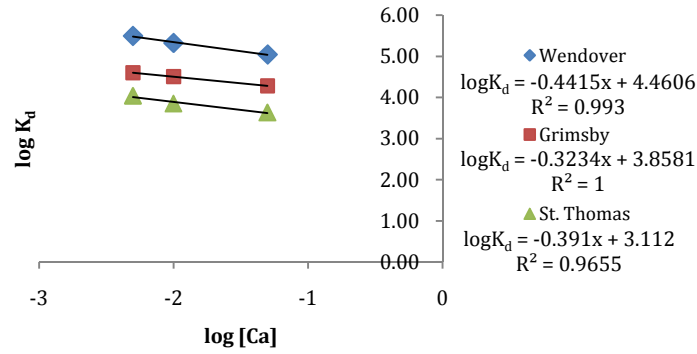
Figure 2.10. Data from Nathwani and Phillips (1979b) describing the relationship between the K_d of radium and the calcium concentration for three different soils.

Vandenhove and van Hees (2007) showed that the correlation between the radium distribution coefficient and both the Ca^{2+} and Mg^{2+} concentrations, produced a better fit with measured K_d values in comparison to only correlating with Ca^{2+} concentrations (figure 2.11). This suggests that one should include both cations when considering the influence of other base-cations on the solid liquid distribution coefficient and to some extent also the concentrations of other alkaline earth elements (Ba, Sr, Ca and Mg).
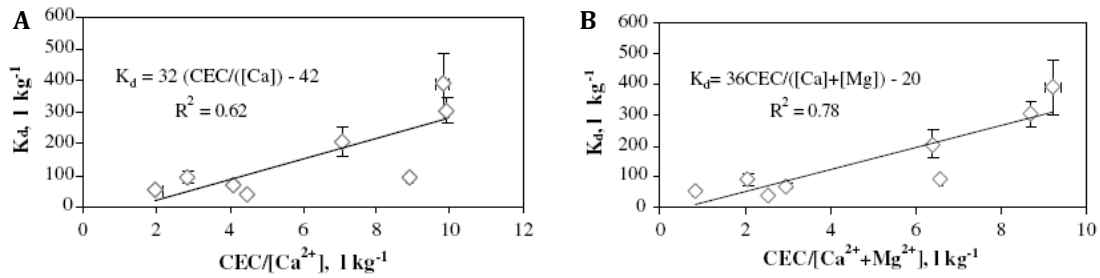
Figure 2.11. Figure from Vandenhove and van Hees, (2007) displaying the relation between radium distribution coefficient, K_d, and (A) CEC/[Ca^{2+}] and (B) CEC/[Ca^{2+} + Mg^{2+}].

In an attempt to obtain a closer fix for the relationship between K_d and the concentrations of Ca and Mg, data were recalculated to exclude CEC, which resulted in the following relationships, further plotted in figure 2.12:

$$logK_d = -8.093log([Ca]) - 9.945 \tag{2.14}$$

$$logK_d = -5.482log([Ca] + [Mg]) - 10.61 \tag{2.15}$$

Figure 2.12. Recalculated log K_d values plotted versus the log concentration of (A) calcium; (B) calcium and magnesium [Vandenhove and van Hees, 2007].

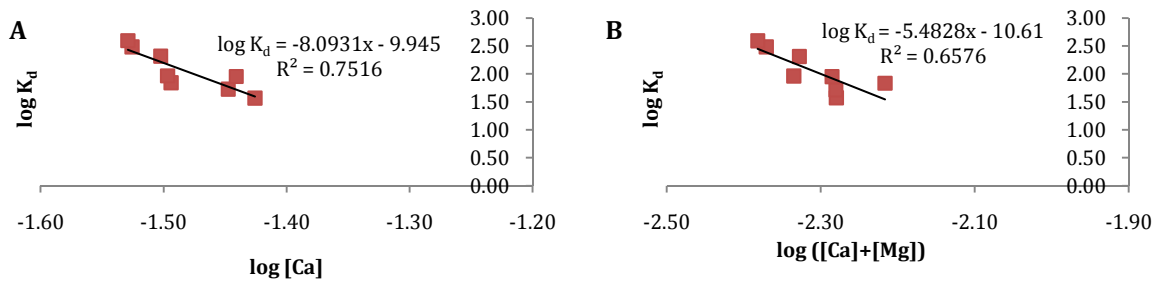Although a decrease in log K_d is observed with increasing Ca and Mg concentrations, as expected, these values are only an estimate and they should be used with caution.

Soil Grain Size

The grain size of a soil has a significant effect on the adsorption of radium. The main differences between soil texture classes such as sand, clay and loam are not only their mineralogical composition, but also to grain size and, more specifically, to surface area, as mentioned earlier in the section 'Soil Textural Fraction'.

As noted by Wang et al (1992), decreasing the particle sizes and hence the surface area of a soil (or in their case crushed rock) can lead to increased adsorption capacity. Figure 2.13 shows that K_d values decreased significantly with particle size. Since surface area increases approximately exponentially with grain size, it may be better to describe the relationship between log K_d and log Mesh Size by including an additional exponent, instead of one linearly.

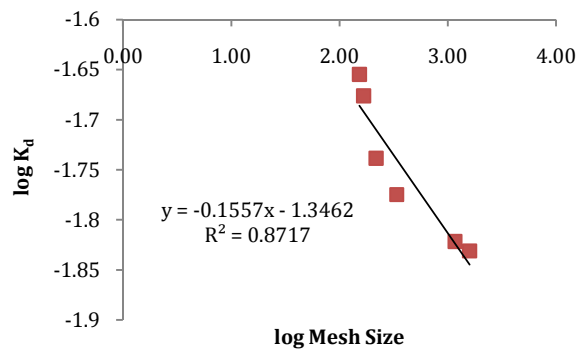*Figure 2.13. Grain size dependence of radium adsorption capacity of Maifanshih [Wang et al (1992)].*

Some of the effects of the mineralogical composition on radium sorption have already been covered in the section on soil textural fractions. Mainly because clays, silts and sandy soils do not only differ in particle size, but generally also in terms of mineralogical composition.

The EPA (2004) concluded that most of the results from crushed rocks and pure mineral phase studies are not necessarily relevant to the mobility and sorption of radium in soils given the complexity of typical soil systems and the strong dependence of partition coefficients on local physical and chemical conditions.

The most important minerals that influence radium mobility are likely iron oxides. The increase in adsorption of cations starts typically at pH values from 6 to 8 and reaches its maximum at a pH of about 10 or less [Cygan, 2002], values that are much higher than those observed in this project. Therefore,

Time to Adsorption Equilibrium

Wang et al. (1992), using Maifanshih rock, determined the adsorption equilibrium time for radium on their medium. Their results (figure 2.14) showed that adsorption approaches equilibrium after an equilibration time of about 11 hour.
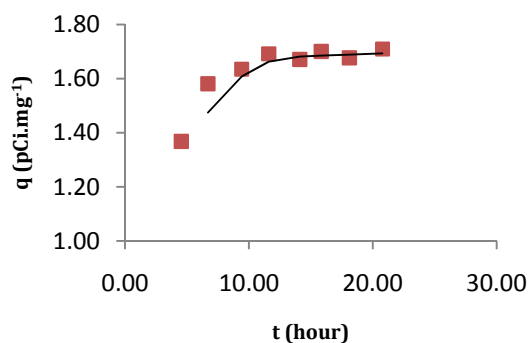
Figure 2.14. Adsorption equilibration of radium on Maifanshih rock [Wang et al. (1992)].

Using coir pith (CP) as organic matter constituent at a pH of 9, Laili et al. (2010) observed that a contact time of 24 hours was sufficient to reach the maximum removal of radium ions from the solution (figure 2.15).
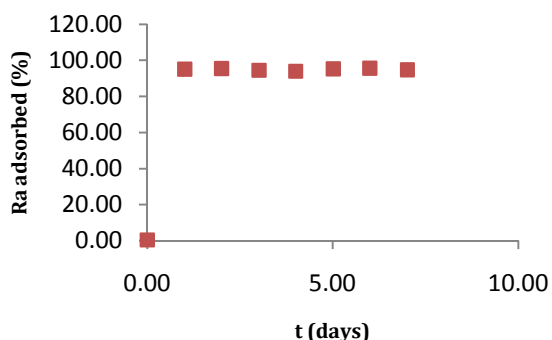

Figure 2.15. Effects of contact time on the adsorption of Ra ions onto CP under the influence of HA's [Laili et al. (2010)].

The relative adsorption equilibrium time of radium to soils is seems to be commonly reached within hours to days. Although flow velocity in transport simulations is the critical parameter to determine if adsorption is in equilibrium or not, the above described experiments are an indication that equilibrium is quickly reached. This suggests that it may be possible to assume instantaneous equilibrium in the modeling experiments.

Temperature

In general, the influence of temperature on radium mobility is complex. Not only does temperature influence chemical reactions but also fluid dynamics. These complex relationships are neglected by assuming a constant temperature in the models.

That the temperature of the system has an effect on K_d values, and can be rather complex, is something shown by Wang et al. (1993) (figure 2.16). Apart from that study, few if any experiments have been carried out about the influence of temperature on the K_d of radium. Hence, no empirical relationship could be established for the effects of temperature on radium sorption.
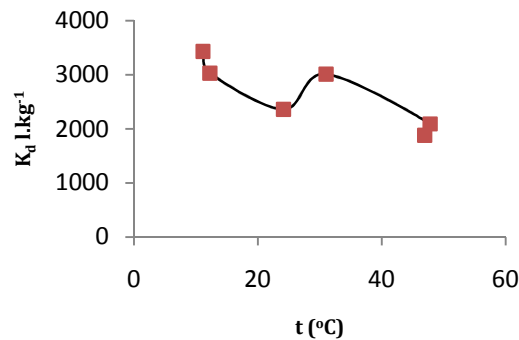

Figure 2.16. Soil (solution) temperature dependence of the radium K_d of Maifanshih rock [Wang et al. 1993].

Redox State (and Microbiological Effects)

Although the redox state of the soil solution may have little effect on the Ra^{+2} cation, with radium existing only as a divalent cation, changing redox conditions as mediated by microorganisms, can certainly influence the matrix in which radium is precipitated or to which radium and other radionuclides are adsorbed [Burnett et al, 1995].

Papanicolaou et al (2010) reported that generally in open phosphogypsum tailing dumps, oxidizing conditions predominate in stabilizing sulphur in the form of hexavalent oxidation state (SO_4^{2-}). However, after application of a soil/vegetative cover and in the presence of natural organic matter, anoxic conditions prevailed (EH<-70mV) resulting in S(VI) reduction to S(-II), from sulphate to sulphide, respectively. Although the sulphide anion can form very insoluble compounds with heavy metal ions leading to very low solubilities, partial reduction of sulphate to sulphide within gypsum may affect the stability of phosphogypsum. This may result in enhanced erosion of the material by rainwater and washing out of contaminants in particulate/colloidal form. Due to a lack of data on the influence of redox conditions on radium mobility, however, this parameter will not be considered in this study.

Plant (roots)

The influence of plants (including plant roots) is not in the scope of this project. However, areas in close vicinity of the roots may be more acidic due to the presence of organic acids, as compared to the general pH of the soil, and therefore increase radium mobility.

2.4.3 - Data from Related Alkaline Earth Elements

Since relatively little research has been done on Ra adsorption, more extensive studies and data on other alkaline earth elements, in particular Ba and Sr, can be used as general guidance in obtaining data for radium migration through soils.

Vandenhove and van Hees (2007) noted that strontium can be characterized by simple and almost reversible ion exchange on clay and organic matter, whereas radium sorption was somewhat more complex. One of their conclusions was that because of the larger ionic size of radium, both calcium and magnesium were less likely to replace radium from the exchange complex than strontium.

Kirby and Salutski (1964) shared this observation. In dilute HCl concentrations the order of elution of earth alkali metals was the same as the order of decreasing hydrated ionic radii. This indicates that the largest hydrated ion, magnesium from the earth alkaline elements, is bound the least tightly and will be eluted first.

These sorption experiments show the same principal in that the affinity of an element for ion exchange relative to other members of its chemical group increases with increasing atomic weight, or decreases with increasing hydrated ionic radius. Relative to other alkaline earth elements, sorption of radium is the strongest of all alkaline earth metals. The sorption trend has been described as $Ra^{2+}>Ba^{2+}>Sr^{2+}>Ca^{2+}>Mg^{2+}$ from strong to weak, respectively [Sposito, 1989].

Thermodynamic properties of radium complexes have been calculated using the properties of related complexes of alkaline earth elements and relating them linearly to the hydrated cation radius [table 2.6] [Langmuir and Riese, 1985]. A similar approach is used to calculate such properties like as adsorption or exchange constants for radium from data of related alkaline earth elements.

Table 2.6. Ionic radii (Å) for alkaline earth elements
[Molinari and Snodgrass, 1990].

Alkaline Earth Element	Ionic Radii (Å)	
	Crystal	Hydrated
Mg^{2+}	0.65	4.28
Ca^{2+}	0.99	4.12
Sr^{2+}	1.13	4.12
Ba^{2+}	1.35	4.04
Ra^{2+}	1.52	3.98

The effect of soil type or soil texture appears to be minimal with respect to the preference for monovalent and divalent cations [de Vries and Leeters, 2001]. Therefore, the difference in cation exchange constants between mono- and divalent cations should be relatively similar for any soil.

Exchange constants reported for A, B and C horizons in podzolic soils, or Fimic Anthrosols were reported by de Vries et al. (1994) [table 2.7]. Exchange constants for the top soil, up to a depth of 30 cm for Fimic Anthrosols have been given by de Vries and Leeters (2001) [table 2.8]. Jacques et al. (2008) reported exchange constants for several cations for sandy soils [table 2.9].

Table 2.7. Average cation exchange constants,
for A, B and C horizons of Podzolic soils [de Vries et al. (1994)].

Soil Horizon	Log K					
	H	Al	Mg	K	Na	NH$_4$
A	4.597	0.342	-0.553	-0.523	-0.161	2.230
B	5.100	1.204	-0.444	0.255	0.431	3.773
C	4.591	0.643	-0.071	0.908	0.602	3.735

Table 2.8. Median values of exchange constants in the mineral
topsoil of a Fimic Anthrosol [de Vries and Leeters, 2001].

Soil Type	Log K						
	H	Al	Fe	Mg	K	Na	NH$_4$
Fimic Anthrosol	3.601	1.083	1.027	-0.654	1.555	-0.653	1.329

Table 2.9. Log K parameters for the cation exchange reactions
of H$^+$, Na$^+$, K$^+$, Ca^{2+} and Mg^{2+} for acid sandy soils [Jacques et al. 2008].

Formula	Log K$_{ix}$
X$^-$ + H$^+$ = HX	4.2
X$^-$ + Na$^-$ = NaX	1.8
X$^-$ + K$^+$ = KX	2.85
2X$^-$ + Mg^{2+} = MgX$_2$	2.8
2X$^-$ + Ca^{2+} = CaX$_2$	3.1

Because no exchange constants were found for Ra, or the reaction 2X$^-$ + Ra^{2+} = RaX$_2$, as well as for several other alkaline earth metals such as Sr and Ba, available data on alkaline earth metals were linearly correlated to the hydrated cationic radius to obtain an approximate value for the radium exchange constant [Langmuir and Riese, 1985].

An example is given here using from de Vries and Leeters (2001) [table 2.8], where the average cation exchange constants related to Ca (K$_{Ca/I}$), of Ca and Mg are linearly correlated to the hydrated ionic radii (H.I.R.) [table 2.6], resulting in the following equation

$$K_{iX} = -4.8636 \times H.I.R. + 21.03 \tag{2.16}$$

where H.I.R. is the Hydrated Ionic Radius (Å) of the divalent cation or alkali earth metal (figure 2.17). From here the K of the remaining alkali earth metals could be calculated and converted into log K values usable in the PHREEQC code [table 2.10].
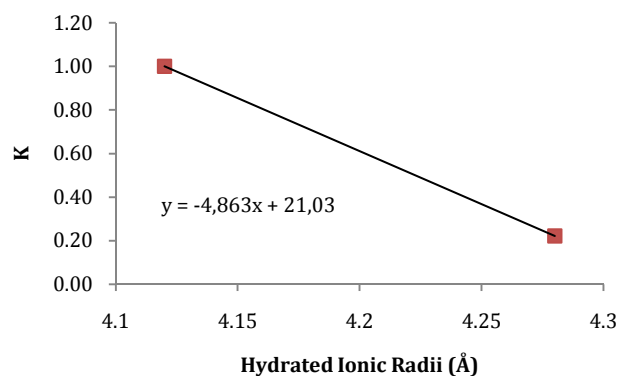
Figure 2.17. Linear correlation of $K_{I/Ca}$ against the Hydrated Ionic Radii resulting in a formula to calculate $K_{I/Ca}$ values for other alkali earth metals.

Table 2.10. Calculated .og K values for the alkali earth elements Sr, Ba and Ra in Fimic Anthrosols [de Vries and Leeters, 2001].

Reaction	Log K	K
$2X^- + Mg^{2+} = MgX_2$	-0,654	0,22
$2X^- + Ca^{2+} = CaX_2$	0,000	1,00
$2X^- + Sr^{2+} = SrX_2$	*0,000*	*1,00*
$2X^- + Ba^{2+} = BaX_2$	*0,143*	*1,39*
$2X^- + Ra^{2+} = RaX_2$	*0,226*	*1,68*

2.4.4 - Field Observations of Radium Adsorption and Distribution through Layers

To compare observed behavior of radium in our modeling experiments, especially those using HP-1, a few field and laboratory observations have been listed.

Observations in column experiments, with deposition of a 6 cm slug on top of 9.5 cm clay, showed that the topmost layer of the soil, to a depth of 0.5 cm, had the maximum activity of 8030 pCi.kg-1. The activity in deepr layers was significantly lower, in total consisting of 2% of the initial activity of the sludge. Activity detected in the effluent from the soil column also showed a non-exchangeable fraction present, presumably 226Ra bound in sulphate form [Paul et al. 1984].

Field studies provided data where the maximum activity was found at 22.5 cm depth. The activity in the top layer was significantly lower, possibly due to leaching over a period of years. The activity at depth 95 cm was comparable to background soil activity of the area, meaning it had not further leached. This low activity at deeper layers suggests that vertical seepage and exchange of radium with subterranean soil is insignificant but still occurs [Paul et al. 1984].

Lindeden (1980) considered a hypothetical case of long-term applications of phosphogypsum to soil used for growing food crops. They assumed an initial gypsum application of 25 tons (25 Mg) per hectare followed by alternate year applications of 13 ton (13 Mg) per hectare. With a radium concentration in the gypsum of 0.6 Bq.g^{-1} and a tillage depth of 15 cm, radium build-up in the top soil would reach 0.2 Bq.g^{-1} after about 100 years.

2.5 - Summary and Conclusions from Literature

2.5.1 - Conclusions on Radium Release

The three studies on leaching of ^{226}Ra from PG [Paul et al., 1984; Cañete et al., 2007; Haridasan et al., 2002] report a different total amount of ^{226}Ra that leached. However, all three studies showed similar trends regarding the ^{226}Ra release over time from PG: a relative large peak soon after addition of PG, followed by a smaller peak and extensive tailing towards a constant ^{226}Ra release process. The following radium phases were found in most studies: a loosely bound fraction, possibly the electrochemical inert $RaSO_4$ (aq) which desorbs quickly in combination with loosely bound radium, possibly Ra^{2+}, which moves down the column in a desorption-sorption cycle; and a chemically exchanged fraction which steadily leaches out [Paul et al. 1984].

The small amounts of ^{226}Ra released (0.9%) after one year can be used as a guideline for the amount of ^{226}Ra that needs to be introduced in our models [Haridasan et al. 2002]. Leaching of ^{226}Ra can be approximated by Fick's law of diffusion with diffusion coefficients ranging from 5 x 10^{-11} to 10^{-13} cm^2 day^{-1} [Nathwani and Phillips, 1978].

2.5.2 - Conclusions on Radium Adsorption

Organic matter content and soil texture (grain size and mineralogical structure) are two important factors that influence the CEC, and thus the amount of adsorption sites available for radium in a soil. Variables of the soil solution that influence radium adsorption significantly are pH, ionic strength and bivalent cation concentrations (mainly Ca^{2+} and Mg^{2+}). These variables need to be included in the K_d-model that will be adopted for radium sorption.

Parameters that likely will affect radium geochemistry and transport, but for which not enough data are available, are temperature and radium concentration in the soil solution. With respect to temperature, only a few data are available in the literature that relates temperature to radium adsorption equilibrium constants [Wang et al. 1993]. In terms of the radium concentration of the soil solution, one study [Laili et al. (2010)] shows that the radium concentration adsorbed to the organic matter increases linearly with the radium concentration in the soil solution. However Wang et al. 1993 showed that the Freundlich isotherm was best used to describe radium adsorption onto Maifanshih rock under changing radium concentrations.

Several parameters mentioned in literature will not be considered in this study or our modeling efforts, mainly because of the too little information in the literature. These parameters include influence of plant roots and microbiological activity. These parameters indirectly influence radium mobility or PG dissolution by affecting the conditions of the surrounding soil such as the pH. If site-specific measurements are available, such as the soil pH, one can assume that most of these influences are taken into account using appropriate values.

Although all of the parameters found in the literature may give an indication of radium adsorption behavior in certain types of soil and under certain conditions, it is always preferred to use site specific information. Judging from field observations, radium will likely be adsorbed most in soil the layers with the highest amounts of organic matter due to the elevated amount of adsorption sites compared other parts of the soil profile.

General speciation calculations can be done with PHREEQC to determine the speciation of radium in the soil solution. This is particularly advised when the soil solution contains significant concentrations of calcium, sulphate (SO_4^{2-}) and phosphate (PO_4^{-}) which might cause complexation and the removal of radium from the soil solution. These conditions, however, are unlikely to occur outside of the PG stack, or when PG is mixed with agricultural soil. It is hence to be expected that formation of [226]Ra solids will not play a role in the mobility of radium once it is introduced into the soil. However, the formation of aqueous species should be considered.

2.5.3 - Summary of Data found in Literature.

The exchange constants, log K, for radium, strontium and barium adsorption have been calculated using the exchange constants of related complexes (notably calcium and magnesium) and relating them linearly to the hydrated cation radius as was done for other thermodynamic properties as well [Langmuir and Riese, 1985] [table 2.11]. Constants from de Vries (2001) will be used in our EC-model.

Table 2.11. Summary of cation exchange constants, log K_{iX}, obtained from various studies. The average, displayed in the last column of the table, is the average of the three studies for the top soil.

Half Reaction	Jacques et al. 2008	de Vries, 2001	de Vries, 1994	Average
	Acidic Sandy Soils	*F.A. depth to 30cm*	*Podzol, Horizon A*	
$X^- + H^+ = HX$	1,10	3,60	4,60	3,10
$X^- + Na^- = NaX$	-1,30	-0,65	-0,16	-0,70
$X^- + K^+ = KX$	-0,25	1,56	-0,52	0,26
$X^- + NH_4^+ = NH_4X$	n.a.	1,33	2,23	1,78
$2X^- + Fe^{2+} = FeX_2$	n.a.	1,03	n.a.	1,03
$3X^- + Al^{3+} = AlX_3$	n.a.	1,08	0,34	0,71
$2X^- + Mg^{2+} = MgX_2$	-0,30	-0,65	-0,55	-0,50
$2X^- + Ca^{2+} = CaX_2$	0,00	0,00	0,00	0,00
$2X^- + Sr^{2+} = SrX_2$	*0,00*	*0,00*	*0,00*	*0,00*
$2X^- + Ba^{2+} = BaX_2$	*0,10*	*0,14*	*0,13*	*0,12*
$2X^- + Ra^{2+} = RaX_2$	*0,16*	*0,23*	*0,21*	*0,20*

Empirical data from the literature were compiled and are listed in table 2.12. The relationships between K_d and a specific parameter are expressed in log K_d equations to facilitate the ease with which they can be used in the K_d-model inside PHREEQC.

Table 2.12. Compilation of radium distribution coefficients (K_d)
as influenced by several parameters found in experimental studies.

Parameters	Formula	R²	Notes	Source
[Ca]	log K_d = -8.093*log[Ca]-9.945	0.751	9 soil types	Vandenhove and van Hees, 2007
	log K_d = -0.4415*log[Ca]+4.4606	0.993	Silt clay	Nathwani and Phillips, 1979b
	log K_d = -0.3234*log[Ca]+3.8515	1	Silt loam	Nathwani and Phillips, 1979b
	log K_d = -0.391*log[Ca]+3.112	0.9655	Sand	Nathwani and Phillips, 1979b
[Mg]	log K_d = -5.482*log([Ca]+[Mg])-10.61	0.657	9 soil types	Vandenhove and van Hees, 2007
Ionic Strength or [NaCl]	log K_d = -1.1231*log[NaCl] + 0.3591	1	Clay, in presence of Sr, pH 5.5	Powell et al., 2010
	log K_d = -0.6301*log[NaCl] + 0.3265	1	Sand, in presence of Sr, pH 5.5	Powell et al., 2010
pH	log K_d = 0.4154*pH - 0.1522	0.6887	Onto Coir Pith (OM)	Laili et al., 2010
	log K_d = 0.2101*pH – 0.3843	0.8966	Crushed sandy sedimentary rock	Meier et al., 1994
Mesh Size	log K_d = 0.1708*log Mesh Size - 2.0304	0.8717	Maifanshih (volcanic rock, feldspar and oxides)	Wang et al., 1993
CEC	log K_d = 0.9305 * log CEC – 0.0047	0.8588		Vandenhove and van Hees, 2007
Organic Matter fraction	Average K_d = 2,400	Studies: 1	Range: N.A.	Thibault et al., 1990
	log K_d = 1.2012 * log OM – 0.7173	0.7173		Vandenhove and van Hees, 2007
Sand fraction	Average K_d = 500	Studies: 3	Range: 57 - 21,000	Thibault et al., 1990
	K_d = 214 to 467 ml.g^{-1}	pH range: 7.6-8.0	Sandy sediment	Serne, 1974
	log Kd = 1.218 * log sand + 6.50	*0.97*	Several soils	Nathwani and Phillips, 1979a
Clay fraction	Average K_d = 9,100	Studies: 8	Range: 696 – 56,000	Thibault et al., 1990
	log K_d = 1.56 + 0.0599* clay	0.13	Compilation of 30 results from several studies	Sheppard et al., 2009
	log K_d = 0.9288 * log clay + 3.8829	*0.99*	Several Soils	Nathwani and Phillips, 1979a
Silt/Loam fraction	Average K_d = 36,000	Studies: 3	Range: 1,262 – 530,000	Thibault et al. 1990

CHAPTER 3 - Methodology

3.1 - Introduction to the HP-1 Modeling Program

In our research the computer code HP-1 is used to model the migration of radium and other components through a one dimensional soil column in the vadose zone. HP-1 combines Hydrus 1D, simulating one-dimensional variably saturated water flow and multicomponent transport in soil systems and sediments, with the PHREEQC geochemical. PHREEQC simulates a broad range of low-temperature biogeochemical reactions in water, soil and sediments, for example aqueous speciation, cation exchange, mineral dissolution/precipitation, and (bio)degradation for mixed equilibrium-kinetic system. A brief overview of HP-1, mostly adopted from the studies by Jacques et al., (2008a, b) is given in this section. The summary identifies the essential processes and equations that define the program and the parts that will be used in this study.

The transport of water, solutes and heat in HP-1 is described by using one dimensional conservation equation for momentum, fluid mass, solute mass and energy. For a porous medium, the conservation equation for water in combination with the Darcy-Buckingham equation for flow gives the Richards equation

$$\frac{\partial \theta(h)}{\partial t} = \frac{\partial}{\partial x}\left[K(h)\left(\frac{\partial h}{\partial x} + cos\alpha\right)\right] - S(h) \tag{3.1}$$

where θ is the soil water content [L^3.L^{-3}], h is the soil water pressure head [L], t is time [T], x is the spatial coordinate (positive upward) [L], K is the unsaturated hydraulic conductivity [L.T^{-1}], α the angle between the flow direction and the vertical axis, and S a sink term [L^3.L^{-3}T-1] which in our case could also be used for uptake of water through evaporation. There is no horizontal flow in the soil profile, only one-dimensional, vertical flow.

The soil is approached as a large unsaturated vadose zone, with the permanent groundwater level always below the profile. To solve the Richards equation, the soil water content, θ, as a function of the soil water pressure head, h, and the unsaturated hydraulic conductive, K, as function of θ or h, must be defined. This can be done by using the van Genuchten equations [van Genuchten, 1980] as follows

$$\theta(h) = \theta_r + \frac{\theta_s - \theta_r}{(1 + \alpha h^n)^m} \tag{3.2}$$

and

$$K(h) = K_s S_e^l \left[1 - \left(1 - S_e^{1/m}\right)^m\right]^2 \tag{3.3}$$

where θ_r is the residual water content [L^3.L^{-3}], θ_s is the saturated water content [L^3.L^{-3}], α [L^{-1}], n [-], and $m \ (= 1 - 1/n)$ [-] are shape parameters, l is a pore connectivity parameter [-], K_s is the saturated hydraulic conductivity [L.T^{-1}], and $S_e = (\theta - \theta_r)/(\theta_s - \theta_r)$ is effective saturation.

Solute transport is calculated by using the advection-dispersion equation, which for each component involved, is a combination of the conservation equation of solute mass and a flux equation accounting for both advective transport and diffusion and dispersion:

$$\frac{\partial \theta C_j}{\partial t} = \frac{\partial}{\partial x}\left(\theta D_w \frac{\partial C_j}{\partial x}\right) - \frac{\partial q C_j}{\partial x} - S C_{r,j} + R_{o,j}$$
(3.4)

where C_j is the total concentration C [M.L^{-1}] of a given component j, D_w is the dispersion coefficient in the liquid phase [L^2.T^{-1}], q the volumetric fluid flux density [L.T^{-1}], S is the sink term in the water flow equation [L^3.L^{-3}.T^{-1}], $C_{r,j}$ is the total concentration in the sink term [M.L^{-3}], and $R_{o,j}$ is a source-sink term that represents various heterogeneous equilibrium and kinetic reactions, such as cation exchange, surface complexation, mineral dissolution, and homogeneous kinetic reactions, such as degradation reactions in the aqueous phase [L^3.M.T^{-1}]. Equations (3.4) assumes that the dispersion coefficient is the same for all components involved.

Equation 3.4 is expressed in terms of the total concentration C [M.L^{-1}] of component j, which was initially written in terms of

$$C_j = c_j + \sum_{i=1}^{N_m} v_{ji} c_i$$
(3.5)

where c_j is the concentration of the jth component, c_i is the concentration of the ith secondary species, v_{ji} is the stoichiometric coefficient of the jth component in the reaction equation for the ith species and N_m is the number of secondary species.

The dispersion coefficient, D_w in equation 3.4 is given by

$$\theta D_w = D_L |q| + \theta D_{i,o} \tau_w$$
(3.6)

where $D_{i,o}$ is the molecular diffusion of the ith aqueous species in free water [L^2.T^{-1}], D_L is the longitudinal dispersivity [L], and τ_w is a turtuosity factor in the liquid phase [-] that is related to the water content.

The geochemical processes used in our model are aqueous complexation and ion exchange. The aqueous complexation reactions are written in terms of components or master species and their stoichiometric coefficients. The general reaction equation for an aqueous species is

$$\sum_{j=1}^{N_m} v_{ji} A_j^m = A_i$$
(3.7)

in which N_m is the number of aqueous master species, $i_e = 1, \dots, N_{sa}$, where N_{sa} is the number of aqueous secondary species, A_j^m and A_i are chemical formula for the master and secondary species, respectively, and v_{ji} represents the stoichiometric coefficients in the reaction.

When assuming equilibrium, the mass law equations with the component conservation equations allow the required speciation calculations. The mass law equations are

$$K_i^l = a_i^l \prod_{j=1}^{N_m} \left(a_j^m\right)^{-v_{ji}} \tag{3.8}$$

in which K_i^l is the thermodynamic equilibrium constant [-], a is the activity [-] defined as $a_i = \gamma c_i / c_i^0$ where c_i is the molal concentration [mol.kg^{-1} H$_2$O], c_i^0 is the standard state (often fixed at 1 mol.kg^{-1} water), γ is the activity coefficient [-], and the superscripts m and l refer to master and secondary aqueous species, respectively.

Using the ion exchange model, sorption on the solid soil phase, can be written in terms of the Gaines and Thomas equation:

$$\sum_{j=1}^{N_m} v_{ji_e}^e A_j^m + v_{j_e i_e}^e X_{j_e}^m = A_{i_e}^e \tag{3.9}$$

in which $j_e = 1, \dots, N_x$, where N_x is the number of master exchangers, $i_e = 1, \dots, N_{se}$, where N_{se} is the number the secondary exchange species, while the superscript e refers to the exchange reactions. When the activity of an exchange species is defined as

$$\alpha_{i_e} = \gamma_{i_e}^e \beta_{i_e, j_e} \tag{3.10}$$

where α is the activity [-], and $\gamma_{i_e}^e$ is the activity coefficient of the i_eth exchange species on the j_eth exchanger [-]. When assuming equilibrium conditions, the mass action laws can now be written as

$$K_{i_e}^e = \gamma_{i_e}^e \beta_{i_e, j_e} \prod_{j=1}^{N_m} \left(\gamma_j^m c_j^m\right)^{-v_{j_e i_e}^e} \left(\gamma_{j_e}^e \beta_{j_e, j_e}\right)^{-v_{j_e i_e}^e} \tag{3.11}$$

HP-1, the code that combines both solute and water transport using Hydrus-1D and chemical reactions using PHREEQC, implements a coupling method in which the governing equations are solved using a sequential non-iterative approach (SNIA). In this approach the physical part (water and solute movement) is solved first without chemical interactions. Chemical reactions are evaluated subsequently in an uncoupled fashion over space (i.e., for each numerical node separately), but coupled over all components.

This section only contained the most important HP-1 formulas for our situation. The model and its possibilities are explained in much greater detail, and with a larger number of example applications such as for heat transport and various geochemical processes, in the papers of Jacques et al. (2008a, b).

The next two sections will give further explanations of the models used in the PHREEQC part of HP-1 (section 3.2) and will state the chemical and physical conditions under which the simulations will be performed (section 3.3) to model the long-term application of PG in a Dutch Fimic Anthrosol.

3.2 - PHREEQC Model

Two approaches to simulate radium interaction with the soil using PHREEQC will be discussed in this section; both use data obtained from the literature, but in different ways.

The first approach, relative simple and highly empirical, calculates the distribution coefficient for radium, K_d, using log-log relationships with parameters found in or derived from the literature. These parameters involve pH, CEC, OM and cation concentrations. This approach, which is named the "K_d-model", gives a first, quick approach to calculate the K_d when such basic soil characteristics as sand/clay fraction, CEC, pH and concentrations of divalent cations are available.

The second approach, referred to as the "Exchange Coefficient" or "EC-model", is based on direct usage of cation exchange constants, K, measured or calculated for alkaline earth elements and other cations in a Fimic Anthrosol. This model automatically takes into account certain parameters such as the CEC through the amount of available sorption sites, and the effect of pH through competition for sorption sites as protons.

3.2.1 - K_d-model

The classical approach to quantify the strength of ion exchange interactions in a soil for a given set of chemical conditions and soil properties is by using the radium distribution coefficient, K_d [ml.g^{-1}]. The distribution coefficient is an equilibrium property that relates the concentration of a contaminant adsorbed onto the solid phase to its aqueous concentration and can be expressed by the following linear relationship

$$S_e = K_d \times C_e \tag{3.12}$$

where K_d [ml.g^{-1}] is the distribution coefficient for radium, S_e [g.g^{-1}] is the amount of radium adsorbed on the soil, usually in terms of Becquerel (Bq) or picoCurie (pCi) per mass of soil, and C_e [g.ml^{-3}] is the concentration of radium in the soil solution. To eliminate the units of K_d, and to be able to implement them easily into PHREEQC using log-log relationship with certain soil properties, K_d, multiplied with the amount of soil used, divided by the volume of the liquid body.

A large distribution coefficient implies that the contaminant is tightly bound to the soil and as such will have little mobility. A small value implies high mobility of the contaminant. Because of the simplicity of a linear relationship, only one K_d value can be used for an entire model, the linear K_d approach is therefore often used in analytical transport models, but often also numerical codes (e.g. HYDRUS1-D).

The K_d approach can be implemented into HP-1 (or PHREEQC) by first defining a surface reaction as

$$A + Surf = SurfA \tag{3.13}$$

where A is the aqueous species, $Surf$ is the free surface species and $SurfA$ is the sorbed species.

The mass action constant is obtained from

$$K = \frac{[SurfA]}{[Surf][A]}$$

(3.14)

where [] denotes activity. The activity of the surface species is calculated as the mole fraction of a given surface-site type [Parkhurst and Apello, 1999].

$$SurfA = \frac{Amount\ of\ sorbed\ A\ in\ the\ system}{Total\ amount\ of\ sorption\ sites\ in\ the\ system}$$

(3.15)

The amount of sorbed A in the system (1 liter of porous medium) is the sorbed concentration $SurfA$ [moles.l$_s^{-1}$]. Rearranging equation 3.15 gives

$$\frac{(SurfA)}{(TSurf)} = \frac{(Surf)}{(TSurf)}[A]$$

(3.16)

where $(TSurf)$ is the concentration of all sorption sites (moles.l$_s^{-1}$). If $(TSurf)$ is chosen to be very large, $(Surf) \approx (TSurf)$. In the classical approach, where the relationship between the sorbed and aqueous concentration is described with a linear distribution coefficient, the activity of A roughly equals the concentration of A:

$$(SurfA) = K(TSurf)\frac{\gamma_A}{m_A^0}(A)$$

(3.17)

where γ_A is the activity correction coefficient, and m_A^0 is the molal concentration in standard state, with a values of 1 and 1 mol.kg$_w^{-1}$, respectively. Equation 3.17 has in essence the same form as the equation that describes the linear distribution coefficient (equation 3.12), except that the units of the sorbed and aqueous concentrations are different. To convert the unit of $(SurfA)$ [moles.l$_s^{-1}$] to units of S [g.g^{-1}], $(SurfA)$ must be divided by the bulk density ρ_b [g.l^{-3}] and by a conversion factor to change between the defined length units to the unit of the geochemical calculations of the system, $Conv_s$ [l.l$_s^{-1}$], while (A) must be multiplied by the density of water ρ_b [kg$_w$.l$_w^{-1}$] and divided by a conversion factor to change the defined length unit to the unit of the geochemical calculations for the water phase, $Conv_w$ [l$_w$.l$_w^{-1}$].

Equation 3.17 can now be written as

$$(SurfA) = K(TSurf)\frac{\gamma_A}{m_A^0}\frac{1}{\rho_b Conv_s}\frac{Conv_w}{\rho_w}(A)$$

(3.18)

where $(SurfA)$ and (A) have now units [g.g^{-1}] and [g.l$_w^{-3}$], respectively.

The other terms in this equation have the unit [L$_w^3$M$_b^{-1}$] which equals K_d. Assuming γ_A equal to one, m_A^0 equal to 1 mol.kg$_w^{-1}$, ρ_w equal to 1 kg$_w$.l$_w^{-1}$ (default value in HP-1) and $Conv_w$ equal to $Conv_s$, the mass action constant corresponding now to the distribution coefficient K_d is

$$K = \frac{K_d \rho_b}{(TSurf)}$$

(3.19)

The log-transform of this function is written as

$$log(K) = log(K_d) + log\rho_b - log(TSurf)$$

(3.20)

Values for these variables can be implemented directly into the PHREEQC part of HP-1. For an example of the implementation of a K_d-model see the attachments.

The model as described above accounts for a linear distribution coefficient. The approach has several limitations. For example, the constant coefficient only describes the partitioning between the solid and aqueous phases for one set of environmental parameters. In case of time-variable chemical conditions (as encountered in typical soil conditions due to transient flow conditions, amongst others) the constant K_d does not account for many chemical variations, such as changing pH and available adsorption sites, which all influence the mobility of a contaminant in the soil.

In the literature section, some important relationships have been identified between several parameters and the linear distribution coefficient. From the relationships found in literature only a few are applicable in our model and our application and thus will be implemented in our K_d-model [table 3.1].

Table 3.1. Summary of the most applicable and important relationships found in literature that influence the radium distribution coefficient (K_d).

Parameters	Formula	R^2	Notes	Source
[Ca]	log K_d = -8.093*log[Ca]-9.945	0.751	9 soil types	Vandenhove and van Hees, 2007
	log K_d = -0.391*log[Ca]+3.112	0.9655	Sand, average of 3 soils.	Nathwani and Phillips, 1979b
Ionic Strength or [NaCl]	log K_d = -0.6301*log[NaCl] + 0.3265	1	Sand, in presence of Sr, pH 5.5	Powell et al., 2010
pH	log K_d = 0.4154*pH - 0.1522	0.6887	Onto Coir Pith (OM)	Laili et al., (2010)
	log K_d = 0.2101*pH – 0.3843	0.8966	Crushed sandy sedimentary rock	Meier et al., 1994

To implement these relationships properly into PHREEQC/HP-1, the K_d is described as

$$K_d = K_{d0} \times (parameter\ 1)^n \times (parameter\ 2)^m \times (... \tag{3.21}$$

or

$$log K_d = log K_{d0} + n\ log\ (parameter\ 1) + m\ log\ (parameter\ 2) + \cdots \tag{3.22}$$

where K_{d0} is the K_d when the parameters (usually concentrations) are unity, consisting of CEC contributed by OM and soil textural fraction, and n and m are empirical coefficients describing the relationship, the slope, between the log of the parameters, concentration or fraction, and log K_d. The number of parameters can be changed subject to the needs of the model and the availability of data.

Using PHREEQC batch experiments (section 3.4.1), the empirical values which best describe the relationship between the log of parameters and the log distribution coefficient of radium will be chosen. These will then be used for the K_d-model formula (equation 3.22) in long-term HP-1 calculations.

Powell et al. (2010) studied the adsorption of radium to several soil types without the presence of organic matter and under controlled conditions regarding ionic strength. Their data provide an opportunity, when linearly plotted against ionic strength and without strontium present, to obtain an estimated of the contribution of a sandy or clay soil to the K_{d0} value when considering fine- and coarse-textured soils under slightly acidic (pH 5.5) conditions. Applying this procedure gives an initial (K_{d0}) estimate of the radium distribution coefficient of 40.05 ml.g^{-1} for sandy soils and 394.37 ml.g^{-1} for clay soils, when [NaCl] is zero (figure 3.1).
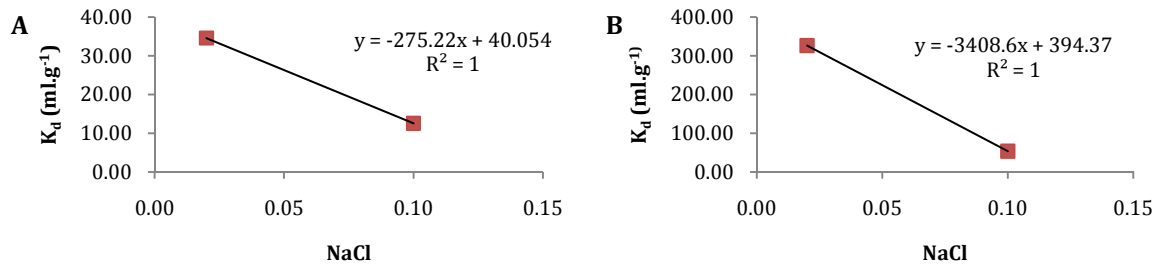
Figure 3.1. Calculation of the starting radium distribution coefficient (K_{d0}),
and the intersect when [NaCl] is zero, for (A) clay and (B) sandy soils by relating K_d to the ionic
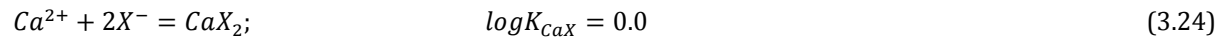*strength of the solution (using data from Powell et al., 2010)*

A second approach to model the mobility of radium in soils with PHREEQC, or the PHREEQC part in HP-1, is by directly using exchange coefficients (EC) obtained from association reactions of the exchanger and ions for the particular soil. As is common by calculating ion exchange reactions in PHREEQC, fully reversible behavior of ion exchange and a limited exchange capacity are assumed. The model is constrained by the fact that all the exchange sites must always be fully occupied by ions [Apello et al. 1997].
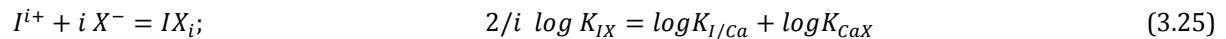
The starting point of the EC-model approach is similar to that of the K_d-model in that an exchange reaction is defined. For example, the exchange reaction of I^{i+} with respect to Ca-X can be written as

$$2/i \ I^{i+} + CaX_2 = 2/i \ IX_i + Ca^{2+}; \qquad logK_{I/Ca} \qquad (3.23)$$

This can also be written in two half reactions:

$$Ca^{2+} + 2X^- = CaX_2; \qquad logK_{CaX} = 0.0 \qquad (3.24)$$

and

$$I^{i+} + i \ X^- = IX_i; \qquad 2/i \ log \ K_{IX} = logK_{I/Ca} + logK_{CaX} \qquad (3.25)$$

where i is the charge of the cation I, Ca^{2+} and I^{i+} are the aqueous species, X^- is the free surface species and CaX_2 or IX_i are the sorbed species. The value of the association constant for IX_i, $log \ K_{IX}$, follows in our case from the known value of $i \ logK_{I/Ca}$, and the reference value of $logK_{CaX} = 0.0$.

The exchange constant K_x depends on temperature and ionic strength, but is also on soil type and the mineral surface area.

The constants found in the databases that are included with PHREEQC need to be replaced by site-specific exchange coefficients for the particular site (in our case a Fimic Anthrosol; see table 3.2) . The soil horizon specific cation-exchange capacity, determined with the bulk density and amount of organic matter, will determine the adsorption limit [Nitzsche and Merkel, 1999].

Table 3.2. Site specific exchange coefficients for a Fimic Anthrosol [de Vries, 2001**]**

Reaction	log K$_{iX}$	Reaction	log K$_{iX}$
$X^- + H^+ = HX$	3,60	$2X^- + Mg^{2+} = MgX_2$	-0,65
$X^- + Na^- = NaX$	-0,65	$2X^- + Ca^{2+} = CaX_2$	0,00
$X^- + K^+ = KX$	1,56	$2X^- + Sr^{2+} = SrX_2$	*0,00*
$X^- + NH4^+ = NH4X$	1,33	$2X^- + Ba^{2+} = BaX_2$	*0,14*
$2X^- + Fe^{2+} = FeX_2$	1,03	$2X^- + Ra^{2+} = RaX_2$	*0,23*
$3X^- + Al^{3+} = AlX_3$	1,08		

3.3 - Problem Definition

The equations used in the HP-1 model have already been described in section 3.1 and 3.2. This section contains general atmospheric and soil data which will be used in HP-1 for a typical agricultural situation in the Netherlands.

3.3.1 - Precipitation Data

Climate charts from the KNMI (the Royal Dutch Meteorological Institute, located in De Bilt, the Netherlands) were used to obtain daily precipitation (figure 3.2), daily average temperature (figure 3.3) and potential evapotranspiration data (figure 3.4) in the Netherlands [KNMI, Daily Data]. Data were obtained for a period of 20 years, from 1990 to 2009, from an automated weather station in the region of Twente, located in the eastern part of the Netherlands, also the location of many Fimic Anthrosols.
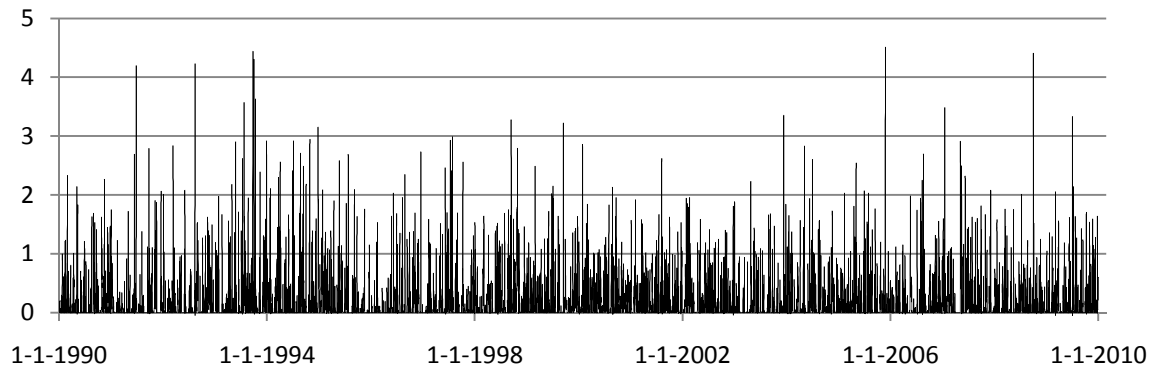

Figure 3.2. Daily precipitation (cm) for Twente, the Netherlands,
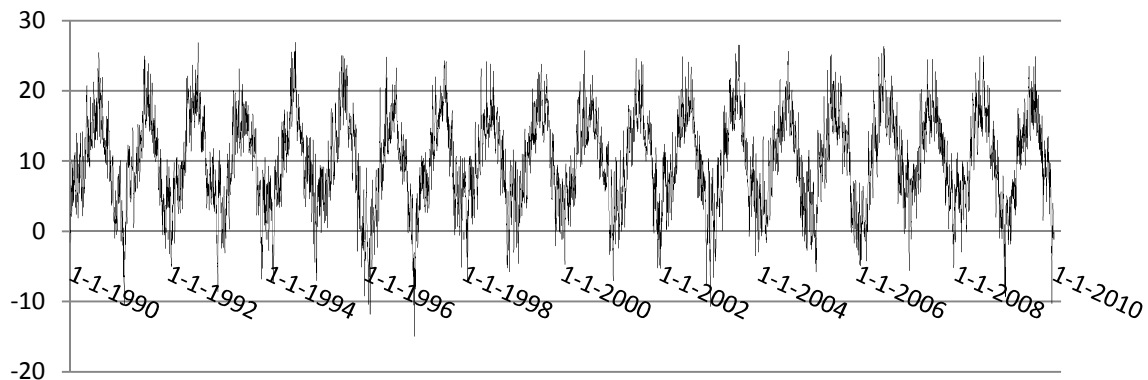measured from January 1st 1990 to December 31st 2009 [KNMI, Daily Data].

Figure 3.3. Daily average temperature (oC) for Twente, the Netherlands,
measured from January 1st 1990 to December 31st 20090 [KNMI, Daily Data].

The daily potential evapotranspiration rates were according to Makkink (figure 3.4). Makkink estimated ET in millimetres per day over 10-day periods for grass lands under cool climatic conditions of the Netherlands as

$$ET = 0.61 \frac{\Delta}{\Delta+\gamma} \frac{R_s}{58.5} - 0.012 \tag{3.26}$$

where R_s is solar radiation, in equivalent millimetres of evaporation per day. Δ is the slope of the saturation vapour pressure curve (in mbar.^{o}C^{-1}), and γ (in mbar.^{o}C^{-1}) is the psychromatic constant. These quantities are calculated as

$$\Delta = 33.8639[0.05904(0.00738T + 0.8072)^7] - 0.0000342 \tag{3.27}$$

$$\gamma = \frac{c_p P}{0.622\lambda} \tag{3.28}$$

$$\lambda = 595 - 0.51T \tag{3.29}$$

$$P = 1013 - 0.1055EL \tag{3.30}$$

where T is temperature (^{o}C), EL is the elevation (in meters), λ (in calories per gram) is latent heat, and P (in mbar) is atmospheric pressure. The specific heat of air c_p (in cal.g^{-1}.^{o}C^{-1}) varies slightly with atmospheric pressure and humidity, ranging from 0.2397 to 0.260, but with a reasonable average value of 0.242 [Xu and Singh 2000].
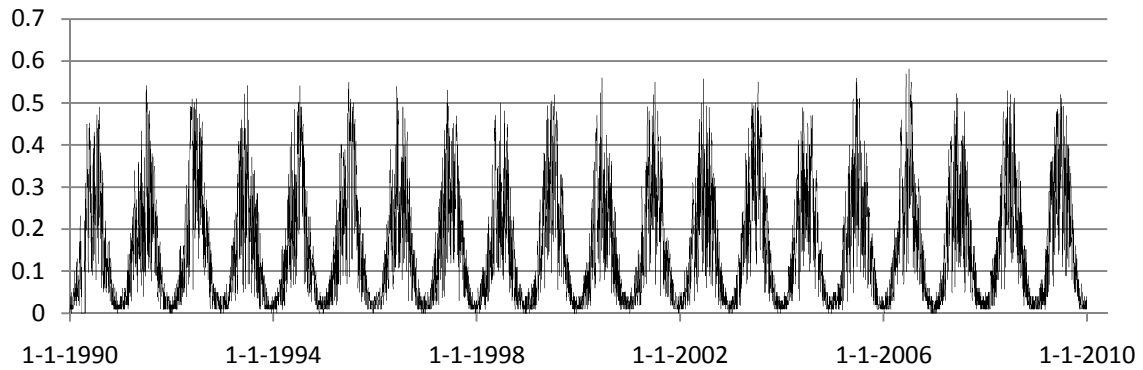
Figure 3.4. Daily potential evapotranspiration (cm) for Twente, the Netherlands, calculated according to Makkink for the period of January 1st 1990 to December 31st 2010.

The precipitation and evaporation data were applied in cycles of 20 years if the modelling time exceeded 20 years, thus repeating the evaporation and precipitation trends as observed at Eibergen, the Netherlands (figure 3.2 and 3.4). In our case no runoff will be modelled, the assumption is made that the soil is able to discharge all the precipitation; excess water is stored as ponded water on the soil surface until allowed to infiltrate when rainfall decreases or becomes zero.

Element concentrations in rainwater were obtained from Stolk (2001) for station 722 located in Eibergen [table 3.3], the Netherlands (figure 3.5). Since PHREEQC requires a non-zero initial concentration for all elements, an arbitrary low value of 10^{-24} mol.l^{-1} was assumed for the radium concentration.

Table 3.3. Average concentration of the main elements
of rainwater in Eibergen, the Netherlands [Stolk, 2001].

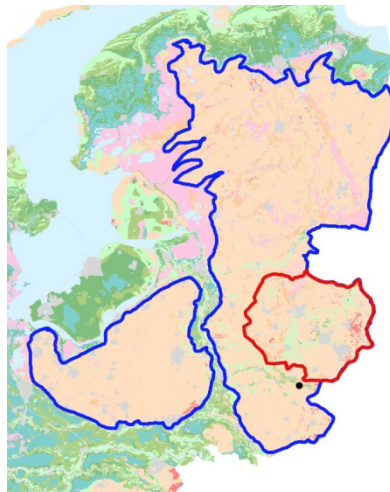| Element	Concentration (mmol.l^{-1})	Element	Concentration (mmol.l^{-1})
N(-3)	9.3×10^{-2}	Na	2.6×10^{-2}
N(+5)	4.4×10^{-2}	K	3.0×10^{-3}
S(6)	2.3×10^{-2}	Mg	4.0×10^{-3}
P	2.0×10^{-4}	Ca	6.0×10^{-3}
F	6.0×10^{-4}	Ra	1.0×10^{-24}
Cl	3.0×10^{-2}	pH	5.74

Figure 3.5. Soilmap of the Netherlands. The red lines indicate the region of Twente where precipitation and evaporation measurements were conducted. The small black dot below that region is Eibergen, the location were the rainwater elemental composition was measured.

In the introduction on Dutch agricultural soils, a few characteristics of the Enkeerdsoil or Fimic Anthrosol were given already. As mentioned earlier, anthropogenic activities over hundreds of years, mainly the agricultural practice of applying manure and peat on sandy soils, resulted in the formation of a thick, about 50 cm or thicker, A-horizon (figure 1.4). In many cases the A- and B-horizons have a relative high amount of loam and organic matter compared to the C-Horizon [table 3.5], which can be found at depths of up to 130 cm [de Vries and Leeters, 2001] [Jongmans and Peek].

The contrast between the A-/B-horizons and the C-horizon is significant. The top layer of a Fimic Anthrosol consists mainly of moderately fine to moderately coarse sand (87%), 160μm - 280μm particle size, combined with silt (10%) and clay (3%) [table 3.4] [Tobor-Kaplon et al., 2005]. By comparison, the deeper C-horizon, generally consists only fine drift sand deposited by glaciers [de Vries and Leeters, 2001]. This difference in soil texture is also reflected by the difference in bulk density, porosity and organic matter content [table 3.5].

Table 3.4. Soil textural composition of the top layer of
a Fimic Anthrosol (0-30cm) [Tobor-Kaplon et al., 2005]

Soil texture type	Volume (%)
sand	87
fine sand	
silt	10
clay	3

Note: the soil is characterized as a fine sand.

Table 3.5. Values of the bulk density, porosity, organic matter content and loam content, and calculated CEC values of the different horizons in a high brown 'Enkeerdsoil' [Locher, W.P. and de Bakker, H., 1990].

Horizon	Depth (cm)	OM (mass %)	Density (kg.dm^{-3})	Porosity (%)	Loam fraction (%)	*CEC in soil (mmol$_c$.kg^{-1})*	*CEC in soil (mmol$_c$.dm^{-3})*
A$_{ap}$	15-20	4.1	1.437	44	22	*27.47*	*39.47*
A$_{a1}$	35-40	3.0	1.483	43	23	*20.10*	*29.81*
A$_{a2}$	52-57	3.3	1.284	50	23	*22.11*	*28.39*
A$_h$	70-75	3.4	1.284	51	23	*22.78*	*29.25*
B$_w$	97-101	3.4	1.290	50	27	*22.78*	*29.39*
B$_c$	111-116	1.1	1.503	43	29	*7.37*	*11.08*
C	130-135	0.2	1.629	39	6	*1.34*	*2.18*

The CEC of the soil, in mmol$_c$.kg^{-1}, has been calculated by making the assumption that 1 mass percent of OM in a Fimic Anthrosol, equals 6.7 mmol$_c$.kg^{-1} [de Vries and Leeters, 2001]. Although the CEC value can change per layer for the EC-model it does not for the K_d-model due to the fact that the concentration of all sorption sites ($TSurf$) is increased to approach ($Surf$) (section 3.2.1). An estimate of that value was given at the end of section 3.2.1.

Using bulk density [table 3.5], the soil textural fractions for a Fimic Anthrosol [table 3.4] for horizon A_{ap} to B_c, and sandy soil characteristics for horizon C, hydraulic properties as described with the van Genuchten (1980) equations can be estimated [table 3.6] by using the Rosetta program. Rosetta is included in HP-1 and was developed to predict van Genuchten (1980) water retention parameters and the saturated hydraulic conductivity (K_s) from soil textural class information, the soil textural distribution and bulk density [Schaap et al. 2001]. Since Rosetta does not account for a difference in the coarse and fine sand fractions, nor the amount of organic matter, the sand fraction for horizon A_{ap} to B_c was decreased to 65% while the silt fraction was increased to 32%, to more closely match expected hydraulic properties of fine sandy soil with high organic matter content [Bear, 1972].

Table 3.6. Estimated soil hydraulic properties [van Genuchten, 1980] for a Fimic Anthrosol calculated by using Rosetta [Schaap et al. 2001].

Horizon	Depth (cm)	Density (g.cm^{-3})	Θ_r	Θ_s	α [cm^{-1}]	n	K_s (cm.day^{-1})
A_{ap}	0-28	1.437	0.0309	0.3694	0.0356	1.4487	73.46
A_{a1}	28-46	1.483	0.0305	0.3598	0.038	1.4459	62.95
A_{a2}	46-64	1.284	0.0323	0.402	0.0295	1.4403	121.65
A_h	64-86	1.284	0.0323	0.402	0.0295	1.4403	121.65
B_w	86-106	1.290	0.0323	0.4007	0.0297	1.4409	119.29
B_c	106-123	1.503	0.0303	0.3557	0.0391	1.4435	58.84
C	123-150	1.629	0.0432	0.3476	0.0398	2.3056	188.2

Note: Θ_r and Θ_s are the residual and saturated water contents, respectively; α and n are shape parameters; and K_s is the saturated hydraulic conductivity.

The van Genuchten (1980) formula calculates the soil hydraulic parameters for the vadose zone. The assumption is made that the groundwater level is well below the C-horizon (i.e., below 1.50 meter). Atmospheric conditions (precipitation and potential evapotranspiration rates) were assumed for the upper boundary of the soil profile, while free drainage conditions were implemented at the lower boundary.

Before exposure to precipitation and evaporation, the entire column was brought into equilibrium with median values of pH and concentrations of the major elements in the soil solution, as observed for the topsoil (0-15 cm depth) of a Fimic Anthrosol [table 3.7].

Table 3.7. pH and the concentrations of major elements in the soil solution
of the topsoil (0-15 cm depth) for Fimic Anthrosols [de Vries and Leeters, 2001].

Element	Concentration ($mol_c.m^{-3}$)	Concentration ($mmol. dm^{-3}$)
pH	*3.4*	*3.4*
N(-III)	*0.21*	*2.10×10^{-1}*
Ca	*0.53*	*2.65×10^{-1}*
N(V)	*0.64*	*6.40×10^{-1}*
S(VI)	*1.0*	*5.00×10^{-1}*
K	*0.21*	*2.10×10^{-1}*

Before the long-term simulations with the PG applications were executed, a 5-year flow simulation was performed without phosphogypsum applications to establish a chemical equilibrium situation between the topsoil and the percolating rainwater.

During the HP-1 simulation a total of 15 solutes were transported: Total_H, Total_O, substituting for general water transport, N(3), N(5), S, P, F, Na, K, Mg, Ca, Cl, Ra, Al and Br. The solution was balanced for charge by Al, since no concentrations for this element in the precipitation was known. This means that the half-reaction of Al^{3+} with Y^-, the definition for a free adsorption site, must also be excluded from the half exchange reactions in the EC-model. Br was added as a tracer in similar concentrations as radium since it did not interact with the system and remained present a Br^- ion.

The US-EPA 1992 requirement for the usage of phosphogypsum restricts the use of phosphogypsum in agricultural applications to a maximum average radiation level of 0.370 $Bq.g^{-1}$, or $1.0x10^{-11}$ $g.g^{-1}$ ^{226}Ra [Alcordo et al., 1999]. This equals 9.99 $pCi.g^{-1}$ radiation emitted or $4.57x10^{-14}$ $mol.g^{-1}$ of radium in phosphogypsum.

Application rates of PG above 10 $Mg.ha^{-1}$ to soils had an adverse effect on wheat biomass production relative to other gypsum amendments, mainly because of the effects of fluoride on soil silicate that started to release Al^{3+}. Optimal application rates in which the germination rate of plants was higher than in the control experiment, were 1.4 and 2.8 $Mg.ha^{-1}$ [Mariscal-Sancho et al., 2009]. These rates will be used in our models, resulting in a PG ($CaSO_4$) application rate of 140-280 $g.m^{-2}$ or 1.03-2.06 $mol.m^{-2}$ [Paul et al., 1984].

From a modeling point of view, two ways of applying radium are possible: via precipitation as was done by Jacques et al. 2008b for uranium in the application of a fertilizer to an agricultural soil (basically assuming that all of the fertilizer dissolved immediately in the soil), or via incorporation of radium in the soil and PG as the solid phase $RaSO_4$. Since HP-1 does not support the repeated application of a solid to the soil, the first option, addition of radium via precipitation, will be used to introduce radium to the model. The application of phosphogypsum through precipitation is assumed not to change any of the physical properties of the soil column.

For modelling purposes, a 'worst-case-scenario' was established where the maximum allowed amount of radium is introduced to the soil. This means applying 280 $g.m^{-2}$ of PG ($CaSO_4$), with an average radiation level of 0.370 $Bq.g^{-1}$, to the soil. This results in a radium input of 103.6 $Bq.m^{-2}$, which is $2.8x10^{-9}$ $g.m^{-2}$ or $1.24x10^{-11}$ $mol.m^{-2}$ ^{226}Ra.

The phosphogypsum in the form of $CaSO_4$, together with the incorporated radium, is assumed to be applied every year on the 1st of May, during the plowing season, in 1 cm, or 10 liter of water per square meter with the same composition as rainwater [table 3.8]. The phosphogypsum is assumed to be completely dissolved in rainwater; this neglects any possible kinetics in the dissolution process of the grains and results in a concentration of $2.06x10^{-1}$ $mol.l^{-1}$ of $CaSO_4$. We do assume however full release of all radium, which would then be added in 1 cm of precipitation with a concentration of $1.24x10^{-12}$ $mol.l^{-1}$ [Ra].

Table 3.8. Composition of the main elements in precipitation in Eibergen, [Stolk, 2001], when combined to 10 liter of a PG solution.

Element	Concentration (mol.l^{-1})	Element	Concentration (mol.l^{-1})
N(-3)	9.3 x10^{-5}	Na	2.6 x10^{-5}
N(+5)	4.4 x10^{-5}	K	3.0 x10^{-6}
S(6)	*2.06* x10^{-1}	Mg	4.0 x10^{-6}
P	2.0 x10^{-7}	*Ca*	*2.06* x10^{--1}
F	6.0 x10^{-7}	*Ra*	*1.24x10^{-12}*
Cl	3.0 x10^{-5}	pH	5.74

3.4 - Additional Experiments

3.4.1 - PHREEQC: batch experiments

Prior to the calculations with HP-1, PHREEQC batch experiments were conducted to compare the effect of using cation-exchange coefficients from de Vries (2001) and the K_d relationships with important parameters as derived previously using literature data. All PHREEQC batch experiments were modeled as accurately as possible by following known experimental conditions, such as cation concentrations, or estimating those conditions within reasonable limits using values observed in a typical soil solution.

A few general assumptions were made for the EC-model batch experiments unless stated differently. The amount of adsorption sites in the soil was 39.47×10^{-3} $mol_c.dm^{-3}$, based on the top layer of a Fimic Anthrosol [Locher and de Bakker, 1990]. Also a bulk density of 1.437 $kg.dm^{-3}$ was used, a radium concentration of 5.00×10^{-09} $mol.l^{-1}$, while the pH of the soil solution was 5.5.

For the K_d-model, data from four studies were chosen to describe the relationship between the distribution coefficient and parameters, [Ca], [Na] and pH. These parameters were first separately modeled in the PHREEQC batch experiments to compare them with the studies from which they were obtained. Those relationships are described as follows

$$logK_d = log40.05 - 0.391\,log[Ca] \tag{3.31}$$

$$logK_d = log40.05 + 0.2101\,pH \tag{3.32}$$

$$logK_d = log40.05 + 0.4145\,pH \tag{3.33}$$

$$logK_d = log40.05 - 0.6301\,log[Na] \tag{3.34}$$

where K_{d0} in equation 3.31 to 3.34 is replaced by the K_{d0} estimate from Powell et al. (2010), and the values for empirical coefficients for [pH], [NaCl] and [Ca] are replaced by the values from Meier et al., (1994), Laili et al. (2010), Powell et al., (2010) and the average of three soils from Nathwani and Phillips, (1979), respectively. Vandenhove et al. (2007) was not considered in these experiments since the slope, the empirical constant, was an average of 9 very different soils, which would not give a good approach to a sandy soil.

After these relationships were studied separately, they were combined into a larger formula, describing the change in K_d for radium depending on 3 parameters as follows

$$logK_d = log40.05 - 0.391log[Ca] + 0.2101pH/0.4145pH - 0.6301[Na] \tag{3.35}$$

This equation was also studied with the PHREEQC batch experiments, thus allowing us to compare the performance of this formula to data from all three studies.

As suggested in the literature section, next to calculations with HP-1, equilibrium speciation calculations for radium should be performed using PHREEQC and the thermodynamic data of Langmuir and Ries (1985) [table 3.9] to obtain better insight in model results and radium behavior. This because the mobility of radium in the soil is controlled through Ra^{2+} ion exchange. If radium is not present as a cation, little to no adsorption will take place.

Table 3.9. Formation constants (log K_{as}) of radium complexes or solubility products (log K_{sp}) of radium solids [Langmuir and Riese, 1985]

Formation Reactions	log K_{as} or log K_{sp}
1) $Ra^{2+} + OH^- = RaOH^+$	0.50
2) $Ra^{2+} + Cl^- = RaCl^+$	-0.10
3) $Ra^{2+} + CO_3^{2-} = RaCO_3$ (aq)	2.50
4) $RaCO_3$ (s) $= Ra^{2+} + CO_3^{2-}$	-8.30
5) $Ra^{2+} + SO_4^{2-} = RaSO_4$ (aq)	2.75
6) $RaSO_4$ (s) $= Ra^{2+} + SO_4^{2-}$	-10.26

The speciation of radium was calculated for conditions similar to those expected in the field, using ion concentrations for standard precipitation [table 3.3], precipitation with the addition of PG in the form of CaSO4, 1.85 mmol.l^{-1} which is 0.9% of the total amount (206 mmol.l^{-1}) added to the soil and Ra, $1.24x10^{-12}$ mol.l^{-1} [table 3.8], precipitation with only Ra, $1.24x10^{-12}$ mol.l^{-1} added and precipitation in addition to PG but with an elevated radium concentration, $1.24x10^{-9}$ mol.l^{-1}. The latter would be the case of the concentration of radium in PG was not 0.370 Bq.g^{-1} but 370 Bq.g^{-1}, a concentration level more often observed in PG when applied in field experiments [Reguigui et al, 2005; Azouazi et al, 2001].

CHAPTER 4 - Results and Discussion

4.1 - PHREEQC Model Batch Experiments

To test both PHREEQC models, batch modeling experiments with settings similar to the lab/field experiments described in the studies, were conducted and results are described here. If experimental settings differed from what was stated in the methods section, this will be noted with the results. Results from the PHREEQC batch experiments using the EC- and K_d-modeling approaches will be compared to literature data and interpreted as such.

4.1.1 - EC-model

Calcium

Two studies, Vandenhove and van Hees (2007), and Nathwani and Phillips (1979b) described relationships between Ca and the K_d of radium which are best applicable to our situation.

With data from the first study [Vandenhove and van Hees, 2007], equation 3.31 was established

$$logK_d = -8.093 \times log[Ca] - 9.945; \qquad (R^2 = 0.751) \qquad (3.32)$$

Reported concentrations of competing ions in this study were 1.50x10^{-3} mol.l^{-1}, 5.00x10^{-4} mol.l^{-1} for Mg^{2+} and K$^+$, respectively. The pH of the soil solution was 5.5 and the Ra concentration 5.00x10^{-9} mol.l^{-1}.
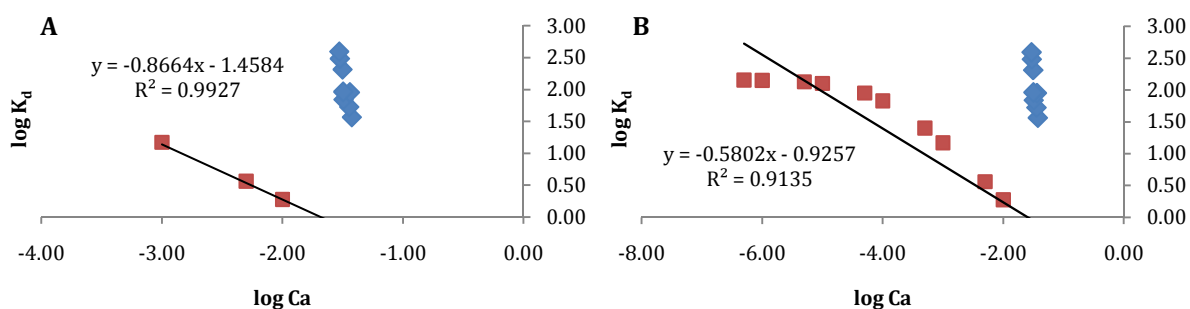
Figure 4.1. Comparison of PHREEQC EC-model results (red) with data from Vandenhove and van Hees, 2007 *(blue). (A) Results obtained using cationic concentrations as given by the paper; and (B) same results but now with a linear trendline drawn through the results over a wider [Ca] range (5.0x10^{-7} to 5.0x10^{-1} mol.l^{-1}).*

The slope obtained from the trendline through the PHREEQC data, with calcium concentration ranges close to the concentration range used by Vandenhove (2007), between 0.001 and 0.1 mol.l^{-1}, was -0.8664 (figure 4.1). This is ten times smaller than the slope obtained from the literature data (-8.093). This large difference may be explained by the fact that Vandenhove (2007) used 9 types of soils, all different in response to changing calcium concentration (with R^2=0.13 for the trendline through the data points). The average response could be far different from what would be expected for a Fimic Anthrosol.

A sensitivity analysis was carried out for the experimental conditions such as cation concentrations (Mg^{2+} and K^+), pH (figure 4.2a), radium concentration and cation exchange capacity (figure 4.2b). Change in cation concentrations, ranging from 1.50×10^{-1} to 1.50×10^{-5} mol.l^{-1} and 5.00×10^{-2} to 5.00×10^{-6} mol.l^{-1} for Mg^{2+} and K^+, respectively, had no significant effect on the K_d of radium while changes in pH and amount of sorption places greatly affected the K_d. If pH decreases (figure 4.2a), competition of calcium ions over adsorption places will be less likely to influence the K_d of radium since most of the adsorption places are occupied by H^+. The more adsorption places are available (figure 4.2b), the stronger radium will bind, resulting in a higher K_d, but no change in sensitivity to changing calcium concentrations.
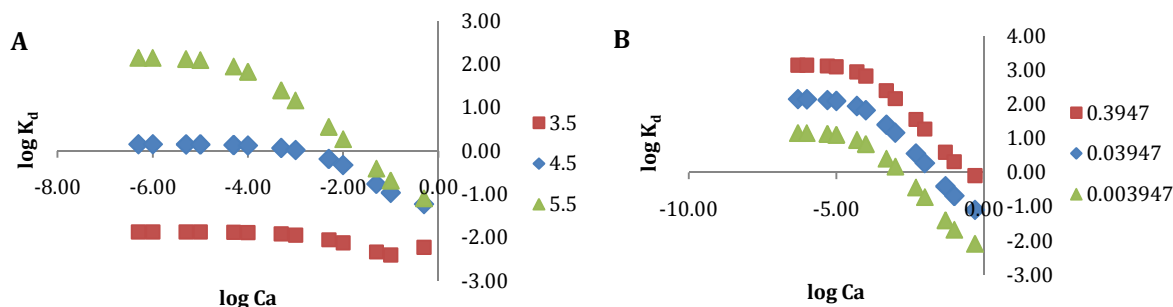
Figure 4.2. Sensitivity analysis for the influence of changing (A) pH; and (B) cation exchange capacity on the K_d of radium under varying calcium concentrations.

The second study of calcium influence on the K_d, Nathwani and Phillips, (1979b), did not, part for a pH of 5.0, report any concentrations for other cations in the soil solution, hence none were added to the PHREEQC batch model. The following formulas were obtained from their study

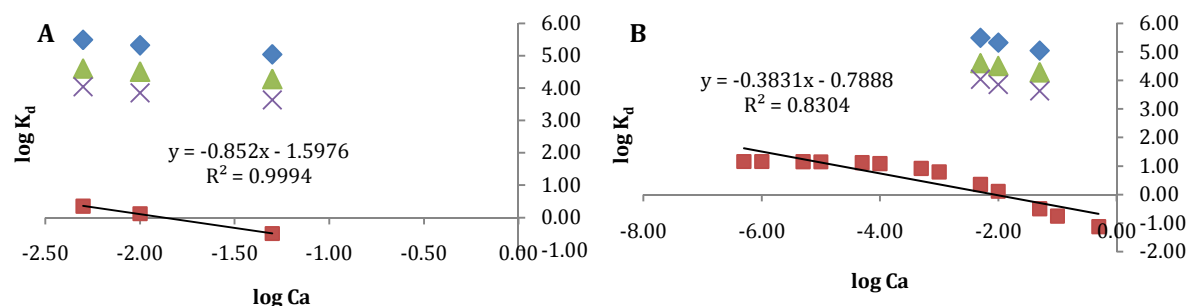|			
Wendover (Silty Clay)	$logK_d = -0.4415 \times log[Ca] + 4.4606;$	$(R^2 = 0.993)$	(4.1)
Grimsby (Silty Loam)	$logK_d = -0.3234 \times log[Ca] + 3.8510;$	$(R^2 = 1)$	(4.2)
St.Thomas (Sandy)	$logK_d = -0.3910 \times log[Ca] + 3.1120;$	$(R^2 = 0.9655)$	(4.3)

Figure 4.3. Comparison of PHREEQC EC-model results (red) with data from Nathwani and Phillips (1979b), by the three soils reported in the study, Wendover (blue), Grimsby (green) and St. Thomas (purple). (A) Results obtained from the PHREEQC model plotted over a [Ca] range similar to Nathwani and Phillips, (1979b), 5.0×10^{-3} to 5.0×10^{-2} mol.l^{-1}; and (B) Same results but now with a linear trendline drawn through results over a wider [Ca] range, 5.0×10^{-7} to 5.0×10^{-1} mol.l^{-1}.

53

The slope obtained from the PHREEQC modeling, using calcium concentrations similar to Nathwani and Phillips (1979b), 0.00 to 0.05 M, was about twice as high as the slope obtained from their data (figure 4.3a). If, however, the slope is taken over the full range of points modeled by PHREEQC (figure 4.3b), the slope decreases and got in range of slope as found in the study. Results from PHREEQC closest match the results from St. Thomas, a sandy soil. This, since Enkeerdsoils mainly consist of sand, was to be expected.

The reason that Nathwani and Phillips (1979b) has significantly higher K_d values for all three soils, might have to do with a difference in cation exchange capacities of the soils compared to what was used in the PHREEQC model. Increasing of the cation exchange capacity of the soil will increase the height of the graph in the simulations, as seen earlier in figure 4.2b, so it can match the observed data from the study by Nathwani and Phillips (1979b) more closely.

Ionic Strength [NaCl]

The paper of Powel et al. (2010) best described the relationship between the Ionic Strength (NaCl concentration) and the K_d of radium for a sandy soil and both were linked by the following formula

$$log K_d = -0.6301 \times log[NaCl] + 0.3265 \tag{2.7}$$

The pH of the solution was about 5.5 and strontium was present in a 6 to 7 magnitude larger than the radium concentration. The radium concentration was estimated at 5.00×10^{-9} mol.l^{-1}, hence strontium was estimated to be present in a concentration of about 5.00×10^{-3} mol.l^{-1}. The solution was allowed to equilibrate with the sandy soil for 48 hour; however no exact ion composition is known after equilibrium with the sandy soil hence no other cations were taken into account during modeling.
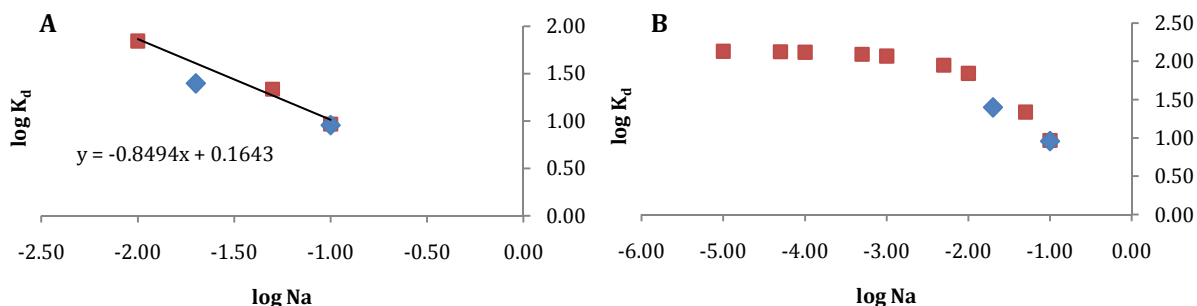

Figure 4.4. (A) Comparison between PHREEQC "EC-model" results (red) and data from Powell et al. (2010) (blue) at similar [Na] concentrations; and (B) results from the same PHREEQC model only over a larger concentration range.

The slope obtained from the PHREEQC batch modeling for the sodium concentrations similar to Powell et al. (2010), 0.002 to 0.1 M, -0.8494, closely matched the slope obtained from their data (figure 4.4a), -0.6301. If the data of PHREEQC is observed over wider [Na] ranges (figure 4.4b), the two data points fitted well in the general trend. The slope of this trend seemed to decline at lower [Na] concentrations, concentrations below 0.01 mol.l^{-1} and the K_d did not change much anymore. This is possibly caused by a constant strontium concentration which, at lower concentrations of sodium, dominates the adsorption sites and becomes the limiting factor in radium adsorption. Caution is advised using this relationship between K_d and Ionic Strength in the "K_d-model", it should be noted that it is based off on a comparison with only two data points.

With data from Laili et al. (2010) a relationship between pH and the K_d for radium, when absorbing to Coir Pith (OM substitute) under influence of Humic Acid, could be formulated as follows

$$logK_d = 0.4145 \times pH - 0.1522; \qquad (R^2 = 0.6887) \qquad\qquad (2.9)$$

The radium concentration reported in this study and used in the PHREEQC batch experiments was an estimate of 1.12×10^{-9} mol.l^{-1}. Furthermore, only an addition of [Na], 2.0×10^{-3} mol.l-1, was reported and used in the simulation.
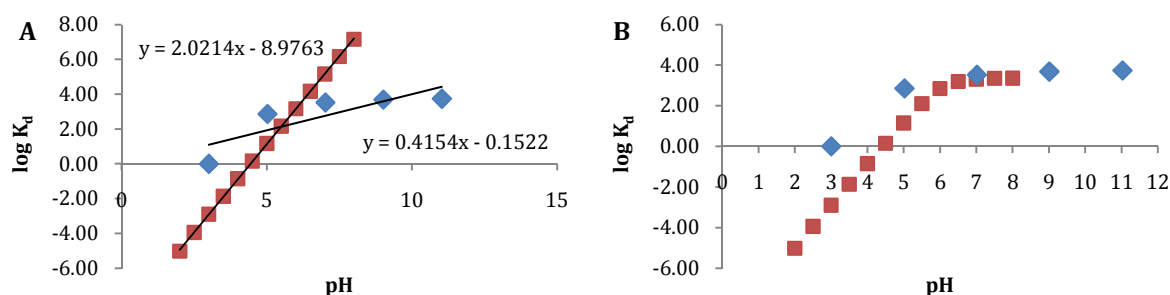
Figure 4.5. Comparison of PHREEQC EC-model results (red) with data from Laili et al. (2010) (blue). (A) Results obtained from model with cationic concentrations as given by the paper; (B) results from the same PHREEQC model with an additional [Ca] of 1.0×10^{-2} mol.l^{-1}.

Comparing the slopes of the linear trendlines drawn through the data points obtained from literature and PHREEQC simulation, a significant difference is noted, a slope of 2.0214 to 0.4154 for the PHREEQC simulation and the results of Laili et al. (2010), respectively (figure 4.5 a). Therefore, using 0.4154 as empirical constant in the log K_d formula for the K_d-model, as stated in the literature section is not advisable, especially when taking in consideration the non-linear behavior of the log K_d curve with regard to pH around comparable ranges.

When calcium in a concentration of 1.0×10^{-02} mol.l^{-1} is added to the PHREEQC simulation, the shape of the graph suddenly resembles much more the data as obtained from Laili et al. (2010) (figure 4.5b). The close resemblance of the results from Laili et al. (2010) and the PHREEQC batch experiments, especially after addition of [Ca], and the fact that the K_d of radium was measured only on organic matter, gives rise to the thought that radium in the soil matrix, mainly adsorbs to the organic matter and not so much the mineralogical interface of the soil.

Data from literature and PHREEQC experiments show that below pH 5, pH 6 for the EC-model, K_d values drop quickly (figure 4.5). In pH ranges observed for soil and precipitation data in the Netherlands, ranging from 3.0 to 5.8, this could lead to a high mobility of radium.

With data from Meier et al., (1994) for crushed sandy sedimentary rock, a similar to Laili et al. (2010) relationship between pH and the K_d for radium could be described

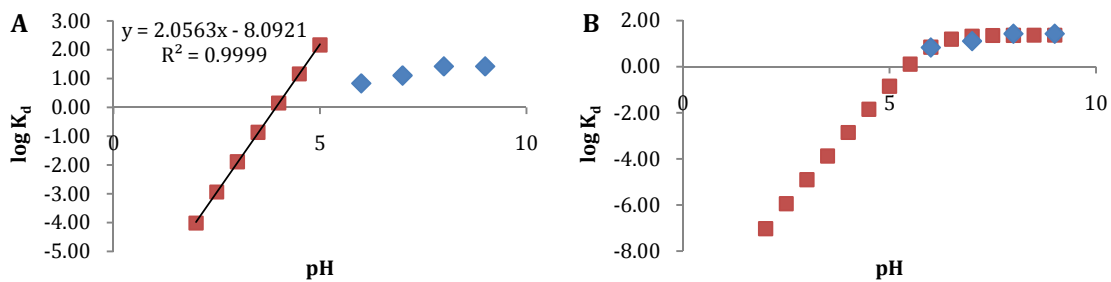$$logK_d = 0.2101 \times pH - 0.3843; \qquad (R^2 = 0.8966) \qquad\qquad (2.8)$$

Figure 4.6. Comparison of PHREEQC "EC-model" results (red) with data from Meier et al., (1994) (blue). (A) results obtained from the PHREEQC model with cationic concentrations as given by the paper; (B) results from the same model with an additional calcium concentration of 1.0×10^{-02} mol.l^{-1} and a CEC two orders of magnitude lower.

Comparing slopes of the linear trendlines drawn through the data points obtained from literature and PHREEQC simulations, shows also in this case a significant difference, 2.05673 to 0.2101 from the PHREEQC data output and the results of Meier et al., (1994), respectively (figure 4.6a).

However, when calcium is added in a concentration of 1.0×10^{-2} mol.l^{-1} and the CEC is decreased by two orders of magnitude, from 39.47×10^{-3} to 39.47×10^{-5} mmol.dm^{-3}, data output from the PHREEQC experiments closely matched the data found in literature (figure 4.6b). This can be explained by the fact that Meier et al., (1994) used crushed sedimentary rock as medium for radium to adsorb on. Naturally, this kind of sandy rock contains little to no organic matter, hence the adsorption of radium is not expected to be high. This observation only strengthens the thought that radium adsorbs mainly to the organic matter fraction of the soil and not so much the mineral phase.

As mentioned in methods, for the K_d-model in the PHREEQC batch experiments, the four defined relationships between the log K_d and the log of the parameters used as empirical constants, were first studied separately from each other and compared to data from their literature study.
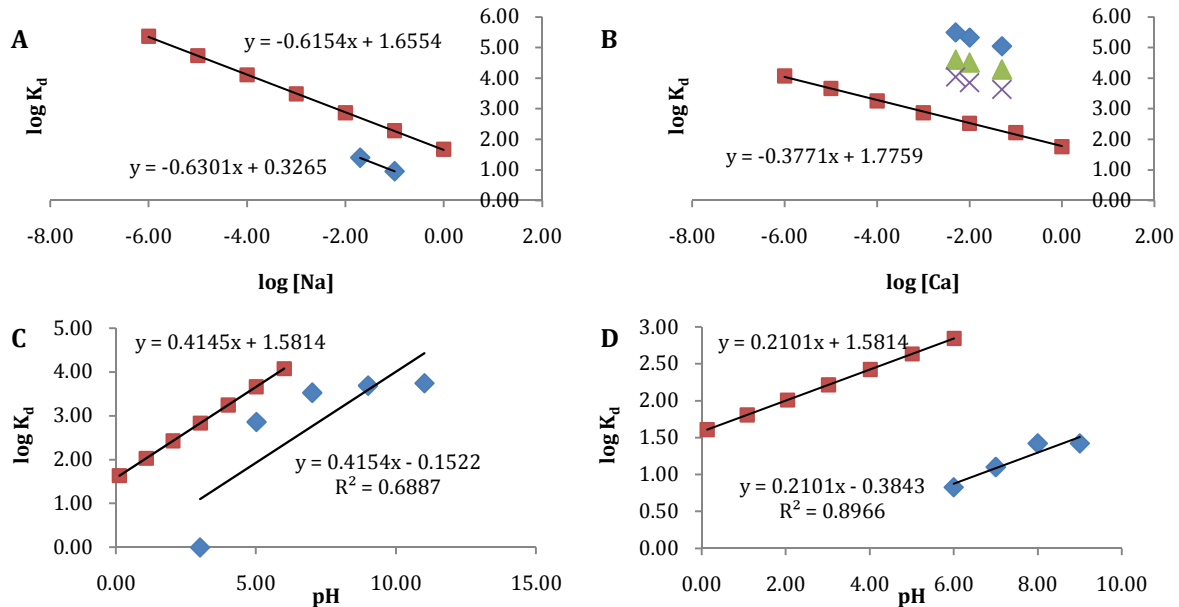

Figure 4.7. Comparison of PHREEQC "K_d-model" output (red) from equation 3.31, 3.32, 3.33 and 3.34 with (A) data from Powel et al. (2010) (blue); (B) data from Nathwani and Phillips (1979b) (blue, green and purple; (C) data from Meier et al., (1994) (blue); and (D) and data from Laili et al. (2010) (blue), respectively.

Generally, the slopes of the trend line through PHREEQC data match well with the slope of the trend line through literature data (figure 4.7 a-d). This is expected since the slope of the trend line through the literature data is used as empirical constant for the PHREEQC batch experiments.

However, the intercept of the trend lines through PHREEQC data differed slightly when compared to their studies. This can be explained by the fact that the amount of CEC used in the PHREEQC experiments was an estimate from the study of Powell et al. (2010) and represents a soil under pH 5.5, with no organic matter and zero ionic strength. The effect of CEC on the K_d was also observed in an earlier section (PHREEQC batch experiments with the EC-model).

Two log K_d vs. pH relationships were studied, one from Meier et al., (1994) (figure 4.7c) and one from Laili et al. (2010) (figure 4.7d). Because of the linearity of data points from Meier et al., (1994) in comparison to data from Laili et al. (2010), is favored when choosing an empirical constant to be used in the HP-1 models. However, Meier et al., (1994) did not study the behavior of the log K_d for pH values below 6 and if done so, it might have shown the same, non-linear behavior as for the study of Laili et al. (2010) (figure 4.7 d).

Having studied all three parameters separately, the following formula was established to describe the change in distribution coefficient for radium under influence of three different parameters

$$logK_d = log40.05 - 0.391log[Ca] + 0.2101pH - 0.6301[Na] \tag{4.4}$$

which can also be written as

$$K_d = 40.05 \times [Ca]^{-0.391} \times pH^{0.2101} \times [Na]^{-0.6301} \tag{4.5}$$

using empirical constants obtained from Nathwani and Phillips, (1979), Meier et al., (1994), and Powell et al., (2010) for [Ca], pH and [Na] respectively.
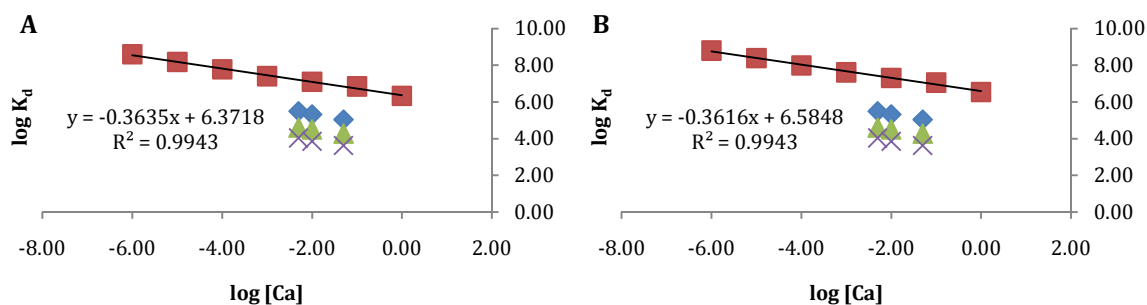
Figure 4.8. Comparison of PHREEQC "K_d-model" output (red) from equation 4.4 with data from Nathwani and Phillips (1979b) (blue, green and purple) for (A) pH 3.5 and (B) pH 4.5.

The results from modeling with equation 4.4 was compared with the literature data from Nathwani and Phillips (1979b) (figure 4.8a). Values for [Na] and pH are estimated at 1×10^{-6} mol.l^{-1} and 3.5 respectively, concentrations commonly observed in our study. With the addition of these parameters, an increase in K_d can be observed. Where the intercept (log K_{d0}) was 1.7759 at first, it has now become 6.3718, increasing about 5 orders of magnitude. The slope of the line has not changed much, -0.3771 to -0.3635 using equation 3.31 compared to using equation 4.4, respectively, meaning that the response of the distribution coefficient to changes in calcium concentrations remains fairly the same. Decreasing the H$^+$ concentration one order of magnitude, results in an increase of 0.2 for the log K_{d0} of radium and a slight decrease in slope (figure 4.8b).

The same, relative large, increase in K_d values is observed when comparing PHREEQC results with data from Powell et al., (2010) and Meier et al. (1994) (figure 4.9). Since this combined formula causes the distribution coefficient to change so drastically with only slight variations in concentrations, it would not be advised to use this whole formula in HP-1 modeling in one simulation, but to study the effects of the influence of the different parameters separately.
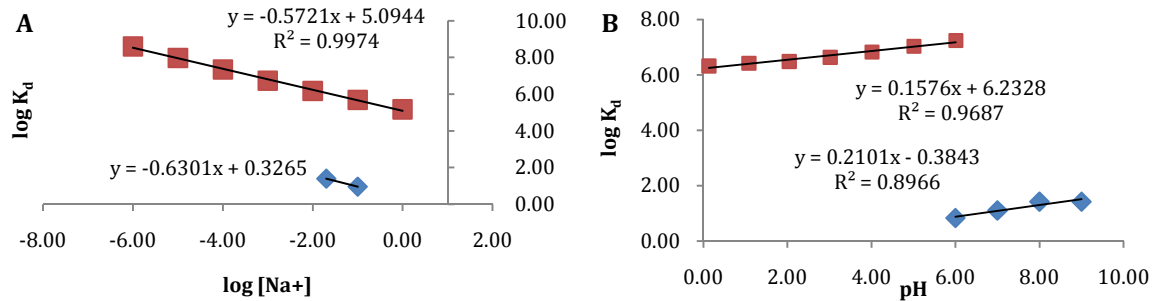

Figure 4.9. Comparison of PHREEQC "K_d-model" output (red) from equation 4.4 with data from (A) Powell et al., (2010) (blue) and (B) Meier et al., (1994).

The speciation of radium was calculated for conditions similar to those expected in the field, using ion concentrations for standard precipitation, precipitation with the addition of PG and radium, precipitation with only an addition of radium and precipitation in addition of PG but with an elevated radium concentration which would be often observed in the field [table 4.1].

Table 4.1. Radium speciation under varying conditions.

Radium speciation (mol.l^{-1})	Standard Precipitation	Prec. + PG + Ra	Prec. – PG + Ra	Prec. + PG + extra (370 Bq.g^{-1}) Ra
Ra^{+2}	9.892e-25	8.545e-13	1.227e-12	8.545e-10
RaSO$_4$ (aq)	1.077e-26	3.855e-13	1.336e-14	3.855e-10
RaCl$^+$	2.179e-29	1.445e-17	2.701e-17	1.445e-14
RaOH$^+$	1.620e-32	1.149e-20	2.009e-20	1.149e-17
Radium speciation (%)				
Ra^{+2}	98.92	68.91	98.92	68.91
RaSO$_4$ (aq)	1.08	31.09	1.08	31.09
RaCl$^+$	0.00	0.00	0.00	0.00
RaOH$^+$	0.00	0.00	0.00	0.00

As observed in table 4.1, radium speciation is mainly dominated by Ra^{2+} and RaSO$_4$ (aq). Under normal precipitation conditions, with a concentration of sulphate of 2.3x10^{-5} mol.l^{-1}, the radium speciation consists for 98.92 and 1.08 % out of Ra^{2+} and RaSO$_4$ (aq), respectively, while under precipitation conditions with the addition of 2.30 mmol.l^{-1} PG (CaSO$_4$), the fully dissolved amount of 280 g.m^{-2} PG, the speciation changed to 68.91 and 31.09 % out of Ra^{2+} and RaSO$_4$ (aq).

The addition of extra radium to the system does not change radium speciation, as can be observed comparing the third and last column of table 4.1, which means that the concentration of sulphate must control the radium speciation in the solution. PHREEQC was used to calculate radium speciation when sulphate concentrations varied from 2.3x10^{-6} to 2.3x10^1 mol.l^{-1} (figure 4.10). These additions were made to the ionic concentrations in precipitation as observed by Stolk (2001).
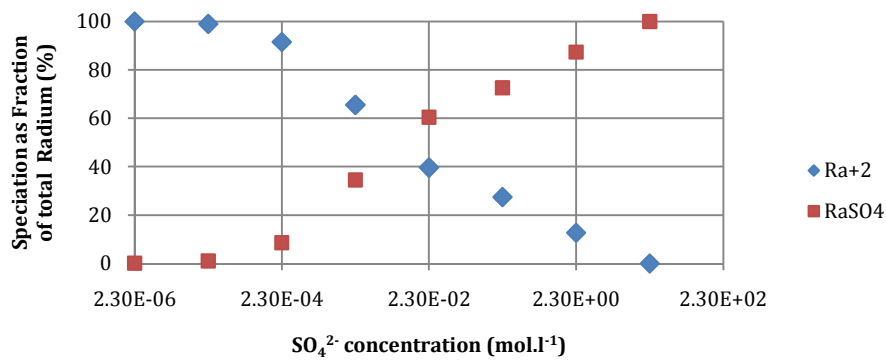
*Figure 4.10. PHREEQC speciation calculations for radium under varying sulphate (SO$_4^{2-}$) concentrations.*

PHREEQC speciation calculations show that the radium speciation is highly dependent on sulphate (SO$_4^{2-}$) concentrations (figure 4.10) for radium and sulphate concentrations of 1.24×10^{-12} mol.l^{-1} and ranging from 2.3×10^{-5} to 1.85×10^{-3} mol.l^{-1}, respectively which are used in our model. This means when PG is instantly added to the soil column through precipitation, the high sulphate concentrations could cause quick migration of radium through the soil column and no adsorption to the ion exchange sites on the organic matter, due to the speciation of radium as the relatively inert RaSO$_4$ (aq).

4.2 - HP-1: Agricultural Application PG

4.2.1 - Soil Hydraulics

The hydraulic parameters, obtained by using pedotransfer fuctions and granulometry of a Fimic Anthrosol in Rosetta, were the same for all situations regardless of the PHREEQC model used. Several the basic hydraulic properties of the soil were obtained and plotted against each other to get characteristic hydrological profiles (figure 4.11).
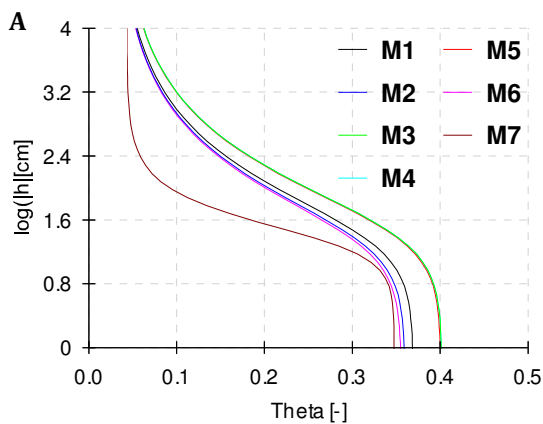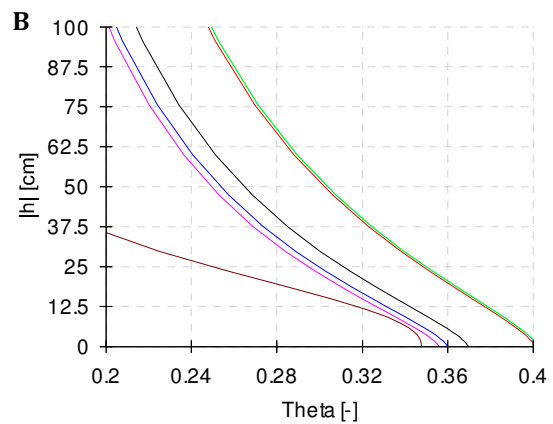

Figure 4.11. Soil hydraulic properties, the colors and conform name (M1 to M7) indicate which horizon is measured, M1 represents the first horizon, horizon A_{ap}, and M7 represents the last horizon, horizon C. Graph (A) and (B) are the water retention curves with the log of the hydraulic head and the hydraulic head, respectively, versus water content, theta.

The retention curve, plotting the log of the head (cm) versus the soil water content, theta (-) (figure 4.11a), is typical for a fine sandy soil with a high organic matter content in most layers. Only hydraulic properties for layer 7 which is also known as horizon C, differs significantly from the other layers. This can be explained by the fact that horizon C is characterized as a pure fine sand, remnant of glacial deposits, and has a very low loam fraction so will not retain water as well as the other layers [table 3.6].
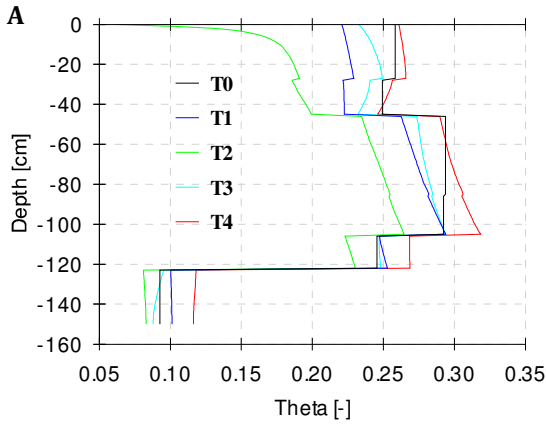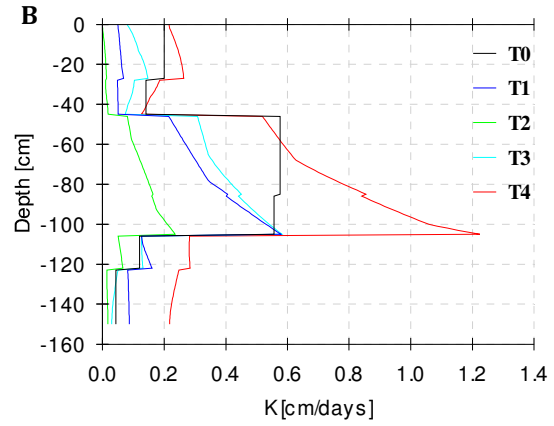
Cum. Actual Surface Flux
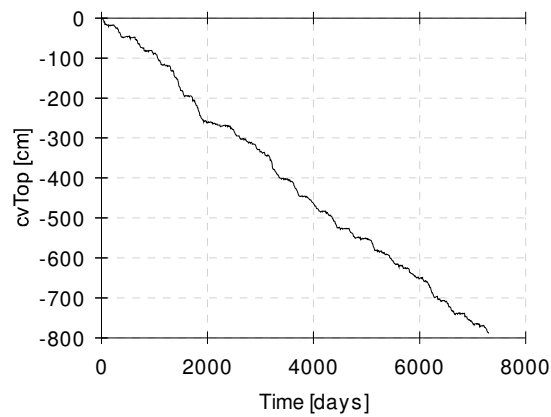
Figure 4.12. The cumulative actual surface flux for the studied soil column after a 20 year application of precipitation and evaporation data.

The cumulative actual surface flux (figure 4.12) is the amount of precipitation (around 1600 cm) that is introduced to the soil column, minus the evaporation (around 800 cm) over a time period of 20 years. The amount of rainfall percolating through the first layer was fairly constant, slightly changing with season and has only one sudden increase in flux around 2000 days, indicating a periods of increased precipitation.
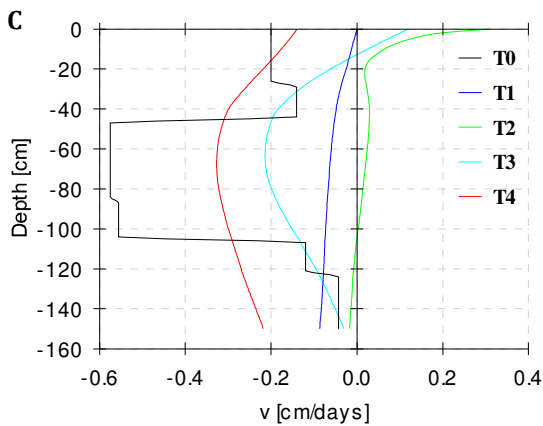
Profile Information: Water Content

Profile Inform.: Hydraulic Conductivity
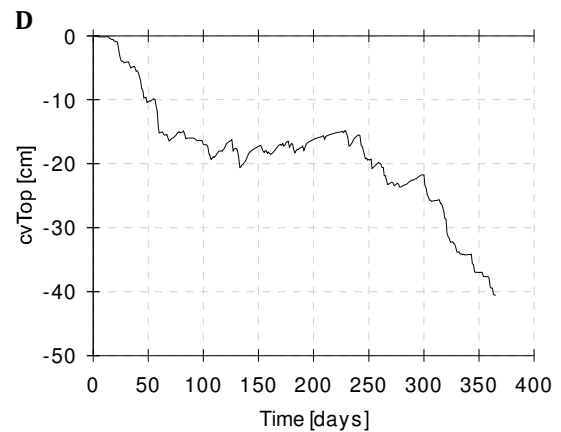
Profile Information: Water Flux

Cum. Actual Surface Flux

Figure 4.13. Hydrological soil profile information for one year of transient flow, from 1-1-1990 to 31-12-1990, where T0= 0, T1= 90, T2= 180, T3=270, T4=365 days. (A) water content; (B) hydraulic conductivity; (C) water flux; and (D) cumulative actual surface flux.

Strong fluctuations in water content, hydraulic conductivity and water flux are observed in the soil when it is modeled with precipitation input over a period of one year, from 1-1-1990 to 31-12-1990. The dry seasons (90 and 180 days) are marked by low water content (figure 4.13 a), lower hydraulic conductivity and nearly no flux while the wet periods (270 and 365 days) are characterized by the opposite. Transport of solutes will most commonly happen during the wet periods, mostly due to the increased water flux.

EC-model

A one year simulation in HP-1, adding PG through 10 mm of precipitation on the first day, results in a radium soil profile with a quick radium migration through the soil profile (figure 4.14a). Radium seems to be partly affected by retardation through ion exchange but within 365 days most of it flushes through the entire soil column. The tracer migrates with same speed through the column but due to the full concentration flushes out, somewhat of tailing is observed (figure 4.14b).
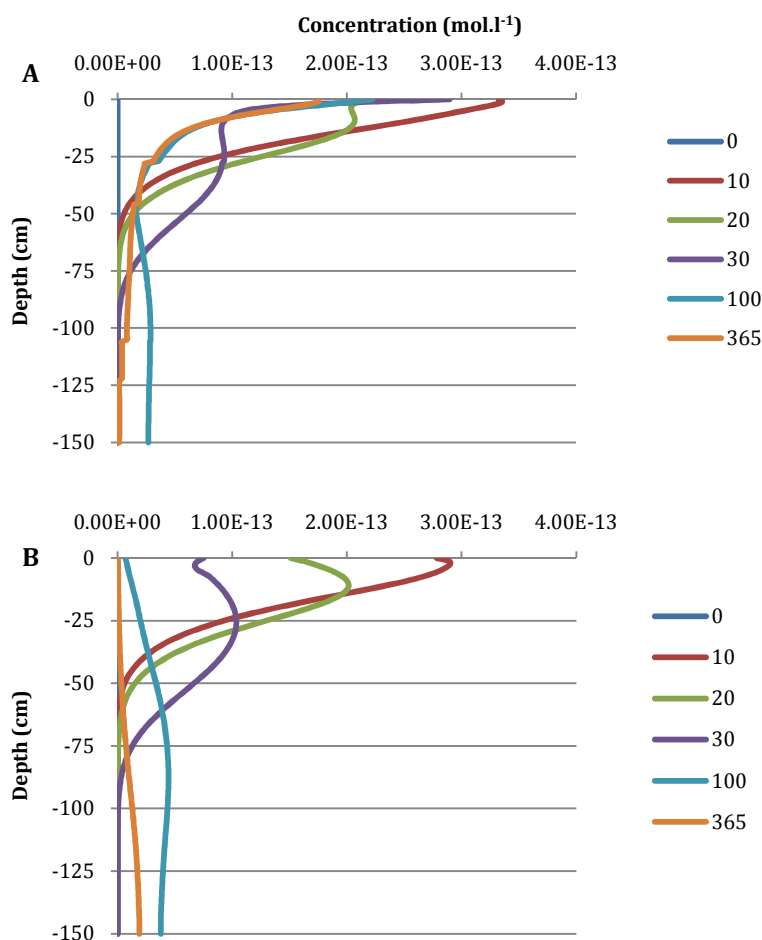

Figure 4.14. (A) Total radium and (B) tracer (bromine) concentrations (mol.dm^{-3} soil) in the soil profile after application of PG and one year of transient flow, profile taken at 0, 10, 20, 30, 100 and 365 days.

A few causes could be behind the quick radium migration as observed in figure 4.14. Since addition of PG to the soil was done through precipitation and the $CaSO_4$ concentration was about 3 times in magnitude larger then usually observed in the soil, radium on the adsorption places might be easily replaced by Ca^{2+} or the concentration of SO_4^{2-} and the resulting speciation of radium, as seen in section 4.1.3, causes the inert $RaSO_4$ (aq) to quickly migrate through the column. This inert form of radium is also observed in field experiments (Paul et al. 1984) and was the main reason some radium was detected in the leachates.

When referring back to the PHREEQC batch experiments in section 4.1.1, where results from the EC-model were compared to literature data, the observation was made that below pH values of 5 or 6, for literature data and the EC-model, respectively, K_d decreased quickly. Even though the pH of precipitation was 5.74 (table 3.3), pH in the soil ranged from around 3 to 5.5 for both one year modeling (figure 4.15a) and modeling for 20 years (figure 4.15b). These strong fluctuations in pH can also be the cause of quickly radium desorption.
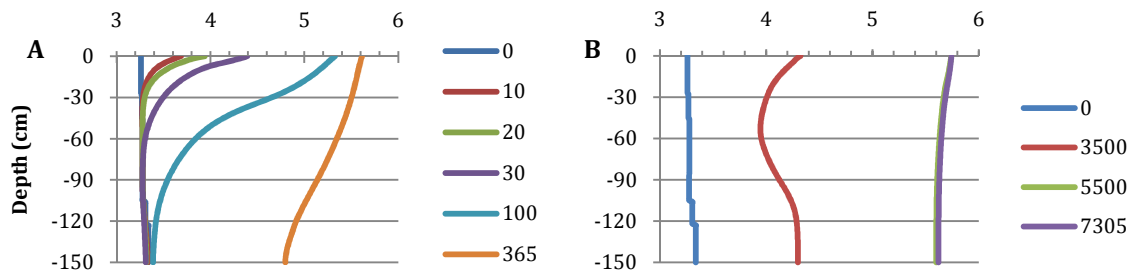

Figure 4.15. pH profiles in the soil observed for (A) a one year simulation with transient flow, profiles taken at 10, 20, 30, 100 and 365 days; and (B) a 20 year simulation with transient flow, profiles taken at 1957, 2323, 3418, 5000 and 7305 days, shortly after PG application.

Modeling for 20 years of transient flow, divided in 5 years normal precipitation to let the column equilibrate with the precipitation, 5 years of PG application (at day 1947, 2313, 2678, 3043 and 3408) and normal precipitation, and 10 years of normal precipitation, results in the following radium concentration profiles (figure 4.16) and breakthrough curves (figure 4.17, 4.18).
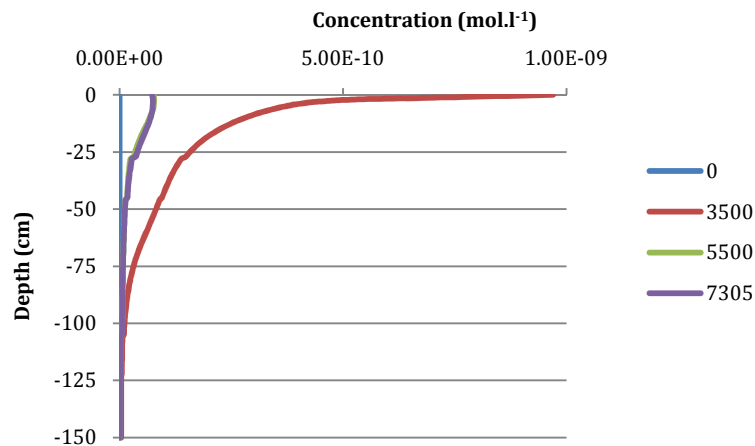

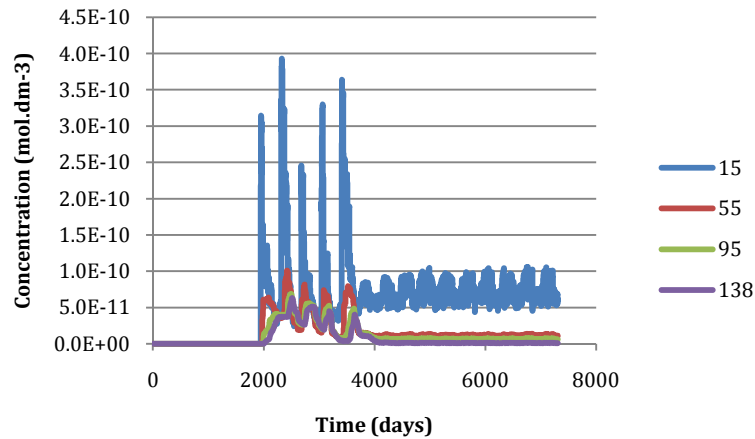*Figure 4.16. Concentration profile of total radium (mol.dm^{-3}) at 3500, 5500 and 7305 days.*

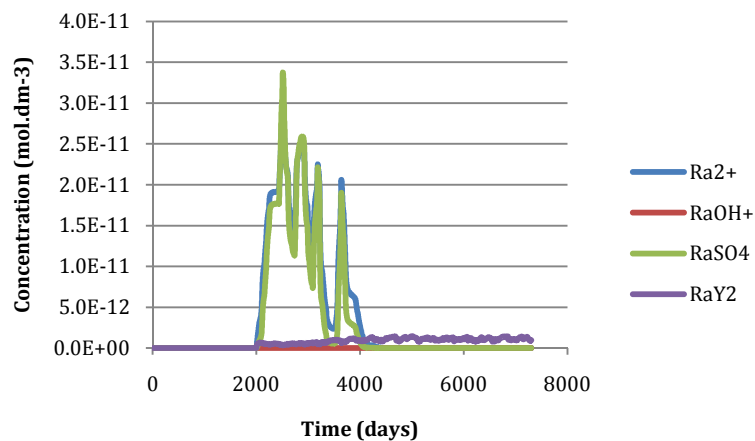*Figure 4.17. Breakthrough curves of radium (mol.dm^{-3}) for nodes at a depth of 15, 55, 95 and 138 cm.*

Figure 4.18. Breakthrough curves for the species Ra^{2+}, RaOH$^+$, RaSO$_4$ (aq) and RaY$_2$ (mol.dm^{-3}), at a depth of 138 cm.

In the 20 year simulation using the EC-model approach with transient flow, the same relative quick migration of radium is observed in the column. This is in particularly clear when the breakthrough curves at depths 15, 55, 95 and 138 cm are watched (figure 4.17). Depending on the speciation, which is about 50 % of both Ra^{2+} and RaSO$_4$ (figure 4.18), a few conclusions can be made. Radium speciation to RaSO$_4$ (aq) might be part of the explanation to the quick migration of radium, however some Ra^{2+} is also observed. This indicates that radium is also prone to competition with other cations, in particular Ca^{2+}, which is present in high concentrations when PG is added, as well as H$^+$, which can strongly fluctuate as seen before (figure 4.15). Remaining concentrations of radium (observed in figure 4.16 and 4.17) in the column are bound to the soil, represented by the RaY$_2$ fraction (figure 4.18) which is the only fraction still present after the full runtime of the model.

An estimated 20% of the initially present radium remains bound to the column, while about 80% leaches through in just a relative short amount of time. Since most of it leaches through so quickly, it is not needed to simulate for longer periods of time, 100 to 200 year, to make conclusions about the fate of radium when applied in agriculture.

The observations of relative quick radium migration reflect back on the estimated exchange constants of radium, and a few other earth alkali elements, which are the foundation of the EC-model. The approach by Langmuir (1985), linking thermodynamic characteristics values to the Hydrated Ionic Radius of the ions, might not be applicable for calculation of the exchange constants as done in our study. Differences between the exchange constants of single charged cations and the alkali earth elements, double charged cations, might be too large. Changing the exchange constants for single charged ions, such as K^+, Na^+ and NH_4^+, by half of their original value, resulted in a profile where radium is strongly bound to the soil and slowly migrates downwards. An interesting observation is the concentration profile of radium at day 365 which differs not much from the profile of day 100. An explanation can be found in the relative high soil pH (figure 4.15a) which, from day 100 to day 365 practically immobilizes radium on its sorption places.
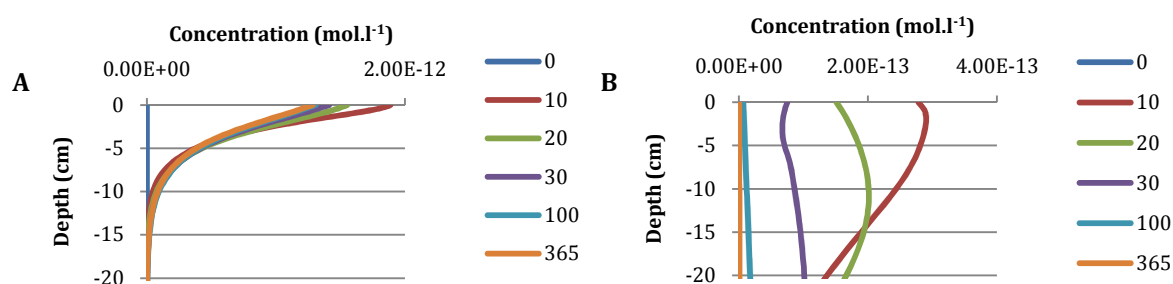
Figure 4.19. The top 20 cm of the soil profile with (A) radium concentrations and (B) bromine concentrations (mol.dm^{-3}) measured at days after application and after adjusting exchange constants for single charged ions and application of PG with radium using precipitation for one year.

The EC-model has successfully been applied before in calculating the mobility of uranium in Podzols [Jacques et al. 2008b]. Those studies however used measured uranium exchange constants, constants not found in literature for radium.

A K_d of 1497 ml.g^{-1} is used to describe a 'standard' relationship between adsorbed radium and radium concentration in soil solution. This is a combined estimate from Powell et al. 2001 and batch experiment for F.A. using Exchange Constants and CEC for top layer, the A$_{ap}$ horizon.

Concentration profiles for radium were obtained using a 5 year simulation (figure 4.20a), applying PG in the second year on May 1st and using a 20 year simulation (figure 4.20b), 5 years of precipitation followed by 5 years in which on May 1st PG was applied (day 1947, 2313, 2678, 3043 and 3408), followed by another 10 years of 'normal' precipitation.
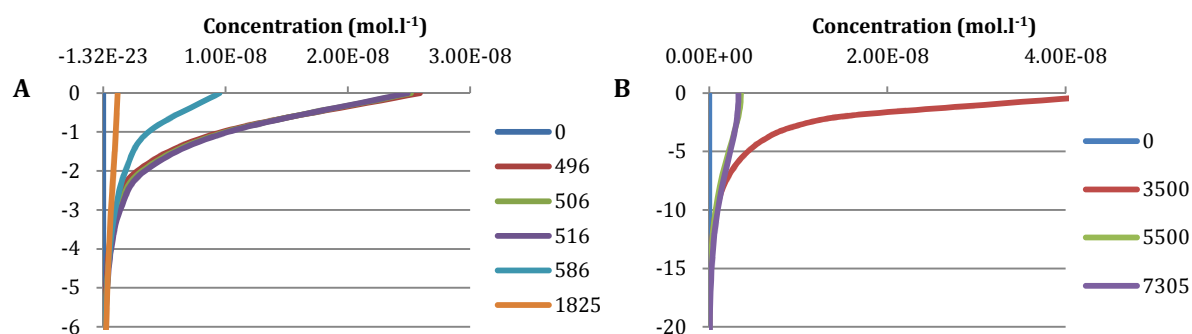

Figure 4.20. Radium concentrations (mol.dm^{-3}) in soil profile
for (A) 5 year simulation; and (B) 20 year simulation.
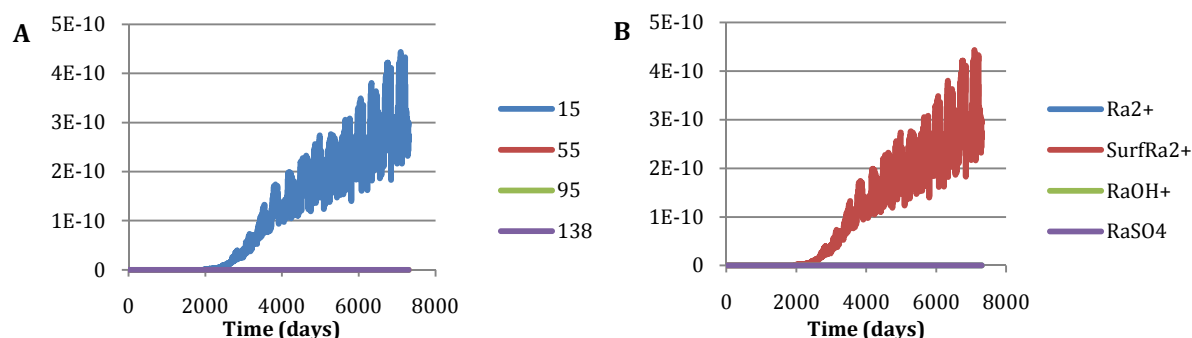
Figure 4.21. (A) total radium concentration at nodes of 15, 55, 95 and 138 cm depth;
and (B) concentrations of various radium species at depth 15 cm.

Even though radium seems to be tightly bound to the soil, some it of leaches away, this happens with a steady release rate as can be seen in the breakthrough curves (figure 4.21a). The leaching is relatively slow, explained by the speciation most observed in the column, that of radium bound to the soil (SurfRa+2) (figure 4.21b).

Three relationships were used to describe the change in K_d for a change in parameter, [Na], [Ca] and pH. With sodium concentrations varying roughly from 1x10^{-5} to 1x10^{-4} mol.l^{-1}, K_d ranges from 13000 to 54000 ml.g^{-1} (figure 4.7a). K_d-values exceed values observed in litaterature by at least one order of magnitude, therefore, radium is expected to immediately adsorp onto the soil and little to no leaching will take place. It must be stated again that the relationship between the log K_d and the log of [Na] was based on only two observation points, and EC-model (figure 4.4) showed a decrease of slope at sodium concentrations below 1x10^{-3} mol.l^{-1}, while the linear approach keeps increasing K_d (figure 4.7a).

With pH values ranging in our model from roughly 3 to 6, K_d of radium ranges from 163 to 695 ml.g^{-1} (figure 4.6). These are K_d values are more often observed in literature [table 2.11]

With calcium concentrations ranging from 1×10^{-1} to 1×10^{-6} mol.l^{-1}, K_d ranges from 65 to 11000 ml.g^{-1}, respectively. These values are in range of values observed in literature [table 2.11], though 11000 ml.g^{-1} is on a high side.

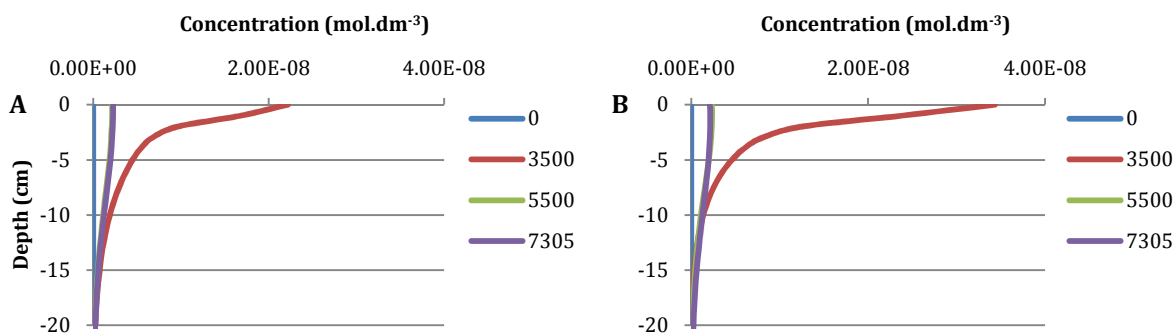Figure 4.22. Concentration profile of radium when K_d depends on (A) pH; and (B) calcium concentration measured at day 3500, 5500 and 7305.
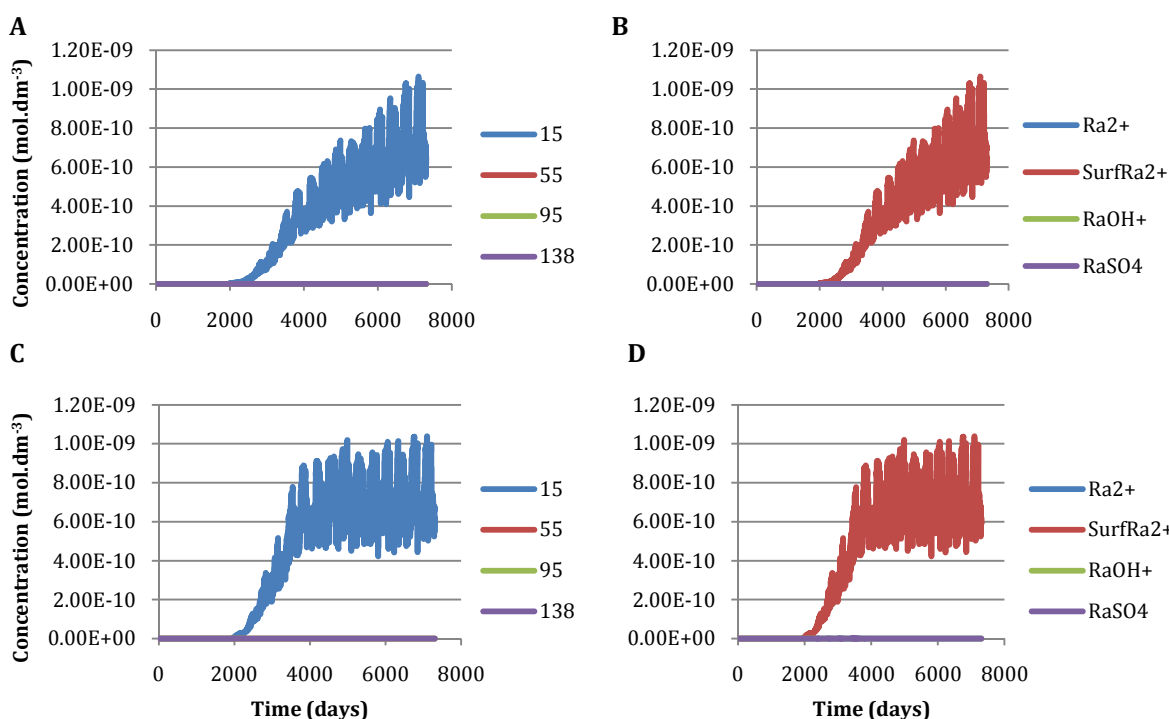

Figure 4.23. Breakthrough curves from HP-1 model using K_d-model approach depending on (A)(B) pH; (C)(D), calcium concentrations. (A) and (C) breakthrough curves of total radium at depths of 15, 55, 95 and 138 cm; and (B) (D) breakthrough curves at depth 15 cm of radium species.

Concentration profiles (figure 4.22a) and breakthrough curves (figure 4.23b) of radium in the soil from the pH dependant model show an increased release of radium compared to the constant K_d-model using a K_d value of 1497 ml.g^{-1} (figure 4.21a, 4.21b). This increased but constant release can be explained by the constant, relative lower, K_d value ranging from 163 to 695 ml.g^{-1}.

Concentration profiles (figure 4.23c) and breakthrough curves (figure 23d) of radium in the soil from the calcium dependant model show an increased release of radium during PG application compared to the constant K_d-model using a K_d value of 1497 ml.g^{-1} (figure 4.21a, 4.21b). This increased release can be explained by the relative high calcium concentrations during PG application, 1×10^{-1} mmol.l^{-1}, effectively lowering the K_d of radium to around 65 ml.g^{-1}. However, as soon as calcium concentrations drop to about 1×10^{-6} mol.l^{-1}, K_d changes to a value around 11000 ml.g^{-1}, immobilizing radium again.

The dominant speciation of radium observed in the breakthrough curves was radium bound to the surface (SurfRa+2) (figure 4.23), implying a relative tight bond of radium to the soil. However, leaching of radium, in the form of Ra^{2+} and RaSO$_4$ still occurred at a depth of 15 cm, be it in relative low concentrations (figure 4.24).
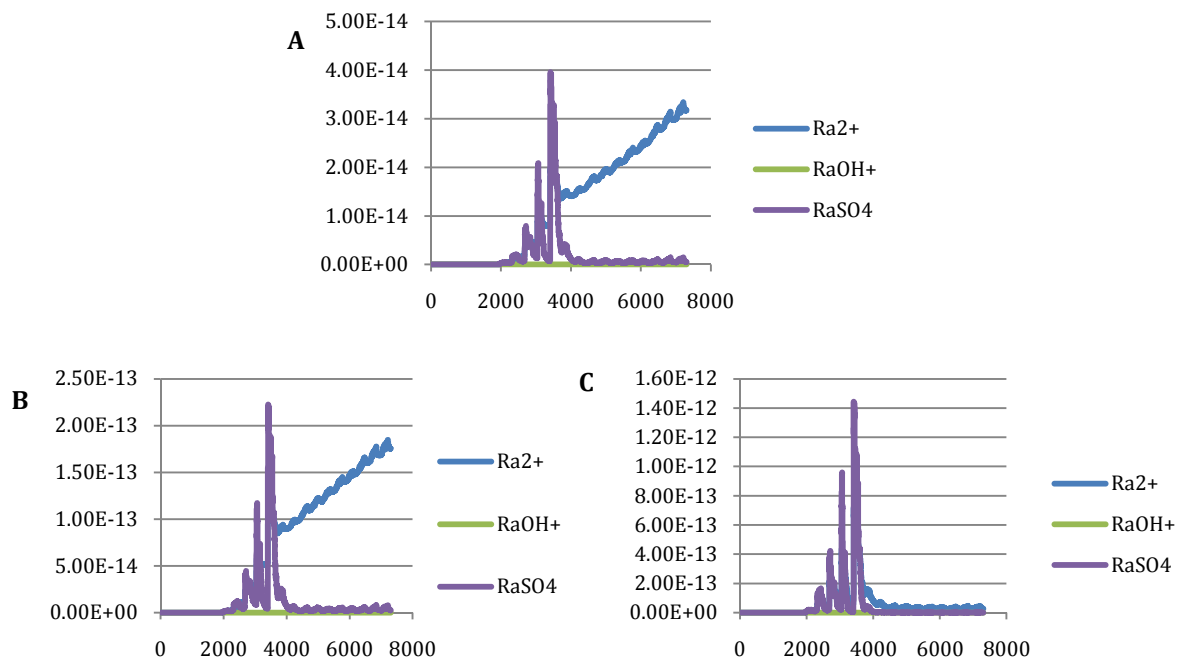
Figure 4.24. Breakthrough curves at a depth of 15 cm for (A) linear K_d-model approach; (B) pH dependant K_d-model approach; and (C) calcium concentration dependant K_d-model approach.

An obvious result of the more simple approach of the K_d-model is observed in the time needed to run a simulation. During a 20 year simulation the K_d-model was significantly faster than the EC-model, 7966 to 11641 seconds, respectively. As stated before, application of the K_d-model for the most important soil parameters might greatly decrease the time needed to run a simulation hence could best be used in multi-dimensional simulations on a larger spatial and temporal scale.

Since the K_d-model does not directly account for changes in multiple parameters, it is very limited. HP-1 models using the K_d-model model radium migration depending on [Ca] and pH well, [Na] showed such examples of extraordinary K_d values, hence this was not modeled.

Going back to radium profiles as observed in field experiments, the following observations were made. Field studies provided data where the maximum activity was found at 22.5 cm depth. The activity in the top layer was significantly lower, possibly due to leach-out over a period of years. The activity at depth 95 cm was comparable to background soil activity of the area, meaning it had not further leached. This low activity at lower depths suggests that vertical seepage and exchange of this activity with subterranean soil is insignificant but still occurs [Paul et al. 1984]. These observations match closest to the K_d-model, with or without K_d dependency on soil parameters and the EC-model with adjusted exchange constants.

CHAPTER 5 - Conclusions

A literature study has carried out to characterize the most important soil parameters which influence radium mobility. Two approaches to account for soil conditions that influence radium mobility have been developed in PHREEQC and results have been compared to data from literature studies. The models were then incorporated in HP-1 for long term modeling of PG application on a Dutch Fimic Anthrosol. Conclusions from this study, those worthy of mentioning, have been listed in this chapter.

Literature conclusions

Literature studies on radium leaching from PG in the soil show that only 0.9% of the radium present in the PG leaches after one year of rainfall and most of the radium remains in the top layers. Three studies indicated a pattern of leaching of radium from PG in three steps, one loosely bound fraction, possibly $RaSO_4$ (aq), a fraction that is retarded by ion exchange, Ra^{2+}, and a long term release of radium caused by (slow) dissolution of PG grains combined with release of radium.

Radium migration through soil was mainly controlled by ion exchange [EPA, 2004][Laili et al. 2010]. Literature study provided several important soil parameters which had their effect on radium mobility. Organic matter content and to lesser extend soil textural fraction provide sorption places which in turn controlled radium sorption. Increasing concentration of bivalent cations, ionic strength resulted in a decrease in radium adsorption while increase in pH resulted in an increase of radium adsorption.

Several of the relationships between the log of the distribution coefficient of radium, K_d, and the log concentrations of soil parameters, such as organic matter, soil textural fraction, [Ca], pH and [Na], could be quantified through literature. Other soil parameters such as temperature, radium concentration, the influence of vegetation through roots and microbiological activity influenced radium mobility, however not enough data was present to quantify and account for these parameters.

Two models for PHREEQC have been developed to approach the influence of soil parameters on the radium mobility and the radium distribution coefficient. The "K_d-model" approach used the slope of the linear trendline through log-log relationships of the radium distribution coefficient and soil parameters to estimate empirical constants. The "EC-model" approach used exchange constants obtained from literature for a Fimic Anthrosol, calculating missing exchange constants for alkali earth elements through the Langmuir approach, and replaced those values in the PHREEQC database.

Batch experiment conclusions

Comparing trends observed from literature with PHREEQC batch experiments using the EC-model, the approach correctly modeled the change in distribution coefficient with regard to change in parameter. An increase in calcium and sodium concentrations, the latter an equivalent of ionic strength, decreases adsorption of radium, while an increase in pH increases the adsorption of radium. An increase in cation exchange capacity leads to an increase in distribution coefficient, in the same order of magnitude over the entire concentration range.

The same comparison was made between trends observed from literature with PHREEQC batch experiments using the K_d-model. Using these empirical constants gave a reasonable approach to the literature studies, however, the linear approach did not account for non-linear behavior as observed for pH.

Combining more than one soil parameter in one formula did not result in viable values for the distribution coefficients. This limits the ability for the K_d-model approach to account for multiple soil conditions even more. Not all log-log relationships between the K_d and the soil parameters were linear, hence caution should be advised while using them.

The EC-model much more accurately models spatial and temporal variations then the K_d-model, especially in studies were the behavior of the log distribution coefficient is not always linear compared to the log of the studied parameter.

Speciation calculations showed that speciation of radium under concentrations of $1x10^{-12}$ to $1x10^{-9}$ mol.l^{-1} added through precipitation is greatly influenced by sulphate concentrations. Formation of the electrostatic inert $RaSO_4$ (aq), is especially observed when PG is applied and introduced to rainwater, causing elevated concentrations of sulphate in the soil column. This, together with the addition of calcium also from PG, might lead to increased leaching of radium from the soil profile. Other complexes, $RaCl^+$ (aq) and $RaOH^+$ (aq) were not observed in significant concentrations.

Long term HP-1 application

Usage of local Dutch precipitation, evaporation and soil patterns results in sharp changes of hydraulic conductivity, water content and hydraulic pressure in the soils, which in turn act on the transport of water and solutes through the soil.

Using the EC-model in a 20 year simulation, quick migration of radium is observed and only an estimated 20% of the initial radium remains in the column. This quick migration is caused by high concentrations of Ca^{2+}, H^+ and SO_4^{2-}. The first two (Ca^{2+}, H^+) concentrations leading to increased competition for adsorption places with regard to radium, the high concentrations of SO_4^{2-} causing the formation of the relative inert $RaSO_4$ (aq). The response of the model is dictated through the exchange constants obtained from literature and estimated through the Langmuir and Riese (1985) approach.

HP-1 models using the K_d-model approach of 20 years were simulated, with radium migration depending on [Ca] and pH. Observed sodium concentrations lead to extraordinary high K_d values, hence this dependency was not used in HP-1. A clear effect of pH and calcium concentration was seen in concentration profiles and breakthrough curves of models using K_d dependencies to pH and calcium concentration, either by mobilizing or immobilizing radium more then when using a constant K_d for radium. For all approaches, most radium remained in the top 10 cm of the soil after a simulation time of 20 years, hence was effectively immobilized.

Comparing the K_d-model to the EC-model approach in HP-1 models for long term simulations, using the first approach results in significantly shortly (about 40%) simulation times. Results obtained from the EC-model can be used to explain observations made in the "K_d-model", for example when considering K_d dependency on sodium.

Field observations closely matched results from the 20 year HP-1 simulations using the K_d-model approach, with or without K_d dependency on soil parameters, and the EC-model with adjusted exchange constants.

This study has effectively used HP-1 modeling and literature data to describe radium migration through soil when PG is applied in an agricultural setting. It has developed models to account for the dynamic interaction of radium with the soil and effectively applied them to HP-1 models, opening the ability to do long-term predictions for the fate of radium.

CHAPTER 6 - Further Research

Computer modeling is a high potential research method to study the long term effects of PG application and to observe the migration of one of its most important contaminants, radium, through the soil column. It provides data which is not yet available from the field, therefore further research to improve the quality of these models is highly encouraged.

Future, experimental, research should focus more on the quantifying the effect soil conditions on radium mobility, for parameters which have not enough data to be included yet in the proposed models; parameters such as temperature, radium concentration, the influence of vegetation through roots and microbiological activity.

Exchange constants for radium and other alkali earth elements should be obtained for the soil that is studied to more effectively apply the EC-model for long-term simulations.

The option to add PG through solid $CaSO_4$ instead of using a dissolved form in precipitation should be investigated. Through addition of PG and radium in the form of $CaSO_4$ and $RaSO_4$, the kinetics of PG dissolution could be taken into account to more gradually release $CaSO_4$ (aq) and radium to the soil. With the addition of solid $CaSO_4$, the mobility of radium should be less influenced through sudden large fluxes of sulphate and calcium ions which control speciation and competition at adsorption places, respectively. Various parameters influencing PG dissolution, already known from literature, could then also be added to the model.

Combining multiple relationships between distribution coefficient and soil parameters in the combined K_d-formula should be investigated and optimized.

Observations made in HP-1 modeling and relationships developed for the PHREEQC models could be used to for large scale, multi-dimensional simulations.

Acknowledgments

A list of people I wish to acknowledge who contributed to the success of this research project because of their contribution through knowledge and insights.

Prof. M. Th. van Genuchten, the main advisor of the project on phosphogypsum. Through his three months visit at Utrecht University in the Netherlands, I came into contact with him and the students working on PG project. Following the summer school and his classes in hydrological modeling, he sparked my interest for this project. His insight in hydrology in general as well as in hydrological modeling using Hydrus 1-D has helped our project a great deal.

Dr. D. Jacques, my other main advisor during this project. I owe him much gratitude for the insights and thoughts that we shared and discussions we had on the models and aspects that should be accounted for in this project. My visits to him in Mol (Belgium) were not without result. Thanks again!

Camila and Marcia, two students from Brazil that worked on the same project. Thanks to their different view on this project due to their background in hydrology, they were able to help me to establish my HP-1 model correctly and provide me with new insights. I wish you both all the best for when you continue with this research and your PhD!

Case van Genuchten, a fellow geochemistry student from Boston who provided us with some helpful thoughts and insights at the start of the project.

Prof. S.M. Hassanizadeh, my secondary advisor in Utrecht. He was of great help in finding the right people at the right places when I could not continue halfway during my research. He was also the teacher who sparked my interest in the field of environmental hydrogeology due to his interesting and challenging courses.

Last but certainly not least, my parents. Without their continuous support I would not have made it this far in my studies and life.

References

- Alcordo, I.S., Rechcigl J.E., Roessler, C.E., Littell, 1999. *Radiological Impact of Phosphogypsum Applied to Soils under Bahiagrass Pasture*. J. Environ. Qual. Vol. 28, pp. 1555-1567.
- Azouazi, M., Ouahidi, Y., Fakhi, S., Andres, Y., Abbe, J.Ch., Benmansour, M., 2001. *Natural radioactivity in phosphates phosphogypsum and natural waters in Morocco.* Journal of Environmental Radioactivity, Vol. 54, pp. 231-242.
- Bear, J., 1972. *Dynamics of Fluids in Porous Media.* Dover Publications.
- Burnett, W.C., Cowart, J.B., LaRock, P., 1995. *Microbiology and Radiochemistry of Phosphogypsum.* Floridat State University, Publication No. 05-035-114.
- Canut, M.M.C., Jacomino, V.M.F., Bratveit, K., Gomes, A.M., Yoshida, M.I., 2008. *Microstructural analyses of phosphogypsum generated by Brazilia fertilizer industries.* Materials characterization, Vol. 59, pp. 365-373.
- Cañete, S.J.P., Palad, L. J.H, Enriquez, E.B., Garcia, T.Y., Yulo-Nazarea, T., 2008. *Leachable 226Ra in Philippine phoshpogypsum and its implicaino in groundwater contamination in Isabel, Leyte, Philippines.* Envrion. Monit. Assess., Vol. 142, pp. 337-344.
- Cygan, R., 2002. *Molecular Models of Radionuclide Interaction with Soil Minerals*. Geochemistry of Soil Radionuclides. Soil Science Society of America, Madison, WI. Edition P. Zhang and P.Brady, pp. 87-110.
- de Vries, W., Kros, J., Salm, van der, C., 1994. *Long-term impacts of various emission deposition scenarios on Dutch forest soils*. Water, Air and Soil pollution, Vol. 75, pp. 1-35.
- de Vries, W., Leeters, E.E.J.M., 2001. *Chemical composition of the humus layer, mineral soil and soil solution of 150 forest stands in the Netherlands in 1990.* Alterra-rapport 424.1, Alterra, Green World Research, Wageningen.
- EPA, 2004. *Understanding Variation in Partition Coefficient, K_d, Values.* Volume 3: Review of Geochemistry and Available K_d Values for Americium, Arsenic, Curium, Iodine, Neptunium, Radium, and Technetium.
- Florida Istitue of Phosphate Research. www.fipr.state.fl.us/index.html, verified 04-08-2010.
- Frenkel, H., Fey, M.V., Noble, A.D., 1989. *Some Factors Limiting the Dissolution Rate of Phosphogypsum in an Acid Soil.* Soil Science Society America, Vol. 53, pp. 958-961.
- Haridasan, P.P., Pillai, P.M.B., Tripathi, R.M., Puranik, V.D., 2009. *An evaluation of radiation exposures in a tropical phosphogypsum disposal environment.* Radiation Protection Disimetry, Vol. 135, No. 3, pp. 211-215.
- Jacques, D., Šimůnek, J., Mallants, D., and M.Th. van Genuchten, 2006. *Operator-splitting errors in coupled reactive transport codes for transient variably saturated flow and contaminant transport in layered soil profiles.* J. Contam. Hydrology, Vol. 88, pp. 197-218.
- Jacques, D., Šimůnek, J., Mallants, D., van Genuchten, M.Th., 2008a. *Modeling coupled water flow, solute transport and geochemical reactions affecting heavy metal migration in a podzol soil.* Geoderma, Vol. 145, pp. 449-461
- Jacques, D., Šimůnek, J., Mallants, D., van Genuchten, M.Th., 2008b. *Modeling coupled hydrologic and chemical processes: long-term uranium transport following phosphorus fertilization*. Vadose Zone Journal, Vol. 7, pp. 698-711.
- Jongmans, T., Peek, G., *Enkeerdgronden, Vorming en gevolgen ervan in het Pleistocene zandlandschap.*
- Kirby, H.W., Salutsky, M.L., 1964. *The Radiochemistry of Radium.* U.S. Atomic Energy Commission.
- KNMI, Daily Data. http://www.knmi.nl/climatology/daily_data/selection.cgi [verified 05-06-2011]
- Langmuir, D., Riese, A.C., 1985. *The thermodynamic properties of radium.* Geochemica et Cosmochimica Acta, Vol. 49, pp. 1593-1601.
- Lindeden, C.L., 1980. *Radiological considerations of phosphogypsum utilization in agriculture.* International Symposium of Phosphogypsum, Lake Buna Vista, Florida. CONF 801161-1.
- Locher, W.P., and de Bakker, H., 1990. *Bodemkunde van Nederland.* Algemene Bodemkunde, Volume 1 & 2, Stiboka, Min. L&V, Malmberg, Den Bosch.

- Mariscal-Sancho, J., Espejo, R., Perigrina, F., 2009. *Potentially Toxic Effects of Phosphogypsum on Palexerults in Western Spain.* Soil Science Society of America Journal. Vol. 73, pp. 146-153.
- Meier, H., Zimmerhacki, E., Zeitler, G., Menge, P., 1994. *Parameter Studies of Radionuclide Sorption in Site-Specific Sediment/Groundwater Systems.* Radiochimica Acta. Vol. 66/67, pp. 277-284.
- Molinari, J., and Snodgrass, W.J., 1999. *The Chemistry and Radiochemistry of Radium and the Other Elements of the Uraniun and Thoriun Natural Decay Series.* International Atomic Energy Agency, Vienna, Austria. The Environmental Behavior of Radium, Volume 1, pp. 11-56
- Nathwani, J.S., Phillips, C.R., 1978. *Rates of Leaching of Radium from Contaminated Soils: an Experimental Investigation of Radium Bearing Soils from Port Hope, Ontario.* Water, Air and Soil Pollution, Vol. 9, pp. 453-465.
- Nathwani, J.S., Phillips, C.R., 1979a. *Adsorption of ^{226}Ra by Soils.* Chemosphere No. 5, pp 285-291.
- Nathwani, J.S., Phillips, C.R., 1979b. *Adsorption of ^{226}Ra by Soils in the Presence of Ca2+ ions.* Chemosphere No. 5, pp 293-299.
- Nitzsche, O., Merkel, B., 1999. *Reactive transport modeling of uranium 238 and radium 226 in groundwater of the Königstein uranium mine, Germany.* Hydrogeology Journal, Vol. 7, pp. 423-430.
- OSPAR Commission, 2002. *Discharges of radioactive substances into the maritime area by non-nuclear industry.*
- Papanicolaou, F., Anoniou, S., Pashalidis, I., 2009. *Experimental and theoretical studies on physico-chemical parameters affecting the solubility of phosphogypsum.* Journal of Environmental Radioactivity, Vol. 100, pp. 854-857.
- Parkhurst, D.L., and Apello, C.A.J., 1999. *User's guide to PHREEQC (Version 2) – A computer program for speciation, batch-reaction, one-dimensional transport and inverse geochemical calculations.* U.S. Geological Survey Water-Resources Investigations Report, Vol. 99-4259, pp. 1-312.
- Paul, A.C., Pillai, P.M.B., Komalan Nair S., Pillai, K.C., 1984. *Studies on the Leaching of Radium and the Emanation of Radon from Fertilizer Process Sludge.* Journal of Environmental Radioactivity, Vol. 1, pp. 51-65.
- Reguigui, N., Felfoul, S.H., Ouezdou, B.M., Clastres, P., 2005. *Radionuclide levels and temporal variation in phosphogypsum.* Journal of Radioanalytical and Nuclear Chemistry, Vol. 264, No.3, pp. 719-722.
- Righi, S., Patrizia Lucialli, P., Bruzzi, L., (2005) *Health and environmental impacts of a fertilizer plant – Part I: Assessment of radioactive pollution.* Journal of Environmental Radioactivity, Vol. 82, Issue 2, pp. 167-182.
- Rutherford, P.M, Dudas, M.J., Samek, R.A., 1992. *Environmental impacts of phosphogypsum*, The Science of the Total Environment, Vol. 149, pp. 1-38.
- Saueia, C.H.R., Mazzilli, B.P., 2006. *Distribution of natural radionuclides in the production and use of phosphate fertilizers in Brazil,* Journal of Environmental Radioactivity, Vol. 89, pp. 229-239.
- Schaap, M.G., F.J. Leij, and M. Th. van Genuchten, 2001. Rosetta: a computer program for estimating soil hydraulic parameters with hierarchical pedotransfer functions. Journal of Hydrology. Vol. 251, pp. 163-176.
- Serne, R.J., 1974. *Waste Isolation Safety Assessment Program Task 4.* Contractor Information Meeting Proceedings. PNL-SA-6957, Pacific Northwest Laboratory, Richland, Washington.
- Sheppard, S.C., Sheppard, M.I., Tait, J.C., Sanipelli, B.L., 2006. *Revision and meta-analysis of selected biosphereparameter values for chloringe, iodine, neptunium, radium, radon and uranium.* Journal of Environmental Radioactivity. Vol. 89, pp. 115-137.
- Sheppard, S., Long, J., Sanipelli, B., Sohlenius, G., 2009. *Solid/liquid partitioning coefficients (Kd) for selected soils and sediments at Forsmark and Laxemar-Simpevarp.* Swedish Nuclear Fuel and Waste Management Co. ISSN 1402-3091, SKB Rapport R-09-27.
- Šimůnek, J., Jacques, D., Twarakavi, N.K.C., van Genuchten, M.Th., 2009. *Selected HYDRUS modules for modeling subsurface flow and contaminant transport as influence by biological processes at various scales.* Biologia, Vol 64(3), pp. 465-469.
- Simon, S., Ibrahim, S., 1990. *Biological uptake of radium by terrestrial plants*. Environmental behavior of radium. Vol. 1, pp. 545-599.

- Smith, B., Amonette, A., 2006. The environmental Transport of Radium and Plutionium: A Review. Institute for Energy and Environmental Research.
- Stolk, A.P., 2001. *Landelijk Meetnet Regenwatersamenstelling.* RIVM Rapport 723101 057 / 2001
- Tayibi, H., Choura, M., López, F.A., Alguacil, F.J., López-Delgado, A., 2009. *Environmental impact and management of phosphogypsum.* Journal of Environmental Management, Vol. 90, pp. 2377-2386.
- Thibault, D. H., Sheppard, M. I., Smith, P.A., 1990. *A Critical Compilation and Review of Default Soil Solid/Liquid Partition Coefficients, K_d, for Use in Environmental Assessments.* AECL-10124, Whiteshell Nuclear Research Establishment, Atomic Energy of Canada Limited, Pinawa, Canada.
- Tobor-Kaplon, M.A., Bloem, J., Römkens, P.F.A.M., de Ruiter, P.C., 2005. *Functional stability of microbial communities in contaminated soils.* Oikos, Vol. 111, Issue 1, pp. 119-129.
- Vandenhove, H., Van Hees, M., 2007. *Predicting radium availability and uptake from soil properties.* Chemosphere, Vol. 69, pp. 664-674.
- Vandenhove, H., Gil-García, C., Rigol, A., Vidal, M., 2009. *New best estimates for radionuclide solid-liquid distribution coefficients in soils. Part 2. Naturally occurring radionuclides.* Journal of Environmental Radioactivity, Vol. 100, pp. 697-703.
- van der Heijde, H.B., Klijn, P-J., Passchier, W.F., 1988. *Radiological Impacts of the Disposal of Phosphogypsum.* Radiation Protection Dosimetry, Vol. 24 (1-4), pp. 419-423.
- van Genuchten, M. Th., 1980. *A closed-form equation for predicting the hydraulic conductivity of unsaturated soils.* Soil Sci. Soc. Am. Vol. 44, pp. 892-898.
- Villa, M., Mosqueda F., Hurtado, S., Mantero, J., Manjón, G., Periañez, R., Vaca, F., García-Tenorio, R., 2009. *Contamination and restoration of an estuary affected by phosphogypsum releases.* Science of Total Environment, Vol. 408, pp. 69-77.
- Wang, R.S., Chau, A.S.Y., Liu, F., Cheng, H., Nar, P., Chen, X.M., Wu, Q.Y. 1993. *Studies on the adsorption and migration of radium in natural minerals.* Journal of Radioanalytical and Nuclear Chemistry, Articles, Vol. 171, No.2, pp. 347-364.
- Yang, J., Liu, W., Zhang, L., Xiao, B., 2009. *Preparation of load-bearing building materials from autoclaved phosphogypsum.* Construction and Building Materials, Vol. 23, pp. 687-693.
- Xu, C. Y., Singh, V. P., 2000. *Evaluation and generalization of radiation-based methods for calculating evaporation.* Hydrological Processes, Vol. 14, pp. 339-349.

Figures

- Alterra, Wageningen UR, Centrum Geo-Informatie, 2006, verified 02-07-2011, http://www.alterra.wur.nl/NR/rdonlyres/7A252DAE-1BBF-491A-BC78-543051F0EC37/105785/ grondsoortenkaart2006.pdf
- DEP, Department of Environmental Protection, verified 03-07-2011, http://www.dep.state.fl.us/secretary/news/2009/12/images/1214_01_drainpipe.jpg
- NBV, Nederlands Bodemkunde Vereniging, verified 02-07-2011, http://www.bodems.nl/canon/venster-33.php
- Niewsarchief, Bibliotheek Wageningen UR, 2010, verified 02-07-2011, http://4.bp.blogspot.com/_Yevlze-YcGY/S81X3z29AVI/AAAAAAAAHho/RiwxQgTiUHA/s1600/ enkeerd.jpg

Attachment A - Additions to PHREEQC Database

To makes sure all radium species were taken into account during PHREEQC/HP-1 calculations, data was gathered from several data bases and literature, and added to the phreeqcU.dat database, renaming it phreeqcUB.dat.

Data from Langmuir (1985) introduced in the phreeqcU.dat database

#Source; "The thermodynamic properties of radium", DONALD LANGMUIR, 1985
SOLUTION SPECIES (Aqueous Complexes)

Ra+2 + H2O = RaOH+ + H+
log_k -13.5

Ra+2 + Cl- = RaCl+
log_k -0.1

Ra+2 + CO3-2 = RaCO3
log_k 2.5

Ra+2 + SO4-2 = RaSO4
log_k 2.75

Data from llnl.dat introduced in the phreeqcU.dat database

PHASES
Ra
     Ra +2.0000 H+ +0.5000 O2 = + 1.0000 H2O + 1.0000 Ra++
          log_k   141.3711
          -delta_H-807.374   kJ/mol   # Calculated enthalpy of reaction Ra
Enthalpy of formation: 0 kJ/mol
     -analytic 4.9867e+001 5.9412e-003 4.0293e+004 -1.8356e+001 6.8421e+002
-Range: 0-200

Ra(NO3)2
     Ra(NO3)2 = + 1.0000 Ra++ + 2.0000 NO3-
          log_k   -2.2419
          -delta_H50.4817kJ/mol   # Calculated enthalpy of reaction Ra(NO3)2
Enthalpy of formation: -991.706 kJ/mol
     -analytic 2.2001e+001 -9.5263e-003 -3.9389e+003 -3.3143e+000 -6.6896e+001
-Range: 0-200

RaCl2:2H2O
     RaCl2:2H2O = + 1.0000 Ra++ + 2.0000 Cl- + 2.0000 H2O
          log_k   -0.7647
          -delta_H32.6266kJ/mol   # Calculated enthalpy of reaction RaCl2:2H2O
Enthalpy of formation: -1466.07 kJ/mol
     -analytic -2.5033e+001 -1.8918e-002 -1.5713e+003 1.4213e+001 -2.6673e+001
-Range: 0-200

RaSO4
    RaSO4 = + 1.0000 Ra++ + 1.0000 SO4--
        log_k   -10.4499
        -delta_H40.309 kJ/mol   # Calculated enthalpy of reaction RaSO4
Enthalpy of formation: -1477.51 kJ/mol
    -analytic 4.8025e+001 -1.1376e-002 -5.1347e+003 -1.5306e+001 -8.7211e+001
-Range: 0-200

Rn(g)
    Rn = + 1.0000 Rn
        log_k   -2.0451
        -delta_H-20.92   kJ/mol   # Calculated enthalpy of reaction Rn(g)
Enthalpy of formation: 0 kcal/mol
    -analytic -3.0258e+001 4.9893e-003 1.4118e+002 8.8798e+000 3.8095e+005
-Range: 0-300

Attachment B - PHREEQC Input in HP-1 Model

K_d-model

The implementation of the "Kd-model" approach in HP-1 will be done according the contaminant, pollution A, Pol_a. The distribution coefficient for a contaminant Pol_a is assumed to be 1 $cm_w^3 \cdot g^{-1}$. The bulk density ρ_b of the porous medium is 1.5 $g \cdot cm^{-3}$. The lines of code are an example of a linear isotherm with the distribution coefficient in the classical approach

Thermodynamic Database

```
1          SOLUTION_MASTER_SPECIES
2          Pola Pola 0.0 Pola 1.0


3          SOLUTION_SPECIES
4          Pola = Pola; log_k 0.0

5          NAMED_EXPRESSION
6          log_bulk_density ; log_k 0.176091259055681
7          log_Kd_pola ; log_k 0.0

8          SURFACE_MASTER_SPECIES
9          Surf      Surf

10         SURFACE_SPECIES
11         Surf = Surf ; log_k   0


12         Sor + Pola = SorPola
13          -log_k -100
14          -add_logk log_bulk_density
15          -add_logk log_Kd_Pola
```

Geochemical model

```
16         SURFACE NODE_NUMBER
17         Surf   1e+100    # TS
18          -no_edl
19          -equilibrate with solution solution_number
```

The new master species, the contaminant Pol_a, is defined in lines 1 – 4. The new surface master species (Surf) and the identity reaction is defined in lines 8-9 and lines 10-11, respectively. The sorption reaction of Pol_a is defined in line 12. The log-transform is written as:

$$\log(K) = \log(K_d) + \log(\rho_b) - \log(TSurf)$$

Each of the three terms are added as individual terms to log(K) in lines 13 to 15. Log(TSurf) is defined in line 13. The two other factors are added as constants to the log_k by using the identifier –add_logk and a name which refers to the name in the PHREEQC data block NAMED_EXPRESSIONS. The first term, $\log(K_d)$, is added in line 15 and defined in line 7. The second term, $\log(\rho_b)$, is added in line 14 and defined in line 6.

To add the sorption model to the HP-1 project, the surface Sor is defined in lines 16-19. The size of the sorption site is 10^{100} (moles.l_s^{-1}) and is equal to the value defined in line 13. The non-electrical surface complexation model is used (line 18) and the initial composition of the surface site is in calculated in equilibrium with a predefined solution, *solution_number* (line 19).

EC-model

The implementation of the "EC-model" approach from PHREEQC requires the following additions to HP-1 code

Thermodynamic Database

```
1       EXCHANGE_MASTER_SPECIES
2            Y    Y-

3       EXCHANGE_SPECIES
4            Y- = Y-
5            log_k    0.0

6            H+ + Y- = HY
7            log_k 3.60
8            Na+ + Y- = NaY
9            log_k -0.65
10           K+ + Y- = KY
11           log_k 1.56
12           NH4+ + Y- = NH4Y
13           log_k 1.33
14           Al+3 + 3Y- = AlY3
15           log_k 1.08
16           Fe+2 + 2Y- = FeY2
17           log_k 1.03
18           Mg+2 + 2Y- = MgY2
19           log_k -0.65
20           Ca+2 + 2Y- = CaY2
21           log_k 0.00
22           Sr+2 + 2Y- = SrY2
23           log_k 0.00
24           Ba+2 + 2Y- = BaY2
25           log_k 0.14
26           Ra+2 + 2Y- = RaY2
27           log_k 0.23
```

```
28      EXCHANGE 1-28 @Layer 1@
29          Y  39.47E-3

30      EXCHANGE 29-46 @Layer 2@
31          Y  29.81E-3

32      EXCHANGE 47-64 @Layer 3@
33          Y  28.39E-3

34      EXCHANGE 65-86 @Layer 4@
35          Y  28.25E-3

36      EXCHANGE 87-106 @Layer 5@
37          Y  29.39E-3

38      EXCHANGE 107-123 @Layer 6@
39          Y  11.08E-3

40      EXCHANGE 124-151 @Layer 7@
41          Y  2.18E-3
```

The new master exchange master species, Y^-, to which cations will adsorb, is defined in line 1-5. Lines 4 - 27 define the exchange species and their corresponding exchange constants which are obtained from literature. Lines 28 – 41 define the amount of CEC, in given concentration of Y^- in $mol.l^{-1}$ soil, which can differ per layer and can be adjusted to the CEC amounts provided by the Organic Matter content or Soil Textural Fraction per layer if so required.